Optimization and Design Modification of Shell and Tube Heat Exchanger for an Economizer: A Case of Awash Melkassa Aluminum Sulfate and Sulfuric Acid Share Company

M.Sc. Thesis

By

Melkamu Embiale Woldie

Thermal and Aerospace Engineering Department

School of Mechanical, Chemical and Materials Engineering

Adama Science and Technology University

Adama, Ethiopia

December, 2018

Optimization and Design Modification of Shell and Tube Heat Exchanger for an Economizer: A Case of Awash Melkassa Aluminum Sulfate and Sulfuric Acid Share Company

A Thesis Submitted to Thermal and Aerospace Engineering Department of School of Mechanical, Chemical and Materials Engineering, Adama Science and Technology University in Partial Fulfillment of the Requirements for the Award of the Degree of Master of Science in Thermal Engineering.

By

Melkamu Embiale Woldie

Advisor: Dr. Addisu Bekele

Adama, Ethiopia

December, 2018

APPROVAL OF BOARD OF EXAMINERS

We, the undersigned, members of the Board of Examiners of the final open defense by Melkamu Embiale have read and evaluated his thesis entitled "Optimization and Design Modification of Shell and Tube Heat Exchanger for an Economizer: A Case of Awash Melkassa Aluminum Sulfate and Sulfuric Acid Share Company" and examined the candidate. This is, therefore, to certify that thesis has been accepted in partial fulfilment of the requirement of the Degree of Masters of Science in Thermal Engineering.

Samuel Gilmuret	[signature]	25/02/2019
Chairperson	Signature	Date
Tatek Temesgen (PhD)	[signature]	28/02/2019
Internal Examiner	Signature	Date
Dr. Abdulkadir Aman	[signature]	14/03/19
External Examiner	Signature	Date

DECLARATION

I hereby declare that this M.Sc. Thesis entitled "Optimization and Design Modification of Shell and Tube Heat Exchanger for an Economizer: A Case of Awash Melkassa Aluminum Sulfate and Sulfuric Acid Share Company" in partial fulfillment of the requirements for the award of the degree of Master of Science in Thermal Engineering is an authentic record of my own work carried out from September 2017 to December 2018 under supervision of Dr. Addisu Bekele, Assistant Professor of Thermal Engineering Department, Adama Science and Technology University.

The matter embedded in this thesis has not been submitted for the award of a degree or diploma in any other university. All relevant resource information used in this paper has been duly acknowledged.

………………………………	……………………….
Student	Signature:

This is to certify that the above statement made by the candidate is correct to the best of my knowledge and belief. This has been submitted for examination with my approval.

………………………………	……………………….
Advisor	Signature:

ACKNOWLEDGEMENT

A lot of thanks to the Almighty God for His willingness without which this thesis work is unthinkable.

I would like to express my immeasurable appreciation and deepest gratitude to my adviser, Dr. Addisu Bekele for his valuable guidance, comments, suggestions and encouragement, without which this work would have not been possible. For his unwavering support, I am truly grateful.

I extend my gratitude to ASTU for providing me a scholarship without which it would have been impossible for me to complete my study.

I would like to thank all member of the AMASSASCo for their kind support during my stay in the factory for data collection.

I would like to thank all my friends who made my life bright and memorable during my under graduate and master's studies (particularly Mamaru Meslie, Getaneh Mehari, and Asmare Getaneh).

Lastly, and most importantly, I wish to thank my family, particularly my mother, Yetemegn Embiale. She bore me, raised me, supported me, taught me, and loved me. To her I dedicate this thesis.

Table of Contents

LIST OF TABLES

LIST OF FIGURES

LIST OF SYMBOLS AND ABBRIVIATIONS

Symbols

$\dot{Q}$	heat transfer rate [W]	N_f	number of fins [-]
$\dot{m}_h, \dot{m}_c$	mass flow rates [kg/s]	h	convective heat transfer rate [W/m^{2}K]
C_{pc}, C_{ph}	specific heats [J/kg.K]	Nu	nussalt number [-]
$T_{c,out}, T_{h,out}$	outlet temperatures [°C]	R_e	Reynolds- number [-]
$T_{c,in,} T_{h,in}$	inlet temperatures [°C]	V_{max}	maximum air velocity in tube bank
U	overall heat transfer coefficient [W/m^{2}K]	D_r	root diameter [m]
ΔT_{lm}	log mean temperature difference [-]	ℓ	fin spacing [m]
F	the correction factor of heat transfer rate [-]	b	fin height [m]
$R_f^{"}$	fouling resistance per surface area [m^{2}K / W]	τ	fin thickness [m]
R_{tot}	total resistance [K/W]	k	thermal conductivity [W/m.K]
R_w	resistance tube wall [K/W]	μ	dynamic viscosity [kg/s.m]
$\dot{Q}_f$	fin heat transfer rate [W]	h_o	Gas-side heat-transfer coefficient [W/m^{2}K]
ε	heat exchanger effectiveness [-]	P_T	pitch distance [m]
A_b	area at the base of the fin [m^2]	D_r	root diameter [m]
θ_b	temrature difference between the base and free stream [°C]	V_{face}	face velocity the average air velocity approaching the first row of tubes [m^2]
T_∞	free stream temperature [°C]	P_r	prandtl number, surface roughness term [-]
A_f	the surface area of the fin [m^2]	ρ	density [kg/m^3]

η_f	fin efficiency [%]	ΔP_s	pressure drop for flow across a bank of tubes [Pa]
η_w	overall surface efficiency [%]	ΔP_t	pressure drop for flow in the tubes [Pa]
$\dot{Q}_t$	total heat rate from the surface area A, associated with both the fins and the exposed portion of the base [W]	**f**	fanning friction factor [-]
G	mass flux [kg/s. m^2]	N_r	number of tube rows [-]
D_f	fin outside diameter [m]	L_2	the core length for flow normal to the tube bank [m]
X_t	pitch in the transverse tube row [m]	A_o	minimum free-flow area [m^2]
X_L	pitch in the longitudinal tube row [m]	**s**	fluid specific gravity [-]
L_1	tube length [m]	**Φ**	viscosity correction factor [-]
L_3	the no flow dimension length [m]		

Subscript

h	hot fluid	∞	free stream
c	cold fluid	**r**	root
in	Inlet	**max.**	maximum
out	Outlet	**min.**	minimum
f	Fin	**t**	in the tube
b	Base	**s**	in the shell

Abbreviation

AMASSAS.Co	Awash Melkassa Aluminum Sulfates and Sulfuric Acid Share Company
STHE	Shell and tube heat exchanger
NTU	Number of transfer unit
ACO	Ant colony optimization

ABSTRACT

This thesis considers detail study of existing shell and tube heat exchanger of an economizer for Awash Melkasa Aluminum Sulfate and Sulfuric Acid Share Company (AMASSA S.Co) and made design modification as well as optimization of this heat exchanger by using univariate optimization technique on Microsoft Excel and using Ant colony optimization technique (ACO) in MATLAB. Here multi-objective optimization of the heat transfer rate and cost of a shell and tube heat exchanger is presented with multiple Pareto-optimal solutions to capture the trade-off between the two objectives in both techniques. Five decision variables were considered: tube layout, tube diameter, fin height, fin space, and fin thickness. For these decision variables sensitivity analysis has been performed in order to observe the variational influences of decision variables over optimization objectives and then focus on more sensitive decision variables in a case of Univariate technique to decrease problem complexities. In this study it is found that tube layout, fin height and fin space have more variational effect on objective variables.

Pareto front graphs are constructed for multi objective optimization and the best solution is selected by comparing the two techniques values based on requirements. Finally, from ACO optimal values, a point at heat transfer rate and total cost of 7.7481$\times 10^5 W$ and 1.1463$\times 10^6$\$ respectively is selected as the best optimum shell and tube heat exchanger.

Key words: Shell and tube heat exchanger, optimization, economizer, Ant Colony Optimization and Univariate Optimization.

CHAPTER ONE

INTRODUCTION

Awash Melkassa Aluminum Sulphate and Sulphuric Acid Share Company (AMASSA S.Co) is located at 15km from Adama city in the south east direction. AMASSAS.Co was established to produce Sulfuric acid 98.5 %, 17,000 tons per year and Aluminum sulfate 17 %, 13,600 tons per year as a public enterprise, on the second august 1986 E.C.

The company was reestablished as a share company on the first January 2000 E.C with paid up capital of birr 94.52 million. As the factory AMASSAS.Co has many devices to execute production process. Of which heat exchanger is one of those devices.

In heat exchangers, typical applications involve heating or cooling of a fluid stream of concern and evaporation or condensation of single or multicomponent fluid streams. In other applications, the objective may be to recover or reject heat, or sterilize, pasteurize, fractionate, distill, concentrate, crystallize, or control a process fluid. In a few heat exchangers, the fluids exchanging heat are in a direct contact. But in most heat exchangers, heat transfer between fluids takes place through a separating wall or separated by a heat transfer surface, for which shell and tube heat exchanger can be an example. Due to manufacturing and design flexibility, shell and tube heat exchangers are the most used heat transfer equipment in industrial processes. They are also easily adaptable to operational conditions. In this way, the design of shell and tube heat exchangers are very important subject in industrial processes. Nevertheless, some difficulties are found, especially in the shell-side design, because of the complex characteristics of heat transfer and pressure drop [1,2]. The shell and tube heat exchanger (STHE) under study for this thesis is found in Awash Melkasa Aluminum Sulfate and Sulfuric Acid Share Company (AMASSA S.Co). Here the heat exchanger works in engineering principle's to extract heat of flue gas (SO_3) in order to make it 180 °C. For the STHE in Awash Melkasa Aluminum Sulfate and Sulfuric Acid Share Company the two system fluids in which heat is going to be exchanged is water and flue gas(SO_3). Flue gas with mass flow rate of 20 kg/s enters in to shell and exit with outlet temperature of 180 °C, whereas water at 80 °C enters the tube side and out at temperature of 130 °C. But the problems is that the tubes are damaged and water leaks from tube to the shell, as a result acid is formed in the shell. Having this information at hand, detail study of this heat exchanger and new geometry optimization will be run using general thermal equations for STHE heat transfer rate (heat load), pressure drop across the system and optimum total cost. The Geometry optimization is done by considering tube diameter, fin thickness, space, height and tube layout (Triangular or Rectangular Pattern). Finally the overall heat transfer rate, Pressure drop and cost are studied and the allowable design will be chosen from thermal design point of view.

1.1 The Research Problem

Awash Melkasa Aluminum Sulfate and Sulfuric Acid Share Company (AMASSA S.Co) is the only sulfuric acid factory in Africa. Even though, it becomes malfunction its work because of problem faced on the economizer (shell and tube heat exchanger) specifically on tube bundles since October, 2015. It was tried to repair many times by replacing it with available seamless pipe in the factory. But, it cannot be solved permanently. It is not possible to manufacture the existing STHE because the tube and the fin made from different materials and there is no enough technology for that locally. The price of new one is also very high and the company is not able to afford it. Therefore, it needs design modification under consideration of manufacturing and cost. Else, in near future the only acid factory in Africa will be closed and other factories taking their raw material from it will also be affected. To solve the problem, this thesis is proposed to modify and design a shell and tube heat exchanger to extract the heat from the flue gas.

1.2 General Objective

The main objective of this study is modifying the design of existing shell and tube heat exchanger (economizer) of AMASSA S.Co and optimize it to perform similar to the original one.

1.3 Specific Objectives

Specific objective of this thesis is:

- Study the detail design of the existing shell and tube heat exchanger
- Modify the design of existing STHE
- Identify the design decision variables for the modified shell and tube heat exchanger
- Develop an objective function for proper functioning of the modified shell and tube heat exchanger
- Optimize the performance of the modified shell and tube heat exchanger

1.4 Significance of the Study

The contribution of this thesis is modifying of existing damaged shell and tube heat exchanger of AMASSA S.Co with a small cost STHE relative to buying another new heat exchanger. The results of this research will open an opportunity for further application of other heat recovery industrial processes in the country. In addition, the result can be used as reference and base for future work.

1.5 Scope of the Study

The scope of this thesis is analytical study of design modification of existing STHE (economizer) of AMASSA S.Co and optimizing it.

1.6 Limitation of the Study

This study did not include:

- Modification of shell size (length, width and height of the shell). To modify economizer shell, evaporator also needs modification because the two devices are interlocked with each other.
- Two phase flow analysis of fluid in the tube. To consider this analysis locally unavailable measuring instruments are required.

1.7 Organization of the Study

The rest of this thesis is organized in to six chapters each having a distinct and related purpose. Chapter Two, literature review gives an overview of the history, present and future trends of the shell and tube heat exchanger optimization. The appropriate material and method is developed at chapter three. Chapter four discuses about the empirical techniques and software tools used and design studies of existing and design analysis of modified STHE. Chapter five is devoted to the analysis and its outcome related to the result. Chapter six draws conclusions, recommendations and future work.

CHAPTER TWO

LITERATURE REVIEW

An extensive research work has been done till date on the Shell and Tube heat exchangers by changing different parameters to meet the industry requirements.

Walraven et al. (2014), carried out an experimental analysis to study on system optimization of organic Rankin cycle parameters together with the configuration of shell-and-tube heat exchangers. They concluded that the 30-tube configurations should be used for the single phase heat exchangers and the 60-tube configuration for the two-phase heat exchangers [3].

Patil et al. (2014), presented a theoretical analysis and an experimental test on a shell and tube latent heat storage exchanger. They performing a comprehensive comparison of the design outputs by IBR and ASME codes of critical component s of a shell and tube type heat exchanger in an attempt to show the redundancy in designing the components using both these codes simultaneously [4].

Arya et al. (2015), performed experimental performance test on the fixed designed STHX and calculate the heat transfer coefficient and effectiveness. Validation is to be carried out using which gives the result comparison with that of experimental result. Here flow parameters are not varied but size and number of tubes are varied and best efficient model is selected as Optimized value. 3 different number of tubes are used with same shell size remaining same. 40 tubes, 32 tubes and 36 tubes were tried. They have been observed for same input temperatures and mass flow rates for three different models one with 36 tubes, 32 tubes model &other with 40 tubes, the temperature variation in 36 tubes is more and also requires less tubes compared to 40 tube model. So it is more effective than tubes model [5].

Fettaka et al. (2013), did a multi-objective optimization of the heat transfer area and pumping power of a shell and tube heat exchanger was presented to provide the designer with multiple Pareto-optimal solutions which capture the trade-off between the two objectives. Considered decision variables were: tube layout pattern, number of tube passes, baffle spacing, baffle cut, tube length, tube outer diameter, and tube wall thickness. The optimization was performed using the fast and elitist non-dominated sorting genetic algorithm (NSGA-II) available in the multi-objective genetic algorithm module of MATLAB. In order to verify the improvements in design that the method offers, two case studies from the open literature were presented. The results showed that for both case studies, better values of the two objective functions can be obtained than the ones previously published [6].

Dubey et al. (2017), have reviewed the enhancement of heat transfer by using twisted tape insert. They observed that the heat transfer phenomenon enhanced by means of finned tubes, inserts, twisted tubes or modified baffles etc. To get better efficiency of industrial system as well as domestic equipment it is required that the effectiveness of heat exchanger to be maximum. And the performance of heat exchanger is related to the governing parameters such as heat transfer area, overall heat transfer coefficient, and mean temperature difference. Finally they reached that among various techniques the most successful development of a component for efficient enhancement of heat exchanger is development of twisted inserts for heat exchanger tubes [7]. Dawit (2014), he has done his project in Harar Brewery Share Company on the STHE at the 9^{th} zone which was malfunctioned that is the temperature of the cold fluid would fluctuate between 35^0C-40^0C. Due to this he has done some optimization and redesign of the machine is done for both mechanical and thermal designs and the simulation for the heat transfer between the two fluids is analyzed using the concept of CFD (Computational Fluid Dynamics) using Gambit and Fluent software's. Then final result of the STHE in HBS.Co which is the redesigned STHE efficiently work to achieve the required outlet temperature 34^0C the temp at which the beer is ready for customer for use [8].

Singh and Sehgal (2013), in this paper, experimental study of shell-and-tube heat exchanger was conducted to calculate the heat transfer coefficient, LMTD, Nusselt number, and pressure drop at different Reynolds numbers (303–1516). After so many experimentation they have given conclusion as follow.

(i) The heat transfer coefficient and the nusselt number increase with increase in Reynolds number in shell-and-tube heat exchanger for both hot fluid inlet and cold fluid inlet.

(ii) The value of LMTD increases with increase in Reynolds number from 303 to 1516.

(iii) The value of temperature constants ξ and ω decreased with increase in Reynolds number.

(iv) The value of pressure drop gradually increases with increase in Reynolds number [9].

Singh and Pal (2016), in this research analysis shell and tube heat exchanger is designed and simulated by using Computational Fluid Dynamic (CFD). After they have been modifying the heat exchanger the effectiveness of heat exchanger is increased by changing the shell side fluid (from water to methanol). Methanol provide sufficient cooling to as compared water in heat exchanger and increase the effectiveness of heat exchanger up to 95.5 percent [10].

Rao and Patel (2011), in this study they explored the use of particle swarm optimization (PSO) and civilized swarm optimization (CSO) algorithms for design optimization of shell and tube heat exchangers from economic view point. Two case studies were also presented and the results of optimization using PSO and CSO algorithms were compared with those obtained by using genetic algorithm (GA). The abilities of both the algorithms were demonstrated using two different case studies and the performance was compared with the GA approach. Savings in total cost ranging from 3.54 to 8.1 per cent (using PSO) and 4.03 to 9.4 per cent (using CSO) were observed compared to the GA approach, shown the improvement potential of the PSO and CSO methods [11].

Patel and Mavani (2012), studied that how to design the shell and tube heat exchanger. In design calculation HTRI software is used to verify manually calculated result and they have concluded that:

- There is increase in pressure drop with increase in fluid flow rate in shell and tube heat exchanger which increases pumping power.
- Genetic algorithm provide significant improvement in the optimal designs compared to the traditional designs.
- It also reveals that the harmony search algorithm can converge to optimum solution with higher accuracy in comparison with genetic algorithm.
- Tube pitch ratio, tube length, tube layout as well as baffle spacing ratio were found to be important design parameters which has a direct effect on pressure drop and causes a conflict between the effectiveness and total cost.

In brief, it is necessary to evaluate optimal thermal design for shell and tube heat exchanger to run at minimal cost in industries [12].

Velazquez et al. (2014), in this paper the Delaware Method published in 1963 is analyzed and upgraded with using correction factors which take into account the undesirable currents of the mean flow. However, this method presented graphically those correction factors which imply an impediment to fulfill the software calculations. Thus, the equations corresponding to the correction factor equations and a Fortran 77 numerical program were established. From this work they have presented the improvements to the Delaware method for the shell and tube heat exchanger design.

These improvements were made up not only of obtaining the correction factor equations which were only available in graphic forma but also of developing the computing program in Fortran 77 language.

Thus, a new and easy tool for the shell and tubes heat exchanger design was available which allows accomplishing the numerical computing in a quick form minimizing the errors of the graphical lecture. This system gave the opportunity to explore different design alternatives in order to find the optimal solution to each proposed problem. The results of this work was a simple software that can perform calculations with the introduction of parameters depending only on the geometry of the heat exchanger, i.e., geometry, temperature and fluid characteristics eliminating the human errors and increasing the calculations speed and accuracy [13].

Thorat et al. (2016), have done this paper on Thermal Design of Shell & Tube Heat Exchanger for the 30MW Concentrating Solar Power Plant. In the first part of this paper, a simplified approach to Theoretical Thermal Design of Shell & Tube Heat Exchanger for Concentrating Solar Power Application. In the second part of this paper, theoretically (analytical) thermal design of STHE compared with the Software (i.e. HTFS) basis design. Theoretical thermal design validate on the basis of HTFS. From the two data they drawn the following conclusions.

1) Inlet & outlet temperature of heat exchanger were achieved by software is exact to calculated by analytical method

2) Overall heat transfer coefficient & Tube side heat transfer coefficient is more than calculated by analytical method.

3) Pressure drop, LMTD & Area of heat exchanger were smaller than calculated.

4) Fouling factor has large influence in the calculation of surface area. So steps like periodic cleaning to maintain lower fouling condition may be less expensive than purchasing

additional surface area.

5) The relative difference between analytical results and software results is very less (<10%).

6) In simulation mode they have got exact results as in rating mode.

Thus, they have proven that thermal design methodology is set to Thermal Design of Shell & Tube Heat Exchanger for Concentrating Solar Power Application by studying various parameters affecting on it [14].

Tari (2010), The shell side design of a shell-and-tube heat exchanger; in particular the baffle spacing, baffle cut and shell diameter dependencies of the heat transfer coefficient and the pressure drop are investigated by CFD modeling a small heat exchanger was discussed and the simulation results compared with the results from the Kern and Bell-Delaware methods. From which they observed that the Kern method always under predicts the heat transfer coefficient. For properly spaced baffles, they observed that the CFD simulation results are in very good agreement with the Bell-Delaware results and the results are also sensitive to the baffle cut selection [15].

Sadeghzadeh et al. (2015), here, an analysis of a radial, finned, shell and tube heat exchanger was carried out, considering nine design parameters: tube arrangement, tube diameter, tube pitch, and tube length, number of tubes, fin height, fin thickness, baffle spacing ratio and number of fins per unit length of tube. The optimization of the objective functions (maximum heat transfer rate and minimum total cost) is performed using a non-dominated sorting genetic algorithm (NSGA-II), and compared against a one-objective algorithm, to find the best solutions. Finally they depicted a set of solutions on a Pareto curve and here the best solution bound (from economic and efficiency points of view) was identified among the possible answers on the Pareto front, all of which account for maximum heat transfer rate and minimum cost. Also, the minimum and maximum objective functions were specified, allowing the designer to select the best points among these solutions based on requirements [16].

Kanizawa and Ribatski (2014), this study presented pressure drop experimental results obtained during single and two-phase upward cross flow of air-water mixtures in triangular tube bundle. Depending up on the result they concluded that: Frictional pressure drop increases with increasing mass flux during single-phase flow. But in case of two-phase flow for reduced liquid superficial velocities, the total pressure drop decreases with increasing the superficial gas velocity, due to the reduction of the gravitational pressure drop parcel. For intermediary and high liquid superficial velocity, the total pressure drop increases with increasing the superficial gas velocity [17].

Lunsford (1998), provided some methods for increasing shell-and-tube exchanger performance. He listed the following heat transfer enhancement methods : operating correctly, increasing pressure drop if available in exchangers with single-phase heat transfer, increased velocity results in higher heat transfer coefficients, periodic cleaning and less conservative fouling factors and through the use of finned tubes, inserts, twisted tubes, or modified baffles [18].

Nakao et al. (2016), discussed the use of fouling rate models in the design of shell-and-tube heat exchanger. They found that availability of fouling rate models can predict the impact of the thermofluidynamic conditions on fouling. In this context, this paper presented a proposal of interconnection between conventional design algorithms and fouling rate models and also it is possible to insert the behavior of the fouling phenomenon during the design phase of the heat exchanger, aiming its mitigation. Finally they concluded that as it is able to modify the design, exploring the predictions of the fouling rate, considering the relevant economic losses associated to fouling and the procedure may be a promise contribution for handling this problem at design level [19].

Sandeep et al. (2015), presented a study of different cross section bundle arrangements such as triangle, rectangular and round for a shell and tube heat exchanger computationally. Ultimately, relationship between pressure drop and heat transfer is evolved for different cross section shape in a counter flow model shell and tube heat exchanger. From computational results, they concluded that there is slight variation in heat transfer performance between three cross-section configurations and simulation results have good agreement with analytical results. Whereas pressure drop variation between three configurations is more. This variation increased with increased in size of heat exchanger. But rectangular cross-section shape is good for tube bundle because it produced less pressure drop on shell side among three configurations. This work carried to experimental investigation with rectangular configuration to compare experimental and CFD results [20].

Caputo et al. (2006), In this paper a formulation of the shell and tube heat exchanger design optimization problem has been proposed based on the utilization of a genetic algorithm. Resorting to the analysis of a number of significant case studies, the paper demonstrated that this optimization algorithm can effectively be utilized to improve the design process and significantly reduce the total discounted cost of heat exchange equipment respect to traditional sizing procedures. When they referring to literature test cases, reduction of capital investment up to 12% and savings in operating costs up to 57% have been obtained, with overall decrease of total discounted cost up to 16%. This shows the improvement potential coming from applying the proposed method [21].

Shukla et al. (2015), explained in their study heat transfer analysis by considering with different fluid combinations such as water-steam, CO_2-steam and SO_2-steam in shell and tube heat exchanger and got the values for Nusselt number, Reynolds number, heat transfer coefficient, pressure drop and friction factor. From the data arrived and drawn they found that as Reynolds number increases Nusselt number increases and friction factor decreases both tube and shell side fluids. Taking steam on shell side and CO_2 and SO_2 on tube side. It was found that Nusselt numbers showed steep increase for SO_2 steam combination than CO_2 steam combination. They also got heat exchanger length and maximum effectiveness 2.16m and 0.65 respectively by fixing area of heat exchanger [22].

Gupta et al. (2017), in this project the theoretical testing of shell -side and tube side heat transfer coefficient was performed by replacing circular tubes with elliptical tubes. From which they concluded that; When the ratio of major axis to minor axis was less than one the increase in tube side flow velocity while when this ratio greater than one they got reduced velocity in tube side. Also, when this ratio was less than one, the heat transfer coefficient in shell side increased by 20.2% and in tube side increased by 14.5%. The overall Heat transfer coefficient increased and reduction in surface area of the tube, also the setup cost of equipment reduced and slightly increment in pressure drop in shell side. But they optimized by taking ratio of axis 0.75 [23].

Mishra et al. (2016), found heat transfer, temperature difference and pressure drop on the shell side of shell-and-tube heat exchanger with and without baffles by using both theoretical and

CFD analysis. From this analysis the following conclusions were drawn: From the theoretical analysis it was found that the heat transfer coefficient, pressure drop and temperature difference was more in case of using baffles as compared to without baffles. And also from the CFD analysis, results were found in similar pattern to increases temperature heat transfer and decreases pressure drop then using in baffles as compared to without baffles [24].

Summary of the literatures

On reviewing the literature, it is found that the optimization can be carried out by numerous configurations for a shell and tube heat exchanger. Different researchers were used different optimization methods to obtain closer solutions towards the exact ones.

In optimization, when many decision variables are considered, the analysis become more complex but better optimal solution can be find out and attain more closer towards exact solution.

CHAPTER THREE

MATERIALS AND METHODOLOGY

3.1 Methodology

The design of STHE involves a large number of geometric and operating variables as a part of the search for an exchanger geometry that meets the heat duty requirement and a given set of design constrains. Usually a reference geometric configuration of the equipment is chosen at first and pressure drop value is fixed. Then, the values of the design variables are defined based on the assumption of several mechanical and thermodynamic parameters in order to have a satisfactory heat transfer coefficient leading to a suitable utilization of the heat exchange surface. The designer's choices are then verified based on iterative procedures involving many trials until a reasonable design is obtained with a satisfying compromise between pressure drops and thermal exchange performances [1]. Likewise in this thesis existing STHE will studied in detail using known input parameters. From which size of the shell and input and output temperature of fluids held constant as input parameter to size the modified STHE. Unknown parameters (decision variables) can be either dependent or independent variables. Then the whole STHE correlations are defined in terms of independent variables. For different independent variable variations, values of heat transfer rate and cost of STHE are different. In a case of optimization using Microsoft Excel, more influential independent variables on values of heat transfer rate and cost will considered in a specified ranges to decrease analysis complexity. But in MATLAB programing all independent variables will be considered. Finally, for each methods one best value will be selected in order to have satisfactory heat transfer rate and total cost. Of which, by compression one solution will take as a final modified STHE.

Detail process of shell and tube heat exchanger design methodology considerations are shown in figurer 3.1.

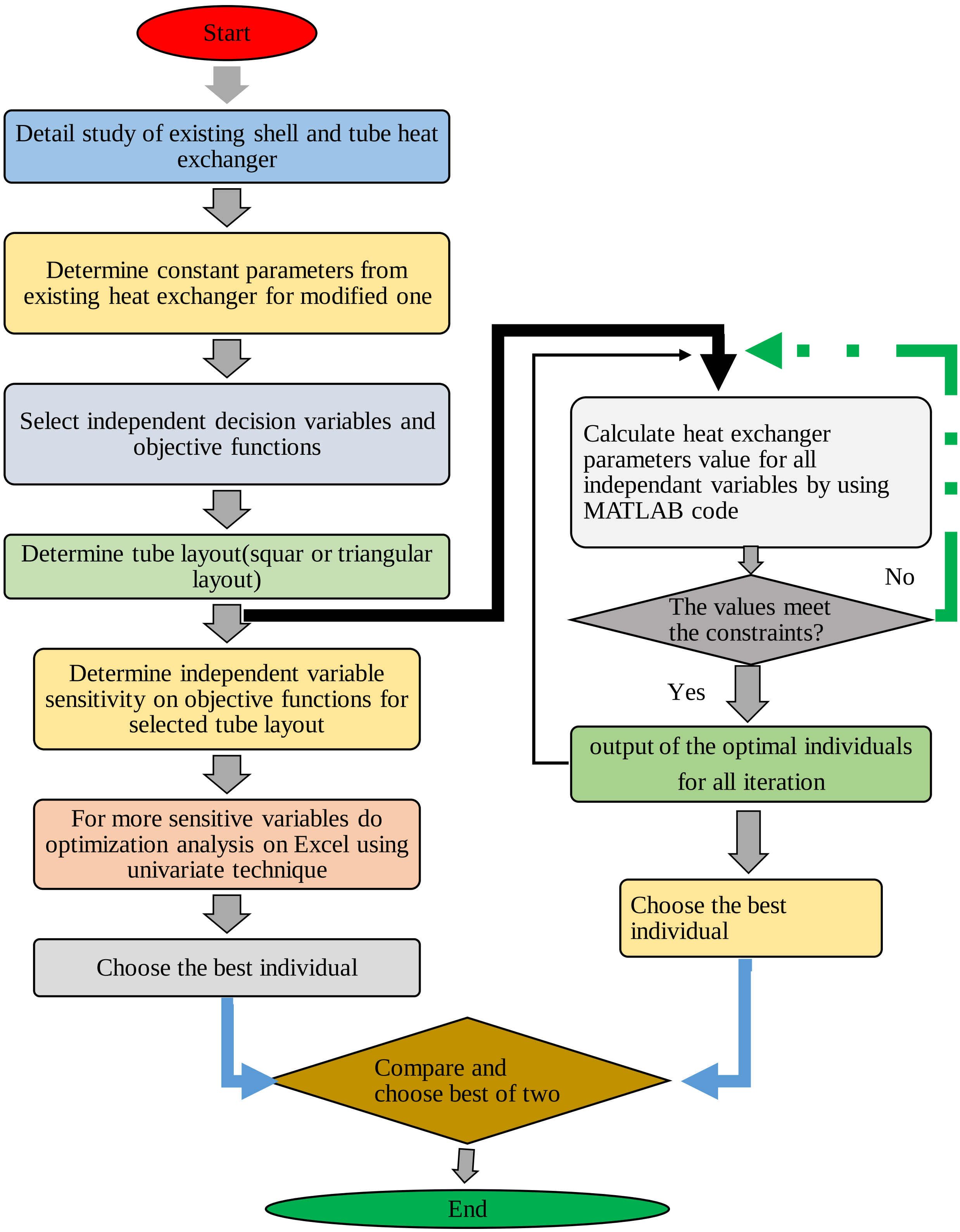

Figure 3. 1 Flow chart for the research work

3.2 Materials

Material applied for data analysis

- ✓ Matlab R2017a
- ✓ Microsoft Excel
- ✓ Catia V5R20

Material used for heat exchanger design

When sulfur (S) -containing fuels are burnt, sulfur oxides (SO_x) are produced, part of which is turned to SO_3. When exhaust gas temperature drops to below a dew point or when the gas is in contact with a low-temperature wall, SO_3 and H_2O, contained in the gas, are combined to form highly-concentrated sulfuric acid that corrodes steel. This is sulfuric acid dew corrosion, which severely corrodes not only carbon steel but also stainless steel. To solve this problem corrosion resistant S-TEN 1 material is extensively applied to the air preheaters of boilers, for power plants, waste incineration plants, and various heating furnaces. At extremely sever corrosion S-TEN 1 (KA-STB380J1) exhibits corrosion resistant about 5-10 times that of stainless steel [25, 26].

S-TEN 1 thermal conductivity between 200 and 300 ˚C is 45.5 W/ (m · K) which is less than the existing heat exchanger tube material (steel K18) thermal conductivity by 50 W/ (m · K). But overall heat transfer coefficient change is insignificant that is only 0.5 % reduction in S-TEN 1.

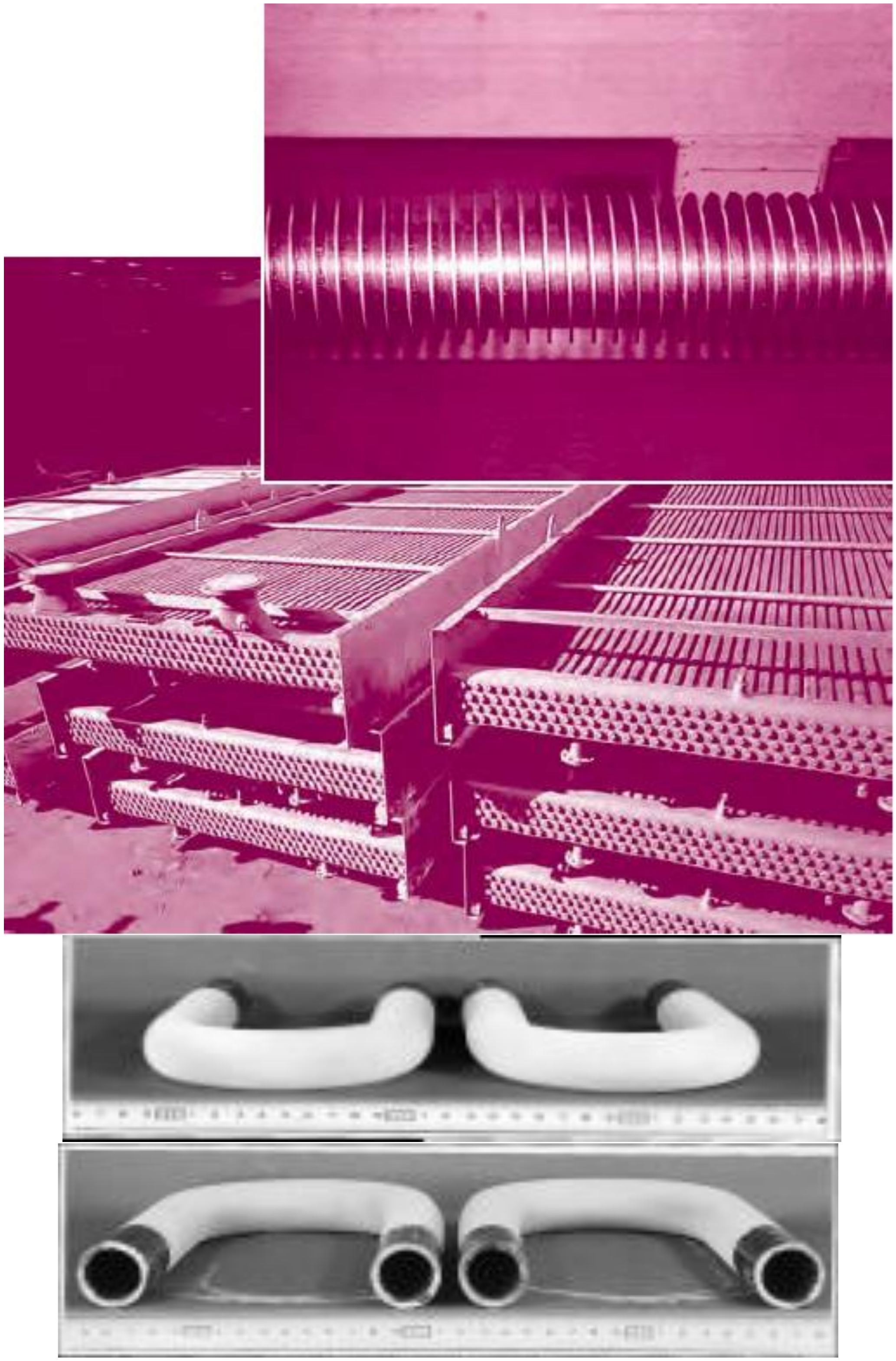

Figure 3. 2 Application examples of S-TEN 1 steel [26].

CHAPTER FOUR

THERMAL ANALYSIS AND OPTIMIZATION OF A HEAT EXCHANGER

4.1 Heat Transfer Assumptions in the Heat Exchanger

To analyze the exchanger heat transfer problem, a set of assumptions are introduced so that the resulting theoretical models are simple enough for the analysis. The following assumptions are made for the exchanger heat transfer problem formulations:

1. The heat exchanger operates under steady-state conditions.
2. Heat losses to or from the surroundings are negligible because it has 50 cm cotton insulation thickness.
3. There are no thermal energy sources or sinks in the exchanger walls or fluids.
4. The temperature of each fluid is uniform over every cross section in exchangers due to turbulence fluids are mixed enough.
5. Wall thermal resistance is distributed uniformly in the entire exchanger.
6. Phase changes in the fluid streams flowing through the exchanger is negligible.
7. Longitudinal heat conduction in the fluids and in the wall is negligible.
8. The fluid flow rate is uniformly distributed through the exchanger on each fluid side in each pass.

4.2 Design Method of Heat Exchanger

Depending on input parameters heat transfer analysis of an exchanger can be performed by using any of the ε -NTU or LMTD methods. Therefore in this heat exchanger heat transfer analysis ε –NTU method is used.

In the ε -NTU method, the heat transfer rate from the hot fluid to the cold fluid in the exchanger is expressed as

$$\dot{Q} = \varepsilon C_{min}\left(T_{h,in} - T_{c,in}\right) = \varepsilon C_{min}\Delta T_{max} \qquad (4.1)$$

Where ε is the heat exchanger effectiveness, sometimes referred to as the thermal efficiency, C_{min} is the minimum of C_c and C_h; $\Delta T_{max} = (T_{h,in} - T_{c,in})$ is the fluid inlet temperature difference (ITD). The heat exchanger effectiveness ε is non dimensional, and it can be shown that in general it is dependent on the number of transfer units NTU, the heat capacity rate ratio $C^* = \frac{C_{min}}{C_{max}}$, and the flow arrangement for a direct-transfer type heat exchanger [27, 28].

Heat Exchanger Effectiveness ε

Effectiveness **ε** is a measure of thermal performance of a heat exchanger. It is defined for a given heat exchanger of any flow arrangement as a ratio of the actual heat transfer rate from the hot fluid to the cold fluid to the maximum possible heat transfer rate if an infinite heat transfer surface area were available in a counter flow heat exchanger. Mathematically:

$$\varepsilon = \frac{\dot{Q}}{\dot{Q}_{max}} \tag{4.2}$$

Or ε can be determined directly from the operating temperatures and heat capacity rates [27].

$$\varepsilon = \frac{C_c(T_{c,out} - T_{c,in})}{C_{min}(T_{h,in} - T_{c,in})} = \frac{C_h(T_{h,in} - T_{h,out})}{C_{min}(T_{h,in} - T_{c,in})} \tag{4.3}$$

Heat Capacity Rate Ratio C*

C* is simply a ratio of the smaller to larger heat capacity rate for the two fluid streams.

$$C^* = \frac{C_{min}}{C_{max}} = \frac{(\dot{m}C_p)_{min}}{(\dot{m}C_p)_{max}} \tag{4.4}$$

C* is a heat exchanger operating parameter since it is dependent on mass flow rates and/or temperatures of the fluids in the exchanger. The C_{max} fluid experiences a smaller temperature change than the temperature change for the C_{min} fluid in the absence of extraneous heat losses [27].

Number of Transfer Units NTU

The number of transfer units NTU is defined as a ratio of the overall thermal conductance to the smaller heat capacity rate:

$$\mathrm{NTU} = \frac{\mathrm{UA}}{\mathrm{C_{min}}} \tag{4.5}$$

NTU designates the no dimensional heat transfer size or thermal size of the exchanger, and therefore it is a design parameter. NTU provides a compound measure of the heat exchanger size through the product of heat transfer surface area A and the overall heat transfer coefficient U [27].

In general heat exchanger effectiveness is dependent on the number of transfer units NTU, the heat capacity rate ratio C*, and the flow arrangement for a direct-transfer type heat exchanger. Therefore for shell and tube, one shell pass (2, 4 . . . tube passes) arrangement heat exchanger effectiveness is represented as:

$$\varepsilon = 2\left\{1 + \mathrm{C}^{*} + (1 + \mathrm{C}^{*2})^{1/2} \times \frac{1 + \exp[-(\mathrm{NTU})(1 + \mathrm{C}^{*2})^{1/2}]}{1 - \exp[-(\mathrm{NTU})(1 + \mathrm{C}^{*2})^{1/2}]}\right\}^{-1} \tag{4.6}$$

4.3 Overall Heat Transfer Coefficient

The overall heat transfer of heat exchangers is the ability of transferring heat through different resistances, it depends upon, the properties of the process fluids, temperatures, flow rates and geometrical arrangement of the heat exchanger. For example, the number of passes, number of baffles and baffle spacing etc. The equation basically sums up all the resistances encountered during the heat transfer and taking the reciprocal gives us the overall heat transfer coefficient [29].

Figure 4.1 below, shows layers of heat transfer media between hot gas in the shell and cold water in the tube.

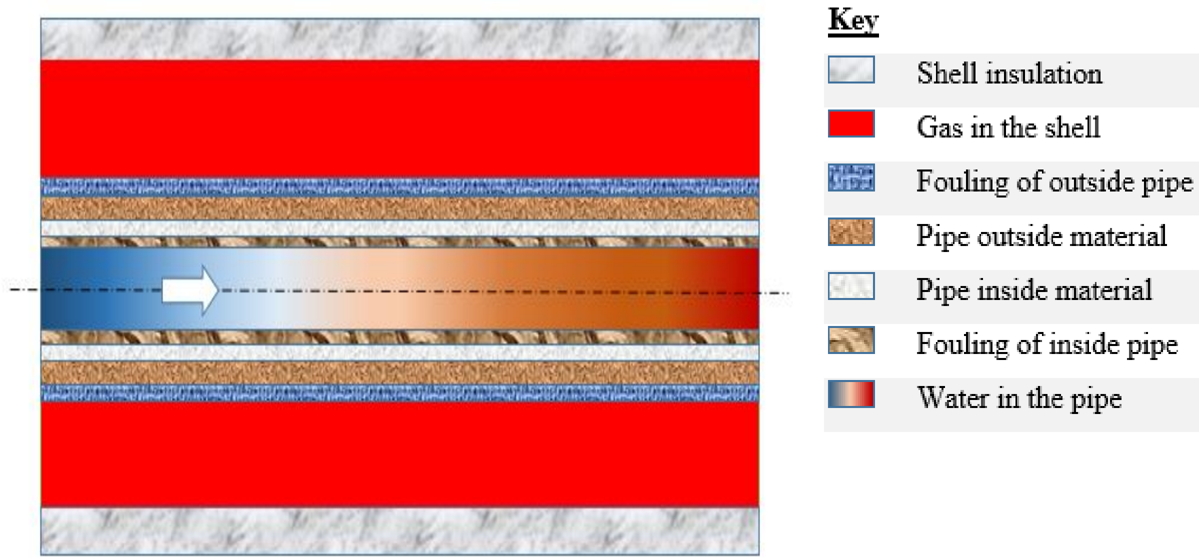

Figure 4. 1 Layers of heat transfer media of existing STHE

The overall heat transfer coefficient is related to the total thermal resistance, and from Equation,

$$U = \frac{1}{AR_{tot}} \tag{4.7}$$

Where, R_{tot} is the sum of surface convection resistances and the conduction resistances through the heat exchanger wall material and layers of fouling material on both sides of the surface.

$$R_{tot} = R_s + R_{f,s} + R_w + R_{f,t} + R_t \tag{4.8}$$

Convection resistances R_t and R_s are calculated from the definition of convection resistance

$$R_{conv} = \frac{1}{hA} \tag{4.9}$$

for in case of a tube of length L_1 and inner and outer diameters of Di and Do , from

$$R_w = \frac{\ln\frac{D_o}{D_i}}{2\pi k_w L_1} \tag{4.10}$$

Fouling layer resistances are in practice rarely calculated from the thickness and thermal conductivity of the fouling layers, which are rarely known precisely enough. Instead, typical values of fouling resistance per surface area $R_f^{''}$ (m^2K / W) for the type fluid and the fouling layer resistance then obtained from [23]

$$R_f = \frac{R_f''}{A} \tag{4.11}$$

From the above thermal resistance equations the value of U can be obtained.

$$U = \left(\frac{A}{A_i h_i} + \frac{\dot{R}_{fDi} A}{A_i} + \frac{\dot{R}_{fDo}}{\eta_w} + \frac{1}{h_o \eta_w} + AR_w\right)^{-1} \tag{4.12}$$

Wall resistance for N_t circular tubes with a multiple-layer wall can be given by equation:

$$R_w = \frac{1}{2\pi L_1 N_t}\left(\sum_j \frac{\ln(D_{j+1}/D_j)}{k_{w,j}}\right) \tag{4.13}$$

Where k_w= wall thermal conductivity, D_j and D_{j+1} = consecutive diameters between a layer and j = number of tube layers.

4.4 Fouling Considerations

Fouling means the undesirable accumulation of solid layers on heat transfer surface. The effect of fouling on heat exchanger performance is to reduce heat transfer due to the added thermal resistance, and sometimes also to increase pressure drop due to the constriction of the free-flow area [23]. From economical point of view, heat exchanger fouling causes additional costs due to:

a) Heat exchangers must be over-sized to account for the reduction of overall heat transfer coefficient due to the expected fouling layers
b) Maintenance costs due to cleaning and possibly treatment of fluids to reduce fouling rates
c) Energy losses due to increased pressure drops and therefore pumping power requirements
d) Loss of production due to maintenance activities

Fouling can happen with a number of mechanisms, depending on the fluids, surfaces and temperatures [30].

Particulate fouling: finely divided solids suspended on the fluid are gradually deposited on the surface

Chemical reaction fouling: a chemical reaction not involving the surface material results in solid material deposited on the surface

Corrosion fouling: heat transfer surface becomes oxidized, creating an additional thermal resistance but more importantly provides a roughened surface suitable for other foulants to attach.

As a general rule, fouling rates tend to be higher on liquid than on gas side, and higher on hot than on cold fluid side.

Although fouling and the resulting thermal resistance are clearly time-dependent phenomena and the fouling rates are frequently dependent on variables at least partly under the designer's control, predicting the fouling rates accurately is difficult at best.

Particularly in heavily fouling increasing efforts are aimed at fouling rate prediction and minimization, the most common design approach for the majority of applications is still to simply assume a certain fouling resistance, calculate the overall heat transfer coefficient U accordingly and thereby find the appropriately over-designed heat transfer area A that accounts for fouling resistances to achieve the required thermal performance. Some over-design (typically about 10% or less) is considered acceptable [30, 31].

4.5 Accounting for the Effects of Extended Surfaces

In a gas-to-liquid exchanger, the heat transfer coefficient on the liquid side is generally one order of magnitude higher than that on the gas side. Hence, to have balanced thermal conductance on both sides for a minimum-size heat exchanger, fins are used on the gas side to increase surface area A. This is similar to the case of a condensing or evaporating fluid stream on one side and gas on the other.

In a tube-fin exchanger, round and rectangular tubes are most common, although elliptical tubes are also used. Fins are generally used on the outside, but they may be used on the inside of the tubes in some applications. They are attached to the tubes by a tight mechanical fit, adhesive bonding, welding, or extrusion.

Depending on the fin type, tube-fin exchangers are categorized as follows:

(1) An individually finned tube exchanger or simply a finned tube exchanger, (2) A tube-fin exchanger having flat (continuous) fins, as shown in Fig. (4.2); and (3) longitudinal fins on

individual tubes.

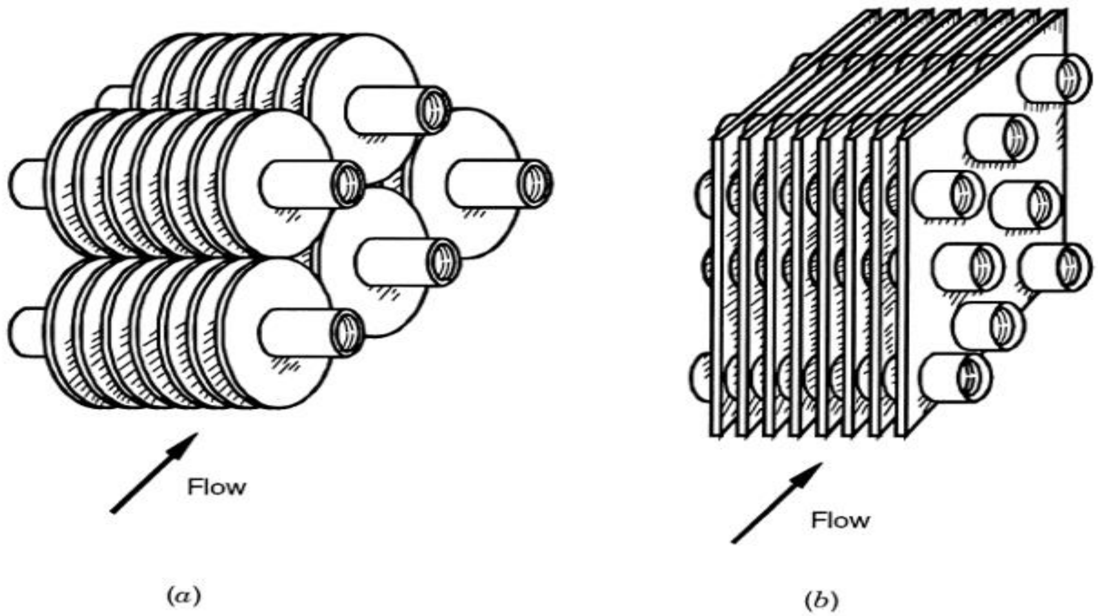

Figure 4. 2 (a) Individually finned tubes; (b) flat (continuous) fins on an array of tubes [32].

The exchanger with flat fins is usually less expensive on a unit heat transfer surface area basis because of its simple and mass-production construction features.

Tube-fin exchangers can withstand ultrahigh pressures on the tube side. The highest temperature is again limited by the type of bonding, materials employed, and material thickness. Tube-fin exchangers usually are less compact than plate-fin units. Tube-fin exchangers with an area density of about 3300 m^2/m^3 are available commercially. On the fin side, the surface area desired can be achieved through the proper fin density and fin geometry. Typical flat fins has a surface area density of about 720 m^2/m^3.

Individually finned tubes are probably more rugged and practical in large tube-fin exchangers [32].

Measure of fin thermal performance is provided by the fin efficiency η_f. The maximum driving potential for convection is the temperature difference between the base (x = 0) and the fluid, $\theta_b = T_{base} - T_\infty$. Hence the maximum rate at which a fin could dissipate energy is the rate that would exist if the entire fin surface were at the base temperature [33].

However, since any fin is characterized by a finite conduction resistance, a temperature gradient must exist along the fin and the preceding condition is an idealization. A logical definition of fin efficiency is therefore

$$\eta_f = \frac{\dot{Q}_f}{\dot{Q}_{max.}} = \frac{\dot{Q}_f}{hA_f\,\theta_b} \tag{4.14}$$

$$\eta_f = \frac{\tanh(m\psi)}{m\psi} \tag{4.15}$$

$$m = \left(\frac{2h_o}{k\tau}\right)^{0.5} \tag{4.16}$$

$$\psi = \left(\frac{D_f + \tau - D_r}{2}\right)\left(1 + 0.35\ln\left(\frac{D_f + \tau}{D_r}\right)\right) \tag{4.17}$$

where A_f is the surface area of the fin.

In contrast to the fin efficiency η_f, which characterizes the performance of a single fin, the overall surface efficiency η_w characterizes an array of fins and the base surface to which they are attached.

$$\eta_w = \frac{\dot{Q}_t}{\dot{Q}_{max.}} = \frac{\dot{Q}_t}{hA\,\theta_b} \tag{4.18}$$

$$A_f = L_1 N_t N_f \left[2\pi\left(\frac{{D_f}^2 - {D_r}^2}{4}\right) + \pi D_f \tau\right] \tag{4.19}$$

$$A_b = \pi D_r (L_1 N_t - L_1 N_t N_f \tau) \tag{4.20}$$

$$A = A_f + A_b \tag{4.21}$$

$$A_i = \pi D_i N_t L_1 \tag{4.22}$$

$$\eta_w = \frac{A_b + \eta_f A_f}{A} \tag{4.23}$$

Where $\dot{Q}_t = \dot{Q}$ is the total heat rate from the surface area A associated with both the fins and the exposed portion of the base (often termed the prime surface). If there are N_f fins in the array, each of surface area A, and the area of the prime surface is designated as A_b, the total surface area is

$$A = N_f A_f + A_b \tag{4.24}$$

The maximum possible heat rate would result if the entire fin surface, as well as the exposed base, were maintained at T_b. The total rate of heat transfer by convection from the fins and the prime (unfinned) surface may be expressed as.

$$\dot{Q}_t = N_t \eta_f A_f h\, \theta_b + h A_b\, \theta_b \tag{4.25}$$

Where the convection coefficient this assumed to be equivalent for the finned and prime surfaces [33]. Hence

$$\eta_w = 1 - \frac{N_f A_f}{A}(1 - \eta_f) \tag{4.26}$$

4.6 Convective Heat Transfer Coefficient

Convective heat transfer occurs when a gas or liquid flows past a solid surface whose temperature is different from that of the fluid. Convection includes energy transfer by both the bulk fluid motion (advection) and the random motion of fluid molecules (conduction or diffusion). Two broad categories of convective heat transfer are distinguished, namely, forced convection and natural (or free) convection.

Heat-transfer coefficient, h, which appears as the constant of proportionality in Fourier’s Law. In particular, h is not a material property. It depends not only on temperature and pressure, but also on such factors as geometry, the hydrodynamic regime (laminar or turbulent), and in turbulent flow, the intensity of the turbulence and the roughness of the solid surface.

From the standpoint of transferring heat, turbulent flow is highly desirable.

The reason that turbulent flow is so effective at transferring heat is that the turbulent eddies can rapidly transport fluid from one area to another. When this occurs, the thermal energy of the fluid is transported along with the fluid itself. This eddy transport mechanism is much faster than the molecular transport mechanism of heat conduction [31, 33].

a) Convective Heat Transfer Coefficient on Shell Side

The flow of gases over banks of finned tubes has been extensively studied and numerous correlations for this geometry are available in the open literature. Among these, the correlation of Briggs and Young has been widely used [31]:

$$N_{us} = 0.134 R_{es}^{0.681} P_{rs}^{1/3} \left(l/_{b}\right)^{0.2} \left(l/_{\tau}\right)^{0.1134} \tag{4.27}$$

Where:

$Nu_s = h_o D_r / k_s$

$R_{es} = D_r V_{max} \rho_s / \mu_s$

The Reynolds number is based on the tube outside diameter and the velocity on the cross flow area of the shell.

V_{max}= maximum air velocity in tube bank

D_r=root diameter

l = fin spacing

b = fin height

τ = fin thickness

k_s = thermal conductivity of gas

ρ_s = density of gas

μ_s = viscosity of gas

h_o = gas-side heat-transfer coefficient

The fin spacing is related to the number,N_f, of fins per unit length by the following equation:

$$l = 1/_{N_f} - \tau \tag{4.28}$$

For an inline tube arrangement:

$$V_{max} = \frac{L_1 L_3 V_{face}}{\left[(X_t - D_r)L_1 - (D_f - D_r)\tau N_f L_1\right] \frac{L_3}{X_t}} \tag{4.29}$$

For the staggered tube arrangement:

$$V_{max} = \frac{L_1 L_3 V_{face}}{\left[\left(\frac{L_3}{X_t} - 1\right)\left[(X_t - D_r) - (D_f - D_r)\tau N_f\right] + (X_t - D_r) - (D_f - D_r)\tau N_f\right] L_1} \qquad (4.30)$$

$$V_{face} = \frac{\dot{m}}{\rho_s A_{face}}$$

Where: V_{face} is face velocity the average air velocity approaching the first row of tubes.

X_t=pitch in the transverse tube row

X_L= pitch in the longitudinal tube row

L_1=tube length

L_3=the no flow dimension length

b) Convective Heat Transfer Coefficient on Tube Side

Heat transfer to fluids flowing inside pipes and ducts is a subject of great practical importance. Consequently, many correlations for calculating heat-transfer coefficients in this type of flow have been proposed. However, the correlations presented below are adequate to handle the vast majority of process heat-transfer applications [31].

For heat-transfer coefficient, hi, the Seider–Tate and Hausen equations are used as follows.

For $R_{et} \geq 10^4$,

$$Nu_t = 0.023 R_{et}^{0.8} P_{rt}^{1/3} \left(\mu_t/\mu_w\right)^{0.14} \qquad (4.31)$$

For $2100 < R_{et} < 10^4$

$$Nu_t = 0.116\left[R_{et}^{2/3} - 125\right] P_{rt}^{1/3}\left(\mu_t/\mu_w\right)^{0.14}\left(1 + \frac{D_i}{L_1}^{2/3}\right) \qquad (4.32)$$

For $R_{et} \leq 2100$,

$$Nu_t = 1.86\left(R_{et} P_{rt} \frac{D_i}{L_1}\right)^{1/3}\left(\mu_t/\mu_w\right)^{0.14} \qquad (4.33)$$

Where

Nu_t = Nusselt Number ≡ $h_i D_i / k_t$

R_{et} = Reynolds Number ≡ $D_i V_t \rho_t / \mu_t$

$$V_t = \frac{4\dot{m}_t(^{n_p}/_{n_t})}{\rho_t \pi {D_i}^2}$$

$\dot{m}_t$= total mass flow rate of tube-side fluid

n_p = number of tube-side passes

N_t= number of tubes

P_{rt}≡ Prandtl Number ≡ $C_{pt}\mu_t/k_t$

D_i = inside pipe diameter

V_t = average fluid velocity

$(^{\mu}/_{\mu_w})^{0.14}$ = viscosity correction factor (dimensionless)

But the value of $(^{\mu}/_{\mu_w})^{0.14}$ is approaches to 1 due to this mostly it is neglected.

C_{pt}, μ_t, ρ_t, k_t = fluid properties evaluated at the average bulk fluid temperature

4.7 Pressure Drop

Fluid must usually be pumped through the heat exchanger, and the pumping power can contribute a significant fraction of the total lifecycle costs of a heat exchanger. The pumping power P [W] is directly proportional to the pressure drop Δp [Pa] through the heat exchanger. Pressure drop increases as fluid flow velocity through the heat exchanger is increased, as does the convection heat transfer coefficient; a good design is therefore always a compromise of sufficiently heat transfer characteristics with acceptable pressure drop.

The causes of pressure drop can be roughly divided into two by their location: the pressure drop in the core of the heat exchanger (the part of heat exchanger where flow is in contact with the heat transfer surface), and pressure drops caused by the devices needed to distribute the flow into the core, and collect it when it exits from it: the inlet and outlet headers, manifolds, etc. Ideally the pressure drop in parts other than the core should be very small compared to the core pressure drop [27, 31].

a) Pressure Drop on Shell Side

The pressure drop for flow across a bank of tubes is given by the following equation:

$$\Delta P_{fs} = \frac{2 f_s N_r G^2{}_s}{\rho_s} \tag{4.34}$$

Where:

f_s = Fanning friction factor

N_r = number of tube rows

$G_s = V_{max}\rho$

$R_{esp} = D_h V_{max} \rho_s / \mu_s$

$D_h = \dfrac{4 A_o L_2}{A}$

L_2=the core length for flow normal to the tube bank

A_o= minimum free-flow area

For an inline tube arrangement:

$$A_o = [(X_t - D_r)L_1 - (D_f - D_r)\tau N_f L_1]\frac{L_3}{X_t} \tag{4.35}$$

For the staggered tube arrangement:

$$A_o = \left[\left(\frac{L_3}{X_t} - 1\right)[(X_t - D_r) - (D_f - D_r)\tau N_f] + (X_t - D_r) - (D_f - D_r)\tau N_f\right] L_1 \tag{4.36}$$

A=total heat transfer area both for fine and prime surface.

$A = A_b + A_f$

$$A_b = \pi D_r (L_1 N_T - N_f L_1 N_T \tau) \tag{4.37}$$

$$A_f = \left[2\pi\left(\frac{{D_f}^2 - {D_r}^2}{4}\right) + \pi D_f \tau\right] N_f L_1 N_t \tag{4.38}$$

For an inline tube arrangement:

$$N_t = \frac{L_2 L_3}{X_t X_l}$$

For the staggered tube arrangement:

$$N_t = \frac{L_3}{X_t}\frac{L_2/X_l + 1}{2} + \left(\frac{L_3}{X_t} - 1\right)\frac{L_2/X_l - 1}{2} \tag{4.39}$$

$$f_s = \left\{1 + \frac{2e^{-\left(a/4\right)}}{1 + a}\right\}\left\{0.012 + \frac{27.2}{R_{e_{eff}}} + \frac{0.29}{R_{es}{}^{0.2}{}_{eff}}\right\} \tag{4.40}$$

Where

$$a = {}^{(P_T - D_f)}/_{D_r}$$

$$R_{e_{eff}} = R_e\left({}^{l}/_{b}\right)$$

$$D_f = D_r + 2b = \text{fin OD}$$

In addition to the tube bank, there are other sources of friction loss on the gas side.

Although the friction loss due to each of those factors is usually small compared with the pressure loss in the tube bank, in aggregate the losses often amount to between 10% and 25% of the bundle pressure drop [27, 31].

b) Pressure Drop on Tube Side

The pressure drop due to fluid friction in the tubes with the length of the flow path set to the tube length times the number of tube passes. Thus,

$$\Delta P_{ft} = \frac{f_t N_t L_1 G^2{}_t}{2000 D_i s \Phi} \tag{4.41}$$

Where:

ΔP_{ft}= pressure drop (Pa)

f_t = Darcy friction factor (dimensionless)

L_1 = tube length (m)

G_t = mass flux (kg /s · m^2)

s = $\frac{\rho_t}{\rho_w}$ fluid specific gravity (dimensionless)

Φ = viscosity correction factor (dimensionless)

= $({}^{\mu_s}/_{\mu_w})^{0.14}$ for turbulent flow

= $({}^{\mu_s}/_{\mu_w})^{0.25}$ for laminar flow

But the value of Φ is approaches to 1 due to this mostly it is neglected.

The minor losses on the tube side are estimated using the following equation:

$$\Delta P_{rt} = 5 \times 10^{-4}\left(2n_p - 1.5\right) {}^{G^2 t}/_{s} \tag{4.42}$$

For turbulent flow in commercial heat-exchanger tubes, the following equation can be used for $R_{et} \geq 3000$:

$$f_t = 0.4137 R_{et}{}^{-0.2585} \tag{4.43}$$

For $R_{et} \leq 3000$, laminar flow the friction factor is given by:

$$f_t = \frac{64}{R_{et}} \tag{4.44}$$

4.8 Tube Layout

The main components of a shell-and-tube heat exchanger are the tube bundle. Tube bundle typically consists of tubes installed in either square or triangular pattern, both of which can be installed in two possible angles relative to the incoming fluid flow, as shown in Fig. 4.3. The 90-degree square arrangement is the only in-line arrangement, while 30-, 45- and 60-degree arrangements are all staggered.

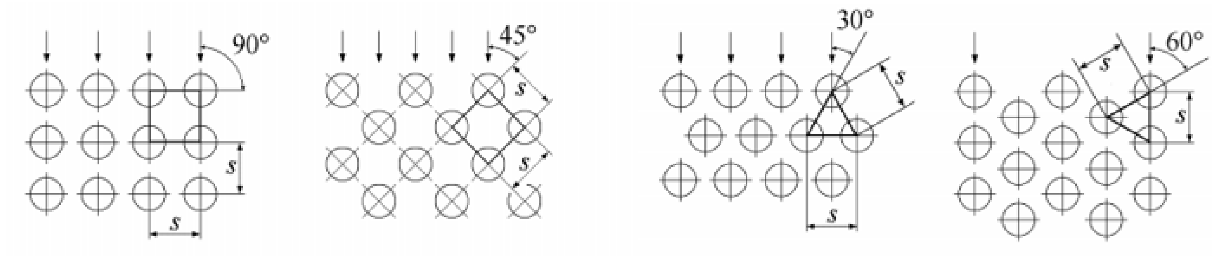

Figure 4. 3 Tube arrangements: 90- and 45-degree square and 30- and 60-degree triangular [34].

30^0 configuration is used in the single-phase heat exchangers (economizer, super heater and de-superheater) and the 60^0 configuration in the two-phase heat exchangers (evaporator and condenser), which will be called the 30- & 60^0-tube configuration. The results below show that the 30- & 60^0-tube configuration performs the best. 30^0- & 60^0-tube configuration can combine high heat-transfer coefficients with relatively low pressure drop in single-phase configurations and two-phase flow, respectively [34].

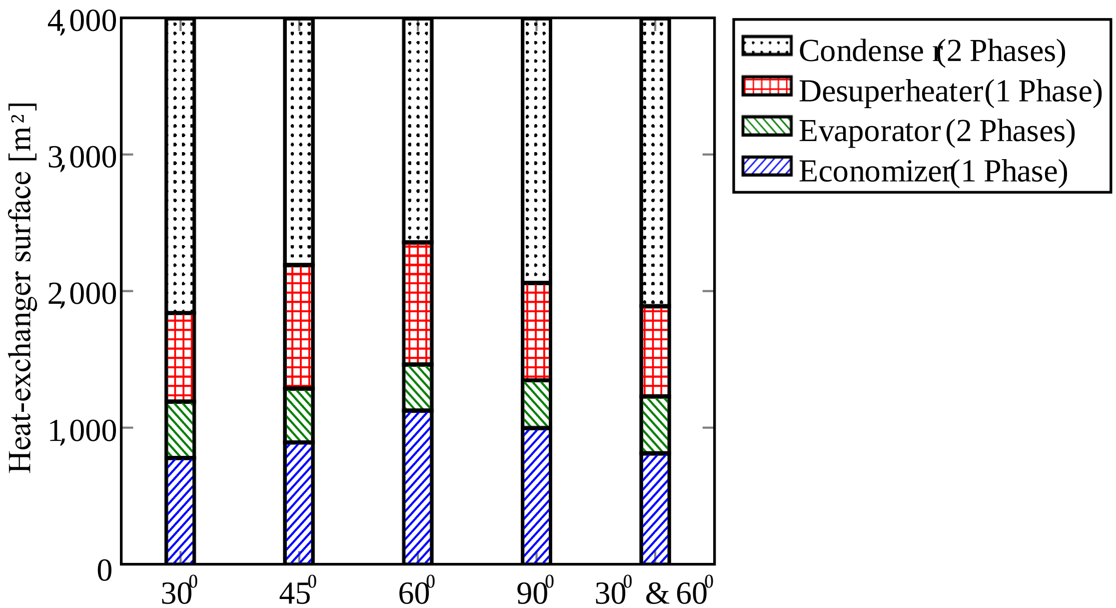

Figure 4. 4 Distribution of the heat-exchanger surface for different tube configurations [34].

Figure 4.4 shows the distribution of the heat-exchanger surface amongst the different heat exchangers for the five investigated tube-configurations. The 30^0-configuration uses a relatively large part of the available surface in the two-phase heat exchangers, while the 60^0- configuration on the other hand uses a relatively large part of the surface in the single-phase heat exchangers. The 30^0& 60^0-tube configuration results in about the same distribution as in the 30^0-case [34].

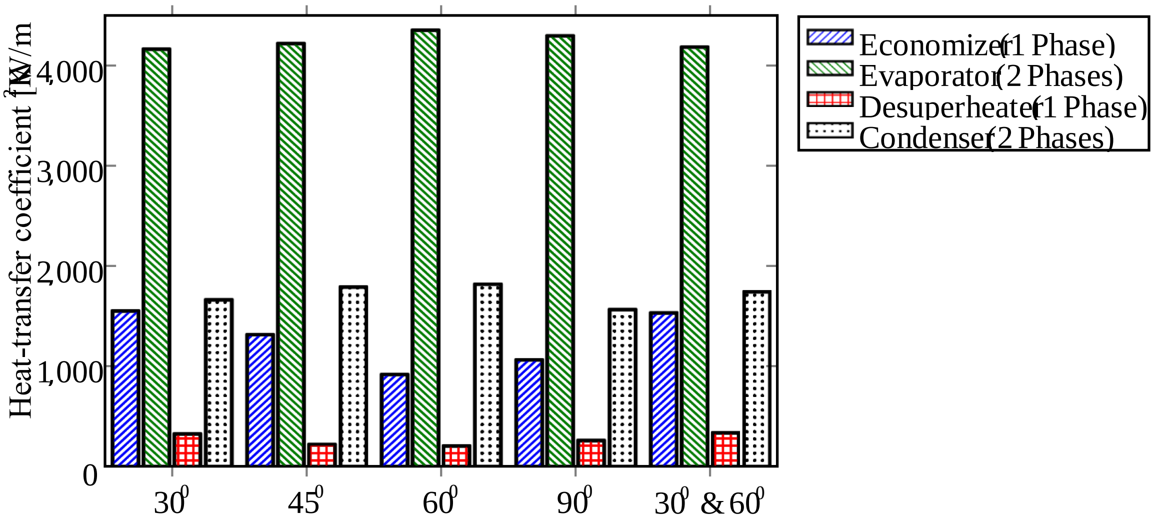

Figure 4. 5 Average heat-transfer coefficient for different tube configurations [34].

The same is seen in figure 4.5. The 30^0-tube configuration and the 60^0-tube configuration have the highest average heat-transfer coefficient in the single-phase heat exchangers and the two-phase heat exchangers, respectively. Combining these two (mono-layout) tube configurations for different heat exchangers results in relatively high heat transfer coefficients in all heat exchangers.

For stand-alone shell-and-tube heat exchangers, it is common practice to select the 30^0-tube configuration for the single-phase heat exchangers and to select the 60^0-tube configuration for phase-change flow [34].

- For the identical tube pitch and flow rates, the tube layouts in decreasing order of shell-side heat transfer coefficient and pressure drop are: 30°, 45°, 60°, and 90°.
- The square pitch (90° or 45°) is used when jet or mechanical cleaning is necessary on the shell side, 90-degree arrangement results in highly inefficient heat transfer, however.
- 60-degree triangular has the same tube density as 30-degree triangular, but relatively higher pressure drop with a flow velocity to produce a given heat transfer coefficient, and is therefore unlikely to be the best choice [30, 34].

4.9 Design Optimization of Shell and Tube Heat Exchanger

Optimization is the act of achieving the best possible result under given circumstances. Optimization techniques are essential in our daily lives, in engineering and in industry. These techniques are applied in almost all fields of applications. Designers can optimize to minimize cost and energy consumption, or to maximize profit and efficiency. Optimization is imperative in the real world because of limitations in resources, time and money. In reality, optimization problems are more complex; the parameters as well as the constraints influence the problems' characteristics. Furthermore, optimal solutions are not always possible. It can only attain suboptimal or even just feasible solutions that are satisfying practically achievable in a reasonable scale. In design, construction, maintenance on which engineers have to take decisions. The goal of all such decisions is either to minimize cost or to maximize benefit. The effort or the benefit can be usually expressed as a function of certain design variables. Hence, optimization is the process of finding the conditions that give the maximum or the minimum value of a function. The main components of an optimizations are [35, 36]:

Objective Function

An objective function expresses one or more quantities which are to be minimized or maximized. The optimization problems may have a single objective function or more objective functions. Usually the different objectives are not compatible. The variables that optimize one objective may be far from optimal for the others.

Variables

A set of unknowns, which are essential are called variables or all the quantities that can be treated as variables are called design or decision variables. The variables are used to define the objective function and constraints.

Constraints

A set of constraints are those which allow the unknowns to take on certain values. They are conditions that must be satisfied to render the design to be feasible [35].

a) Classification of Optimization Problems

Optimization problems can be classified based on the type of constraints, nature of design variables, nature of the equations involved and number of objective functions. Of which Based on the number of objective functions: objective functions can be classified as single-objective and multi-objective problems.

Single-objective problem: Problem in which there is only a single objective function.

Multi-objective problem: Multi-objective optimization can be formulated as a decision making problem of simultaneous optimization of two or more design objectives that are conflicting in nature [35].

b) Solutions of Optimization Problems

The choice of suitable optimization method depends on the type of optimization problem.

Direct method: for multi-dimensional problem random search or univariate search types of direct method can be used. As the name implies, the random search method repeatedly evaluates the function at randomly selected values of independent variables. If a sufficient number of samples are used, the optimum will eventually be located. In univariate search method, change is made in one variable at a time to improve the approximation while the other variables are held constant. The univariate search method is more efficient than random search method.

Algorithm method: Algorithm method is developed to arrive at near-optimum solutions to a large scale optimization problem. The problem having very large number of decision variables and non-linear objective functions are often solved by algorithms.

Many classification algorithms already exist, such as Ant Colony Optimization (ACO) has been introduced during the past 10 years.

Ant Colony Optimization, ants are able to find the shortest path between a food source and the nest without the aid of visual information. It was found that the way ants communicate with each other is based on pheromone trails. While ants move, they drop a certain amount of pheromone on the floor, leaving behind a trail of this substance that can be followed by other ants. The more ants follow a pheromone trail, the more attractive the trail becomes to be followed in the near future [35, 37, and 36].

In this paper, ant colony optimization (ACO) algorithms using MATLAB17a will be used with the principal of shorter road and getting food in ant food searching activities analogous to minimum cost and maximum heat transfer rate in a case of STHE respectively.

c) Pareto Curve

The basic underlying rule behind the Pareto principle is that in almost every case, 80 % of the total problems incurred are caused by 20 % of the problem causes. Therefore, by concentrating on the major problems first, majority problems can be eliminated or solved.

Mostly there is no unique optimal solution but rather a set of efficient solutions, also known as Pareto solutions or Pareto fronts. The set of all these Pareto solutions or the Pareto front, represents the problem trade-offs, and being able to sample this set in a representative manner is a very useful aid in decision making and Pareto curve constructed from Pareto solutions of Multi objective optimization [39].

4.10 Design Study of Existing Shell and Tube Heat Exchanger

The heat transfer analysis of an exchanger can be performed by using the ε-NTU method. Sizing the shell and tube heat exchanger is done by changing the decision variable values and the effects on the device will be analyzed. But before new sizing will start, it is better to determine the existing STHE parameter values for tube layout shown below in figure 4.6.

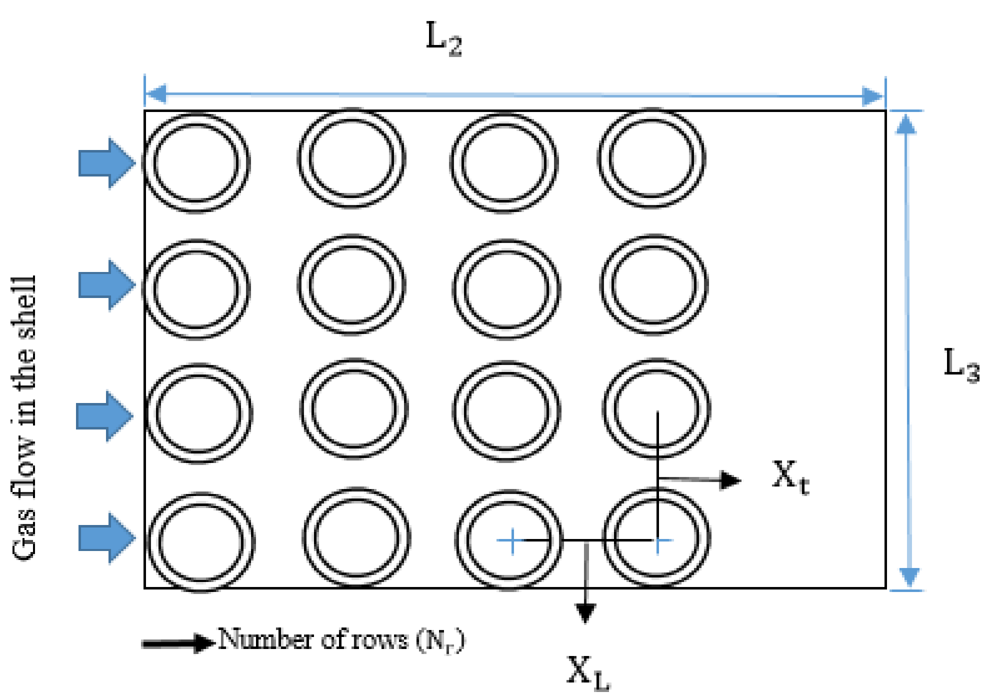

Figure 4. 6 Tube layout of existing STHE (rectangular)

Where X_t=pitch in the transverse tube row, X_L= pitch in the longitudinal tube row, L_3=the no flow dimension length and L_2=the core length for flow normal to the tube bank.

Table 4. 1 Existing (original) heat exchanger impute parameter values

Parameter name	Shell side (SO_3)	Tube side (Water) at average temperature $^{(80+130)}/_{2} = 105℃$
Root diameter D_r(m)	-	0.075
Inside diameter D_i(m)	-	0.04
Fin spacing ℓ(m)	-	0.023
Fin height b(m)	-	0.02
Fin thickness τ(m)	-	0.007
Number of fins per leng. N_f	-	74
Number of tube passes n_p	-	2
Number of tubes N_t	-	64
Thermal conductivity $k(W/m.K)$	? (unknown value)	0.682
Density $\rho(kg/m^3)$	?	954.575
Viscosity $\mu(kg/(m.s))$	?	2.67×10^{-4}
Prandtl number (P_r)	?	1.67
Pitch diameter P_T(m)	-	0.13
Fin diameter D_f(m)	-	0.115
Tube length L_1(m)	-	2.2
Pipe thickness	-	0.012
Mass flowrate $\dot{m}(^{kg}/_{s})$	20	?
T(°C) inlet and outlet respectively	**?**, 180	80, 130

From the above parameters the heat transfer rate and inlet temperature of SO_3flue gas (in the shell) as well as mas flow rate of water in the tube can be calculated by using ε-NTU method as follow.

Let's take inlet temperature of SO_3 flue gas (in the shell) is 230 ℃ and iterate to get the right temperature of SO_3 flue gas.

By using average temperature of SO_3 flue gas properties can be find.

$$\frac{180\ ℃ + 230\ ℃}{2} = 205\ ℃$$

Table 4. 2 SO_3 flue gas properties values [31]

At 205℃	
$\rho_s (\mathrm{kg/m^3})$	0.7388
$C_{ps} (\mathrm{J/kg.K})$	1027
$k_s (\mathrm{W/m.K})$	0.03826
$\mu_s (\mathrm{kg/(m.s)})$	2.628×10^{-5}
P_{rs}	0.705

Then convective transfer coefficient on the tube side(h_i) can be calculated as follow.

Average fluid velocity in the tube.

$$V_t = \frac{4\dot{m}_t \left({}^{n_p}/_{N_t}\right)}{\rho_t \pi {D_i}^2} = 0.026\dot{m}_t\ \mathrm{m/s} \tag{4.45}$$

Reynolds Number in tube

$$R_{et} = D_i V_t \rho_t / \mu_t = 3{,}725.537\dot{m}_t \tag{4.46}$$

From energy balance

$$\dot{Q} = \dot{m}_t C_{pt}(T_{t,o} - T_{t,i}) = \dot{m}_s C_{ps}(T_{s,i} - T_{s,o})$$

$$= \dot{m}_t \times 4216.25(130 - 80) = 1.027 \times 10^6\ \mathrm{W}$$

$$\dot{m}_t = 4.872\ \mathrm{kg/s}$$

With Reynolds Number, $R_{et} = 18151.82$

Nusselt number of water in tube when $R_{et} \geq 10^4$

$$N_{ut} = 0.023 R_{et}^{0.8} P_{rt}^{1/3} = 19.63{\dot{m}_t}^{0.8} \tag{4.47}$$

$$= 69.677$$

Water heat transfer coefficient from eq. (3.31)

$$h_i = N_{ut}\, k_t / D_i = 334.67 \dot{m}_t^{\,0.8} \tag{4.48}$$

$$= 1187.907\ \mathrm{W/m^2.K}$$

Convective heat transfer coefficient on the shell side(h_o) will be calculated:

Area of face is $A_{face} = L_1 L_3 = 0.53 \times 2.2 = 1.166\ m^2$

Face velocity the average air velocity approaching the first row of tubes

$$V_{face} = \frac{\dot{m}_s}{\rho_s A_{face}} = 23.217\ \mathrm{m/s}$$

From eq. (4.29) maximum gas velocity in tube bank is:

$$V_{max} = \frac{L_1 L_3 V_{face}}{[(X_t - D_r)L_1 - (D_f - D_r)\tau N_f L_1]\frac{L_3}{X_t}} = 66.35\ \mathrm{m/s}$$

Reynolds number of flue gas in the shell is from eq. (4.27)

$$R_{es} = D_r V_{max} \rho_s / \mu_s = 1.399 \times 10^5$$

For turbulent flow Nusselt number can be calculated as

$$Nu_s = 0.134 R_{es}^{0.681} P_{rs}^{1/3} (l/b)^{0.2} (l/\tau)^{0.1134} = 448.25$$

Then heat transfer coefficient in shell side is evaluated from (4.27)

$$h_o = Nu_s k_s / D_r$$

$$= 228.667\ \mathrm{W/m^2.k}$$

Base area of the tube from eq. (4.20)

$$A_b = \pi D_r (L_1 N_t - N_f L_1 N_t \tau) = 25.28\ m^2$$

Eq. (4.19) Fin area is calculated as:

$$A_f = \left[2\pi\left(\frac{D_f^{\,2} - D_r^{\,2}}{4}\right) + \pi D_f \tau\right] N_f L_1 N_t = 69.26\ m^2$$

Total area for heat transfer is in eq. (4.21)

$$A = A_f + A_b = 94.54\ m^2$$

Total inner tube area can be evaluated from eq. (4.22)

$$A_i = \pi D_i N_t L_1 = 17.7\ m^2$$

Performance of single fin as well as efficiency of array of fin can be calculated by using thermal conductivity of fin (St41k) is $k = 51.7\,W/m.k$ as follow

$$m = \left(\frac{2h_o}{k\tau}\right)^{0.5} = 35.55$$

$$\psi = \left(\frac{D_f + \tau - D_r}{2}\right)\left(1 + 0.35\ln\left(\frac{D_f + \tau}{D_r}\right)\right) = 0.0275$$

$$\eta_f = \frac{\tanh(m\psi)}{m\psi} = 76.926\ \%$$

$$\eta_w = \frac{A_b + A_f\eta_f}{A} = 83.096\ \%$$

Wall resistance of composite circular tube can be calculated by using materials thermal conductivity (pipe steel k18, $k = 48.75\ W/m.k$), (St41k, $k = 51.7\ W/m.k$) at diameter of 51 and 75 mm respectively. From eq. (4.13)

$$R_w = \frac{1}{2\pi L_1 N_t}\left(\sum_j \frac{\ln(D_{j+1}/D_j)}{k_{w,j}}\right) = 1.406 \times 10^{-5}\ K/W$$

And a typical values of fouling resistance per surface area for inside and outside of the tube in $[m^2K / W]$ will find out bellow.

$\dot{R}_{Do} = 4.403 \times 10^{-4}\ m^2K / W$

And

$\dot{R}_{Di} = 1.7611 \times 10^{-4}\ m^2K / W$

Overall heat transfer coefficient from eq. (4.12) is

$$U = \left(\frac{A}{A_i h_i} + \frac{\dot{R}_{Di}A}{A_i} + \frac{\dot{R}_{Do}}{\eta_w} + \frac{1}{h_o\eta_w} + AR_w\right)^{-1} = 79.625\ W/m^2.K$$

From which number of transfer unit is

$$NTU = \frac{AU}{C_{min}} = 0.3665$$

From eq. (4.4) heat capacity rate ratio

$$C^* = \frac{C_{min}}{C_{max}} = 0.99$$

Then modified temperature is find out from eq. (4.6)

$$\varepsilon = 2\left\{1 + C^* + (1 + C^{*2})^{1/2} \times \frac{1 + \exp[-(NTU)(1 + C^{*2})^{1/2}]}{1 - \exp[-(NTU)(1 + C^{*2})^{1/2}]}\right\}^{-1} = 0.264$$

$$= \frac{1}{C^*}\left(\frac{T_{h,in} - 180}{T_{h,in} - 80}\right)$$

$$T_{h,in} = 215.87\ ℃$$

This iteration step has to be continuous until the temperature converges to the some value. Then final Values found from all iterations are summarized in table 4.3. From which the final extracted heat transfer rate and mass flowrate of water are 5.133×10^5 W and $2.435\ kg/s$ respectively.

Table 4. 3 Existing shell and tube heat exchanger calculated results

Name of parameters	**Iterations with respect to its average temperatures (℃)**						
	1 (205)	**2 (197.935)**	**3 (195.15)**	**4 (194.105)**	**5 (193.3)**	**6 (192.85)**	**7 (192.52)**
$\rho_s (kg/m^3)$	0.7388	0.7489	0.75388	0.7556	0.757	0.757	0.757
$C_{ps} (J/kg\ K)$	1027	1025.676	1025.23	1025	1024.9	1024.9	1024.9
$k_s (W/m.k)$	0.0382	0.0378	0.03764	0.03757	0.03752	0.0375	0.03747
$\mu_s (kg/m.s)$	2.628×10^{-5}	2.6×10^{-5}	2.589×10^{-5}	2.585×10^{-5}	2.582×10^{-5}	2.58×10^{-5}	2.5787×10^{-5}
P_{rs}	0.705	0.705	0.705	0.705	0.705	0.705	0.705
$h_i (W/m^2.k)$	1187.9	909.74	794.575	750.3	718.8	696.6	682.05
$V_{face} (m/s)$	23.217	22.904	22.75	22.7	22.66	22.66	22.66
$V_{max} (m/s)$	66.35	65.455	65.023	64.875	64.76	64.76	64.76
R_{es}	1.399×10^5	1.414×10^5	1.42×10^5	1.4223×10^5	1.424×10^5	$1.424\ 2 \times 10^5$	1.4248×10^5
N_{Us}	448.25	451.533	452.8388	453.3156	453.713	453.713	453.713
$h_o (W/m^2.k)$	228.67	227.57	227.265	227.1	227	227	227
$\eta_f (\%)$	76.926	77	77.03	77.0425	77.048	77.048	77.048
$\eta_w (\%)$	83.096	83.155	83.171	83.181	83.1856	83.1856	83.1856

$T_{h,in}$(°C)	230	215.87	210.3	208.21	206.6	205.7	205.04
U($W/m^2.k$)	79.625	71.66	67.514	65.74	64.41	63.5	62.8

From the above calculated parameter values, the existing shell and tube heat exchanger pressure drop both in the tube and shell side can be calculated.

Pressure drop on the shell side:

The fin spacing is related to the number, N_f, of fins per unit length by the following equation:

$$N_f = \frac{1}{\ell + \tau} = 34$$

$$a = \frac{P_T - D_f}{D_r} = 0.2$$

For an inline tube arrangement:

$$A_o = \left[(X_t - D_r)L_1 - \left(D_f - D_r\right)\tau N_f L_1\right]\frac{L_3}{X_t} = 0.3075\ m^2$$

Hydraulic diameter of shell to calculate pressure

$$D_h = \frac{4A_o L_2}{A} = 0.02914\ m$$

Reynolds number:

$$R_{es} = D_h V_{max} \rho_s / \mu_s = 5.544 \times 10^4$$
$$R_{e_{eff}} = R_{es}\left(\frac{\ell}{b}\right) = 6.375 \times 10^4$$

Mass flux of flue gas SO_3 is,

$$G_s = \rho_s V_{max} = 49.075\ \ kg/s.m^2$$

The friction factor for tube banks,

$$f_s = \left\{1 + \frac{2e^{-(a/4)}}{1+a}\right\}\left\{0.012 + \frac{27.2}{R_{e_{eff}}} + \frac{0.29}{{R_e}^{0.2}{}_{eff}}\right\} = 0.1142$$

Number of tube rows N_r = 16

The pressure drop for flow across a bank of finned tubes is given by the following equation:

$$\Delta P_{fs} = \frac{2 f_s N_r G^2{}_s}{\rho_s} = 11.1\ kPa$$

This Pressure loss is only on the tube banks.

In addition to the tube bank, there are other sources of friction loss on the gas side, in aggregate the losses often amount between 10 % and 25 % of the bundle pressure drop [31]. From which a pressure loss 10% can be taken because of one shell and added to tube bunk pressure drop to get overall pressure drop on the shell side due to flue gas SO_3 flow.

$$\Delta P_{fsT} = 10\ \%\ \Delta P_{fs} + \Delta P_{fs}$$
$$\underline{\underline{= 12.209\ kPa}}$$

Pressure drop on tube side:

The pressure drop due to fluid friction in the tubes can be calculated as follow,

Mass flux:

$$G_t = \frac{\dot{m}_t (n_p/N_t)}{\pi\, D_i{}^2/4} = 60.55\ kg/s.m^2$$

$$R_{e_t} = \frac{4\dot{m}_t (n_p/N_t)}{\pi D_i \mu_t} = 9.388 \times 10^4$$

Specific gravity of water at an average temperature (105℃) is,

$$s = \frac{\rho_t}{\rho_w} = 0.9547$$

Friction factor,

For turbulent flow in tubes, the following equation can be used for Re ≥ 3000 [31]:

$$f_t = 0.4137 R_e{}^{-0.2585} = 0.02144$$

The pressure drop due to fluid friction in the tubes with the length of the flow path Thus,

$$\Delta P_{f_t} = \frac{f_t N_T L_1 G^2{}_t}{2000 D_i s} = 144.938\ Pa$$

But this is not the only pressure drop on a tube side rather there is other loss on fittings and also on inlet outlet pipes.

The losses on bending's are estimated using the following equation:

$$\Delta P_r = 5 \times 10^{-4}\left(2n_p - 1.5\right) {G^2{}_s}/{s}$$
$$= 4.8\ Pa$$

Here pressure drop on the inlet and outlet of the pipe is omitted because number of passes is small and the effect is insignificant.

Therefore the total pressure drop on the pipe side is calculated by adding the two drops, which is,

$$\Delta P_{tT} = \Delta P_r + \Delta P_{f_t}$$
$$= 149.74\ Pa$$

4.11 Design Analysis of Modified Shell and Tube Heat Exchanger

4.11.1 Cost Estimation

Cost is always an important consideration in designing any process equipment. In heat exchanger cost can be broken into two principal components – capital or investment cost and operating cost.

The capital cost for heat exchangers increases with increase in the heat transfer area whereas operating cost is primarily pumping cost. The pumps must provide work to overcome the pressure drop on the tube side and that on the shell side.

The operating cost C_{op} and the initial investment C_{in} for the shell and the tube can be approximated as follows.

$$C_T = C_{in} + C_{op} \tag{4.49}$$

$$C_{in} = F_p F_m F_l C_B \tag{4.50}$$

Where, F_p, F_m, C_B, F_l are pressure factor, material factor, tube length factor and types of heat exchanger respectively.

For carbon steel shell and steel tube materials

$$F_m = a + (\frac{A}{100})^b\text{, a=1.55, b=0.05}$$

Pressure factor F_p=0.9876, $F_l = 1.25$ for length 2.44 m.

$C_B = exp(11.667 - 0.809[ln(A/0.093)] + 0.009005[ln(A/0.093)]^2)$, A is in m^2

$$C_{op} = \sum_{k=1}^{n_y} \frac{C_o}{(1+i)^k} \tag{4.51}$$

Where C_o is the annual cost, n_y lifetime, and i is the annual inflation rate.

The total operating cost is dependent on the pumping power to overcome the pressure drop from both shell and tube side flow [40].

$$C_o = P \times kel \times H \tag{4.52}$$

$$P = \frac{1}{\eta}\left(\frac{\dot{m}_s \Delta P_{sfT}}{\rho_s} + \frac{\dot{m}_t \Delta P_{tT}}{\rho_t}\right) \tag{4.53}$$

Where kel the unit price of electrical energy, P is pumping power; H is the hours of operation per year and η is the pumping efficiency.

4.11.2 Selection of Decision Variables

Existing shell and tube heat exchanger has been studied above in detail. Standing from which the modified design STHE will be studied.

Impute data used in modified STHE is: Inlet and outlet temperature and mass flowrate of both fluids along with their physical properties, tube length, tube thickness, and length, width and height of the shell. Which is taken from the existing STHE because this heat exchanger is erected with in one frame with evaporator and erecting it alone and changing the shape is leading to another cost.

Here, the total cost and the heat transfer rate are the two objective functions. To fulfill the two needed objective functions optimization problem should be required.

Optimization problem is exactly that, a problem for which the one want to select the best possible, optimal, solution from a set of alternatives.

The main objective of this optimization is to find out the minimum value for the total cost and maximum heat transfer rate of the heat exchanger simultaneously.

The existing shell and tube heat exchanger study was rating problem that stands from design parameters and some operating conditions with those unknown values operating parameters were calculated. But modified design will be opposite of this that is sizing problem.

Objective functions subjected to constraint taken from existing STHE heat transfer rate and total cost:

$\dot{Q} \geq 5.133 \times 10^5$ W and CT $\leq 1.8294\times 10^6$ \$

In modification, shell size is not considered because it is inter locked with evaporator and leads to additional cost. So that modified STHE design decision variable parameters are reduced to:

- ✓ Tube diameter (D_i)
- ✓ Fin spacing (ℓ)
- ✓ Fin height (b)
- ✓ Fin thickness (τ)
- ✓ Tube layout (triangular and square)
- ✓ Number of tubes(N_t)
- ✓ Number of rows(N_r)
- ✓ Number of passes(n_p)
- ✓ Pitch length(P_T)
- ✓ Number of fin(N_f)

The variables listed above are both dependent and independent variables. The last five are dependent whereas the first five are independent variables. Since dependent variables can be expressed with independent values, it doesn't need to change the values of dependent variables rather it can be varies whenever changing independent variables.

Due to these decision variables are decreased to five variables: fin space, fin height, tube diameter, Tube layout and fin thickness.

4.11.3 Mathematical Model of Triangular Tube Layout Shell and Tube Heat Exchanger

Most of equations used in triangular tube layout design will be the same as the square tube layout STHE. But some equations are different and simplified due to value directly from existing design.

Figure 4.7 Shows that cross flows of gas in triangular tube layout of STHE.

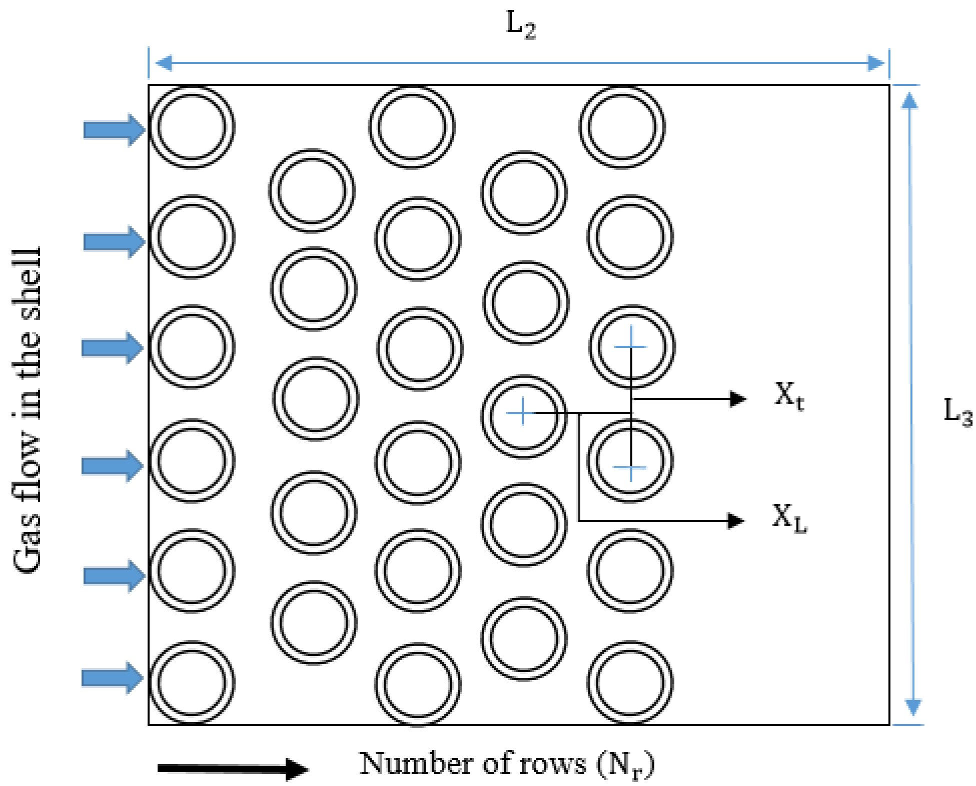

Figure 4. 7 Triangular tube layout of STHE

Where X_t=pitch in the transverse tube row, X_L= pitch in the longitudinal tube row, L_3=the no flow dimension length and L_2=the core length for flow normal to the tube bank.

For consistency Simplified equations is used for accurately determining the heat transfer coefficients and the shell side pressure drop for triangular tube layout is listed below.

Heat transfer coefficients

For shell side:

$$P_T = 1.15D_r$$

$$P_T = X_t$$

$$X_L = \frac{\sqrt{3}}{2}P_T$$

From eq. (4.28)

$$N_f = \frac{1}{\ell + \tau}$$

From eq. (4.40)

$$D_f = D_r + 2b$$

$$n_p = 19.5548 N_t {D_i}^2$$

For the staggered tube arrangement it is different from the inline arrangement of tube in original STHEX.

From eq. (4.30)

$$V_{max} = \frac{12.01}{\left[\left(\frac{0.53}{X_t} - 1\right)\left[(X_t - D_r) - \left(D_f - D_r\right)\tau N_f\right] + (X_t - D_r) - \left(D_f - D_r\right)\tau N_f\right]}$$

Reynolds number of flue gas in the shell is from eq. (4.27)

$R_{es} = 2.9355 \times 10^4 D_r V_{max}$

Nusselt number

$Nu_s = 0.12 R_{es}^{0.681} ({}^{l}/_{b})^{0.2} ({}^{l}/_{\tau})^{0.1134}$

$h_o = 0.03747 Nu_s / D_r$

Base area of the tube from eq. (4.20)

$$A_b = 6.9115 D_r N_t \left(1 - N_f \tau\right)$$

Fin area from eq. (4.19)

$$A_f = 6.9115\left[\left(\frac{{D_f}^2 - {D_r}^2}{2}\right) + D_f \tau\right] N_f N_t$$

Total heat transfer area from eq. (4.22)

$$A = A_b + A_f$$

For the staggered tube arrangement number of tubes eq. (4.39)

$$N_t = \frac{1}{2X_tX_L}(1.1872 + 0.53X_L + (0.53 - X_t)(2.24 - X_L))$$

Area on the tube side eq. (4.22)

$$A_i = 6.9115N_tD_i$$

$$\psi = 0.5\left(D_f + \tau - D_r\right)\left(1 + 0.35\, ln\left(\frac{D_f + \tau}{D_r}\right)\right)$$

$$m = \left(\frac{2h_o}{k\tau}\right)^{0.5}$$

$$\eta_f = \frac{tanh(m\psi)}{m\psi}$$

$$\eta_w = \frac{A_b + \eta_f A_f}{A}$$

For tube side

$$R_{et} = 1.202 \times 10^5 n_p/(N_tD_i)$$

For $R_{et} \geq 10^4$, from eq. (4.31)

$$Nu_t = 0.0273{R_{et}}^{0.8}$$

For $2100 < R_{et} < 10^4$, from eq. (4.32)

$$\mathrm{N_{ut}} = 0.1376\left[{R_{et}}^{2/3} - 125\right]\left(1 + \frac{D_i}{2.2}^{2/3}\right)$$

For $R_{et} \leq 2100$, from eq. (4.33)

$$\mathrm{N_{ut}} = 0.9122(\, R_{et}D_i)^{1/3}$$

$$h_i = 0.682Nu_t/D_i$$

Overall heat transfer coefficient eq. (4.12)

$$U = (\frac{A}{A_ih_i} + \frac{1.7611 \times 10^{-4}A}{A_i} + \frac{4.403 \times 10^{-4}}{\eta_w} + \frac{1}{h_o\eta_w} + AR_w)^{-1}$$

$$NTU = \frac{AU}{10266.57}$$

Heat exchanger performance from eq. (4.6)

$$\varepsilon = 2\left\{1 + C^* + (1 + C^{*2})^{1/2} \times \frac{1 + exp[-(NTU)(1 + C^{*2})^{1/2}]}{1 - exp[-(NTU)(1 + C^{*2})^{1/2}]}\right\}^{-1}$$

$$\dot{Q} = 1.32496 \times 10^6 \varepsilon$$

Pressure drop

For shell side

From eq. (4.40)

$$a = \frac{P_T - D_f}{D_r}$$

For the staggered tube arrangement from eq. (4.36)

$$A_o = 2.2\left[\left(\frac{0.53}{X_t} - 1\right)\left[(X_t - D_r) - \left(D_f - D_r\right)\tau N_f\right] + (X_t - D_r) - \left(D_f - D_r\right)\tau N_f\right]$$

$$D_h = \frac{8.96 A_o}{A}$$

From eq. (4.34)

$$R_{esp} = 29341.1 D_h V_{max}$$

$$R_{e_{eff}} = R_{esp}\left(\frac{\ell}{b}\right)$$

From eq. (4.40)

$$f_s = \left\{1 + \frac{2e^{-(a/4)}}{1 + a}\right\}\left\{0.012 + \frac{27.2}{R_{e_{eff}}} + \frac{0.29}{R_e{}^{0.2}{}_{eff}}\right\}$$

$$G_s = 0.757 V_{max}$$

$$N_r = \frac{2.24}{X_L}$$

From eq. (4.34)

$$\Delta P_{fs} = 2.642 f_s N_r G^2{}_s$$

$$\Delta P_{fsT} = 0.10\Delta P_{fs} + \Delta P_{fs}$$

For tube

From eq. (4.41)

$$G_t = 3.1831 \frac{n_p}{N_t {D_i}^2}$$

For $R_{et} \geq 3000$, from eq. (4.43)

$$f_t = 0.4137 {R_{et}}^{-0.2585}$$

For $R_{et} \leq 3000$,

$$\mathrm{f}_t = \frac{64}{\mathrm{R_{et}}}$$

From eq. (4.41)

$$\Delta P_{f_t} = 1.1522 \times 10^{-3} \frac{f_t N_t {G^2}_t}{D_i}$$

From eq. (4.42)

$$\Delta P_r = 5.2374 \times 10^{-4} (2n_p - 1.5) {G^2}_t$$

$$\Delta P_{tT} = \Delta P_r + \Delta P_{f_t}$$

From variables listed above, tube layout (square and triangular) effects with the same parameter values are listed in table 4.4.

Table 4. 4 Comparison between square and triangular tube layouts

Tube layout	N_T	n_p	A	h_i	h_o	U	ε	$\dot{Q}$	N_r	ΔP_{fst}	ΔP_{tT}
Square (Existing)	64	2	94.54	682.05	227	62.8	0.39	513300	16	12209	149.74
Triangular (modified)	70	2	102.08	4207.6	221.86	103.37	0.54	715519.6	20	13857.22	146.22

U, h_i and h_o are expressed in (W/m^2k) and $\dot{Q}$ (W), $\Delta P_{fst}(Pa)$, $\Delta P_{tT}(Pa)$ and $A(m^2)$

Here the table values were calculated from the same impute parameters that is fluids temperature, mass flow rate, tube length, tube diameter, tube thickness, number of fin, fin length, fin space, fin height and shell length, width and height. These results tells that number of tubes and rows increase due to compactness of the tube in triangular tube layout. Heat transfer area which is direct related to capital cost of STHE increases by 7.39 % whereas heat transfer coefficients in the tube and shell decreases because of decrease of Reynolds number. But overall heat transfer coefficient improved by 64.6 %. Heat transfer rate and performance of heat

exchanger are raised by 39.4 and 37.17 % respectively with 13.5 % shell pressure drop penalty and 2.35 % tube pressure drop benefit.
Finally, conclusion can be drawn that triangular tube layout can be a good choice for modified shell and tube heat exchanger design if its parameters are adjusted in optimized way.

4.11.4 Sensitivity Analysis

Sensitivity analysis can be performed in order to observe the variation influences of design parameters over optimization objectives. Virational effects of four decision variables on the problem objectives of heat transfer rates and total cost of heat exchanger is shown below in Figure 4.8 to 4.11. Best solutions will be selected by influences of decision variables over problem objectives. The remaining variables stays constant during evaluations. Decision variables and their range of variation are listed in Table 4.5.

Table 4. 5 Decision variables and their range

Decision variables	**Range(m)**
Tube diameter (D_i)	0.034, 0.036, 0.038, **0.04**, 0.042, 0.044, 0.046
Fin spacing (ℓ)	0.017, 0.019, 0.021, **0.023**, 0.025, 0.027, 0.029
Fin height (b)	0.014, 0.016, 0.018, **0.02**, 0.022, 0.024, 0.026
Fin thickness (τ)	0.013, 0.011, 0.009, **0.007**, 0.005, 0.003, 0.001

Values written in the bold are taken from the existing STHE. To test the influence of decision variables over problem objectives back and forth of this values can be used.

Table 4. 6 Diameter effects from appendix C

D_i	**A**	**A_i**	**U**	**$\dot{Q}$**	**ΔP_{fs}**	**ΔP_{Tt}**
0.034	121.2632	27.00622	117.4943	797522.7	12475.31	327.1139
0.036	119.3312	27.3046	118.2336	794643.1	12583.11	292.1725
0.038	117.4376	27.54709	118.9084	791592.2	12684.63	262.4165
0.04	115.5827	27.73984	119.5268	788393.4	12780.23	236.9093
0.042	113.7665	27.88829	120.0955	785066.4	12870.24	214.9142
0.044	111.989	27.99726	120.6203	781627.7	12954.95	195.8455
0.046	110.2499	28.07101	121.1059	778091.5	13034.63	179.2329

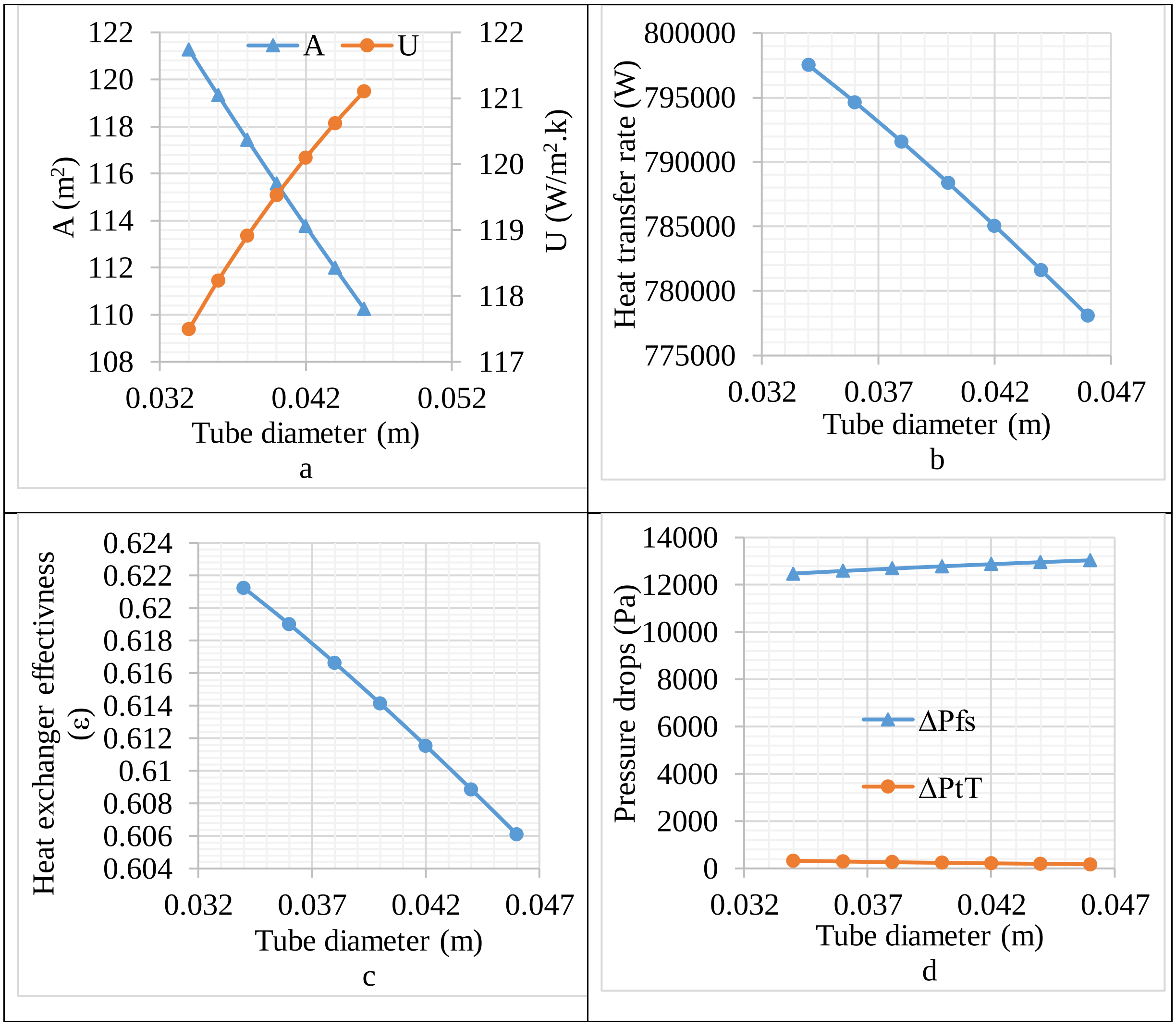

Figure 4. 8 Effects of diameter on objective functions

As shown the fig. a-d above when internal diameter of the tube increases from 0.034 to 0.046 mm: overall heat transfer coefficient increase and blockage of gas in the shell is increase which leads pressure drop on the shell side are increasing in a small amount. Total area and heat exchanger effectiveness (heat transfer rate) decrease in a small amount. Here only pressure drop on the tube side is decreasing rapidly due to decrease of friction in the tube. The effects on heat transfer rate and heat exchanger effectiveness have the same profile since $\dot{Q} = 1.283731757 \times 10^6 \varepsilon$.

Table 4. 7 Fin space effects from appendix D

ℓ	**A**	η_w	**U**	$\dot{Q}$	ΔP_{fsT}
0.017	134.7694	0.799476	109.5587	807860	15241.76
0.019	127.3899	0.801304	113.0594	800682.3	14245.88
0.021	121.0646	0.803198	116.3745	794221.6	13442.56
0.023	115.5827	0.805139	119.5268	788393.4	12780.23
0.025	110.786	0.807109	122.5349	783124.5	12224.24
0.027	106.5536	0.809098	125.414	778351.6	11750.41
0.029	102.7915	0.811095	128.1768	774019.9	11341.41

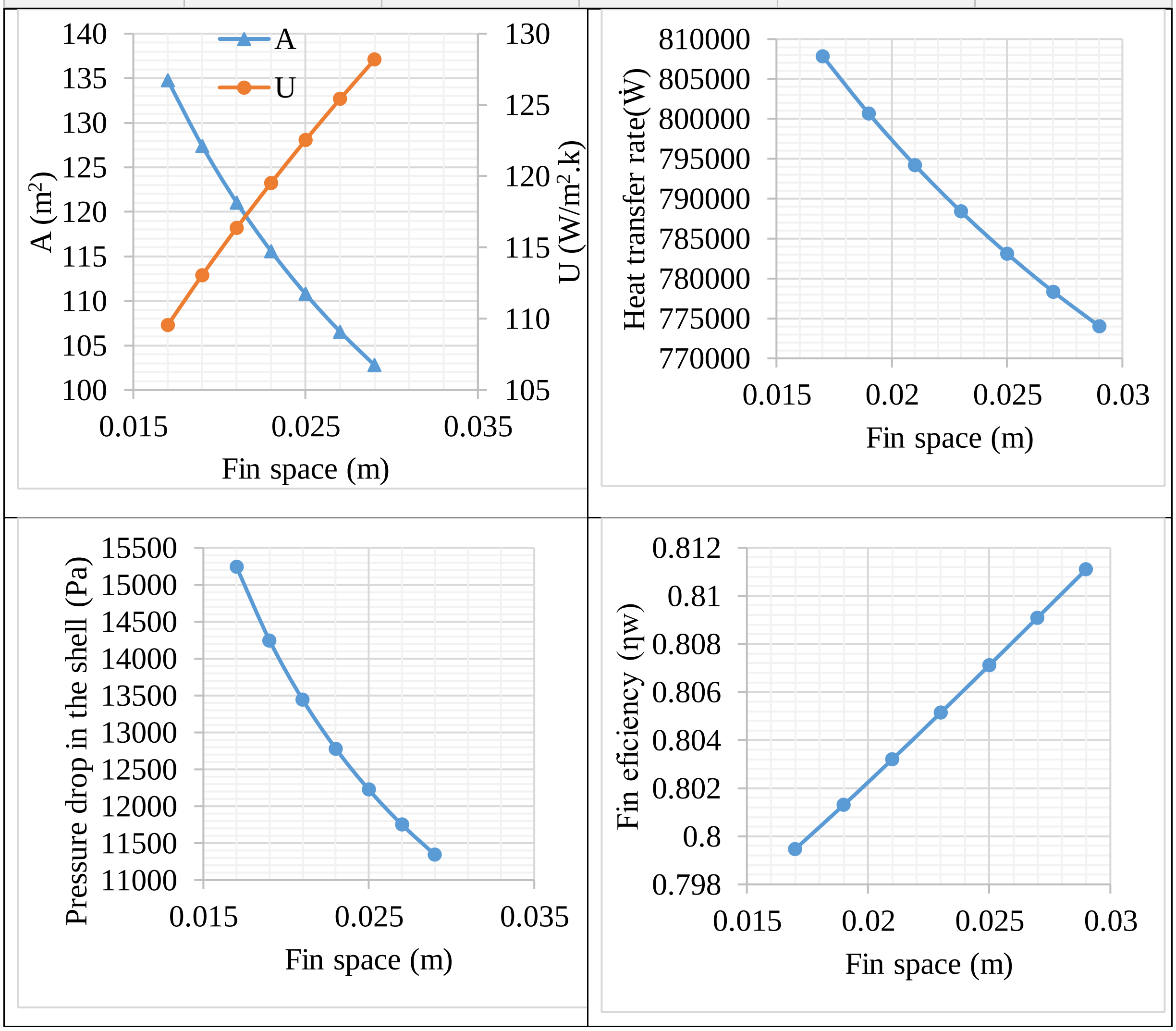

Figure 4. 9 Effects of fin space on objective functions

Figure 4.9 shows that whenever the fin space increase from 0.017 to 0.029 mm:

- ✓ Area of heat exchanger decrease due to fin area decrease.
- ✓ Overall fin efficiency $\eta_w = \frac{A_b + \eta_f A_f}{A}$ improved with a very small amount because of heat transfer area decrease but individual fin efficiency decrease.
- ✓ Overall Heat transfer coefficient increase due to overall fin efficiency increase.
- ✓ Shell side pressure drop decrease due to less turbulence in the shell.
- ✓ But heat transfer rate decrease moderately compared to values on diameter.

Table 4. 8 Fin height effects from appendix E

b	A	Ai	η_w	U	$\dot{Q}$	ΔP_{fsT}	ΔP_{Tt}
0.014	117.3681	36.71576	0.878688	153.069	859786.1	18925.84	314.5016
0.016	116.7938	33.30621	0.854756	140.2836	836498.8	16377.88	285.0278
0.018	116.1963	30.33845	0.830114	129.2201	812632.7	14380.95	259.3729
0.02	115.5827	27.73984	0.805078	119.5268	788393.4	12780.23	236.9093
0.022	114.9584	25.45205	0.779921	110.9512	763965.3	11472.63	217.1325
0.024	114.3277	23.4278	0.754875	103.3058	739513.4	10387.18	199.6339
0.026	113.6935	21.62844	0.730134	96.44731	715184.1	9473.61	184.0793

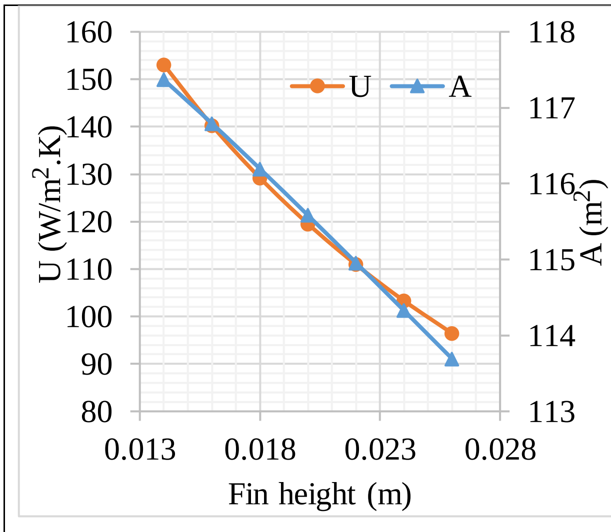

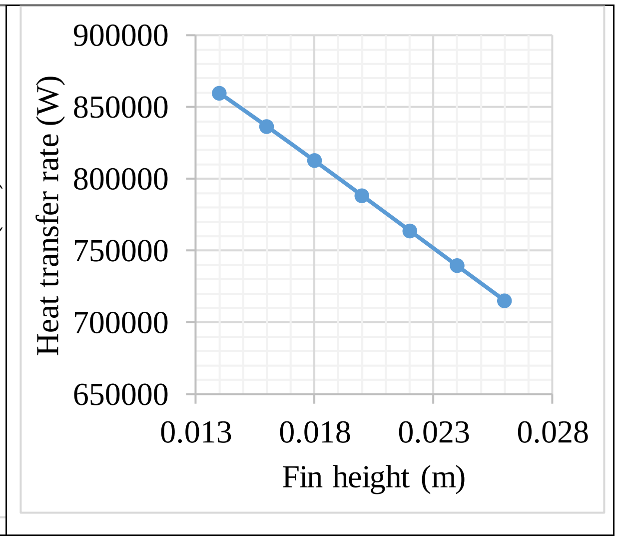

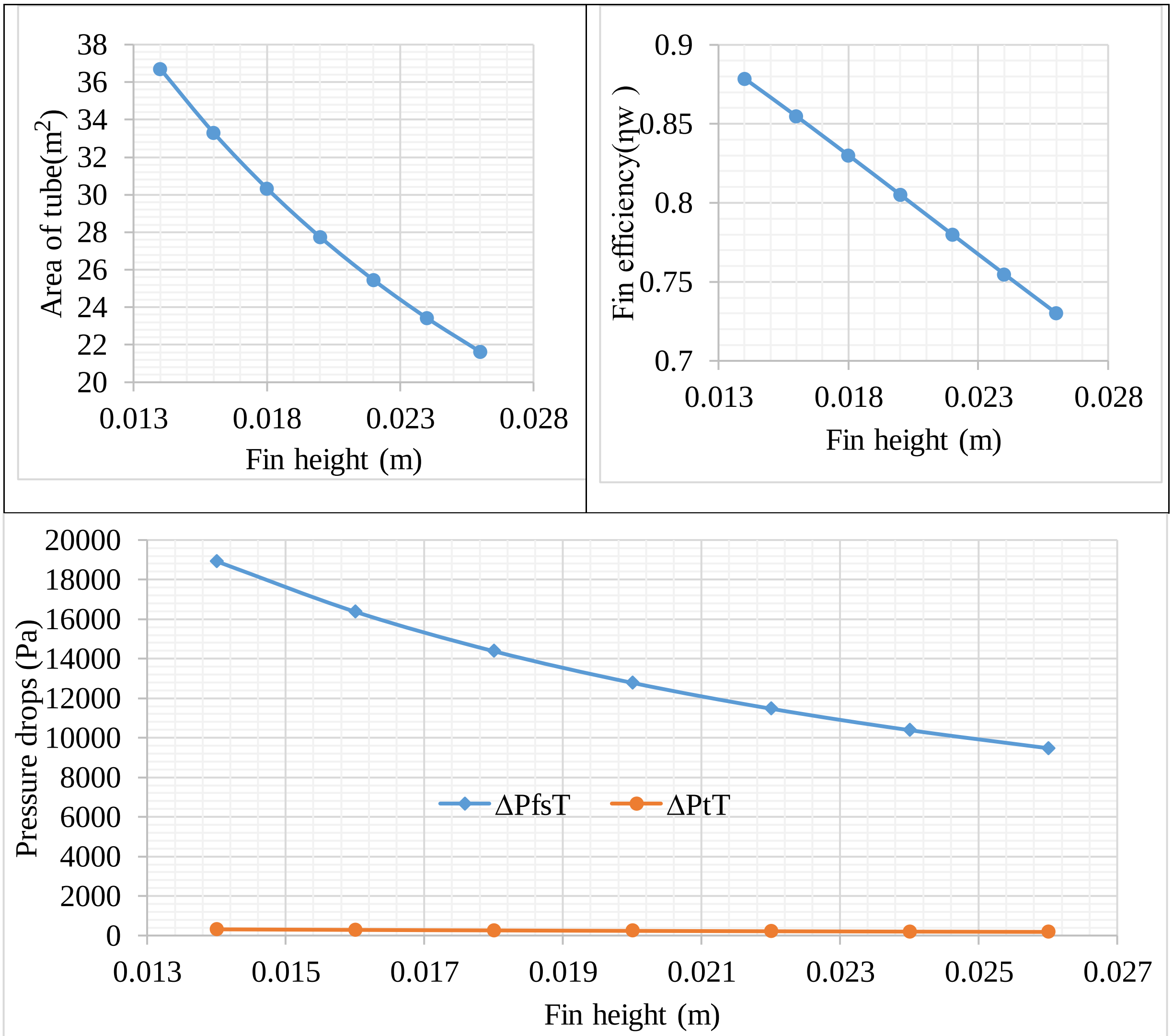

Figure 4. 10 Effects of fin height on objective functions

As shown values above from table and graph fin height has more variational effects. When fin height increase from 0.014 to 0.026 mm fin efficiency, heat transfer coefficient, heat transfer rate and pressure drop both on shell and tube side are increasing rapidly whereas total area change is small almost negligible.

Table 4. 9 Effects of fin thickness from appendix F

τ	**A**	**η_w**	**U**	**$\dot{Q}$**	**ΔP_{fsT}**
0.001	127.8344	0.563536	96.5455	753603.1	9508.287
0.003	123.1222	0.713878	109.7159	781634.5	10595.38
0.005	119.0832	0.774121	115.6901	787558.7	11687.29
0.007	115.5827	0.805139	119.5268	788393.4	12780.23
0.009	112.5197	0.823193	122.4266	787529.6	13871.03
0.011	109.8171	0.834408	124.803	786003.8	14957.04
0.013	107.4148	0.841587	126.836	784210	16036.07

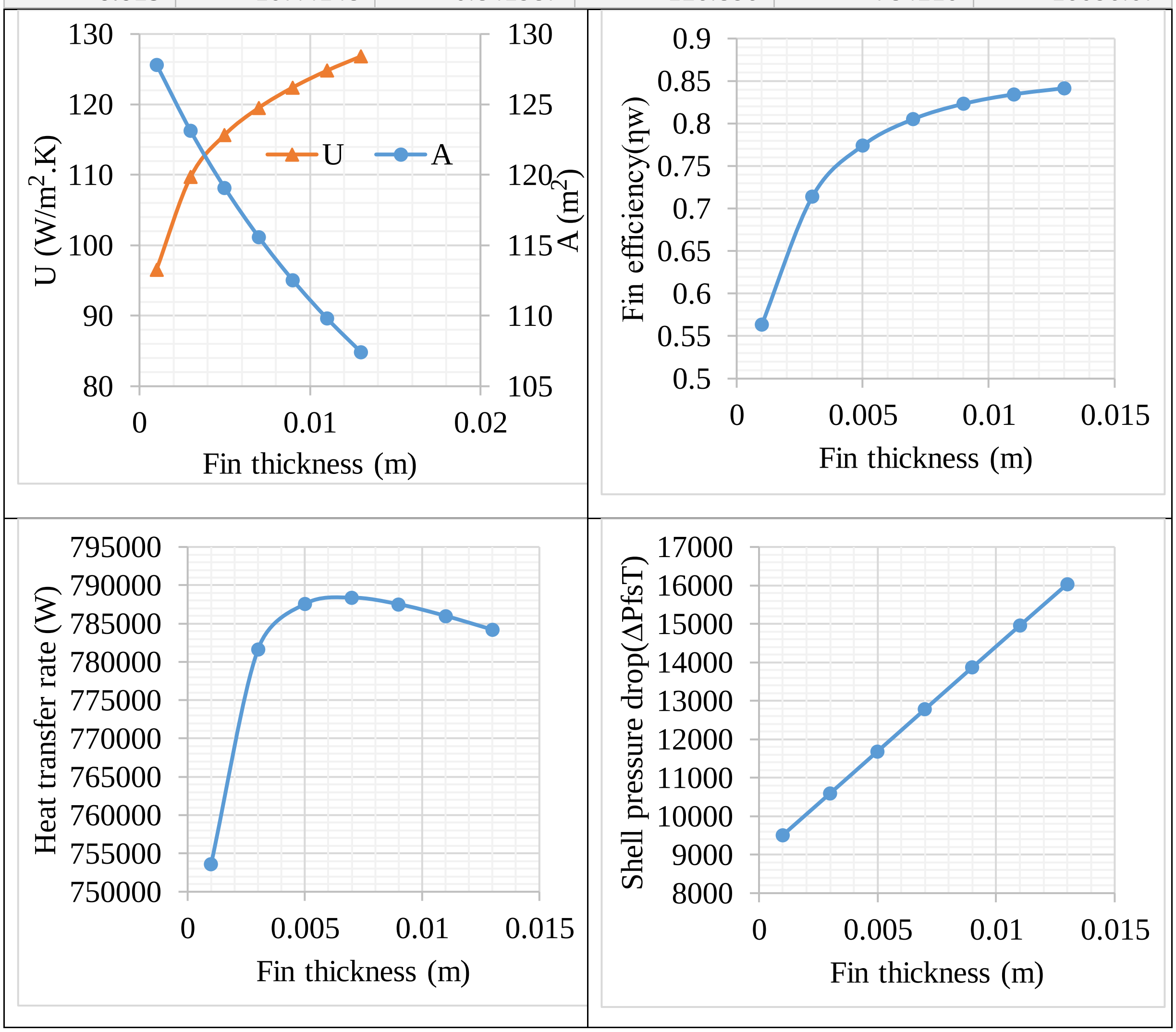

Figure 4. 11 Effects of fin thickness on objective functions

Table 4.9 and fig.4.11 shows that whenever fin thickness increases from 0.011 to 0.013:

- ✓ Fin efficiency, heat transfer coefficient and shell side pressure drop also increases. But pressure drop increase more rapidly
- ✓ Total surface area of STHE decrease.
- ✓ Heat transfer rate first increases after a while it is decreasing but in a very small amount almost negligible.

In optimizing, the sensibility analysis needs to decide which adjustable variables of the problem are more important than others. Depending on sensitivities of variables over the objective functions, inside tube diameter and fin thickness have no significant effect on heat transfer rate. But fin height is more sensitive over the heat transfer rate and pressure drops which is related to operating cost. Fin space also more sensitive on heat transfer rate than fin thickness and diameter. Therefor from these result decision variables can be reduced to two decrease problem complexities that is:

- ✓ Fin height and
- ✓ Fin space.

By using these two decision variables design optimization of STHE will be performed in the next Chapter.

CHAPTER FIVE

RESULT AND DISCUSSION

5.1 Comparison of Univariate Results

From sensitivity analysis, all values of heat transfer rate and heat exchanger performances are greater than constraint values set above, which is due to change of tube layout. Therefore, for the next analysis calculated by the two decision variables (fin height and fin space) can be unconstrained univariate optimization type.

Table 5. 1 Selected decision variables and their range

Decision variables	**Range(m)**
Fin height (b)	0.011, 0.014, 0.017, **0.02**, 0.023, 0.026, 0.029
Fin spacing (ℓ)	0.014, 0.017, 0.02, **0.023**, 0.026, 0.029, 0.032

In Table 5.1, there are two variables, fin height (b) and fin spacing (ℓ) which have seven different values. By using these different values, 49 different alternative shell and tube heat exchanger can be found.

These 49 different solutions are there in appendix from G up to M. From there some required parameter values are single out and presented in Tables below.

Table 5. 2 Effects of fin height (b) and fin space (ℓ) over heat transfer area

ℓ (m) / **b (m)**	**Heat transfer area (m^2)**						
	0.014	**0.017**	**0.02**	**0.023**	**0.026**	**0.029**	**0.032**
0.011	143.0868	132.7023	124.6254	118.1639	112.8773	108.4717	104.744
0.014	145.6392	133.8596	124.6976	117.3681	111.3712	106.3737	102.1451
0.017	147.3617	134.5016	124.4993	116.4974	109.9505	104.4947	99.87822
0.02	148.4742	134.7694	124.1101	115.5827	108.6057	102.7915	97.87184
0.023	149.1309	134.7612	123.5848	114.6436	107.3282	101.2319	96.07359

0.026	149.4422	134.5469	122.9617	113.6935	106.1104	99.7912	94.44417
0.029	149.4886	134.177	122.268	112.7408	104.9458	98.45004	92.95358

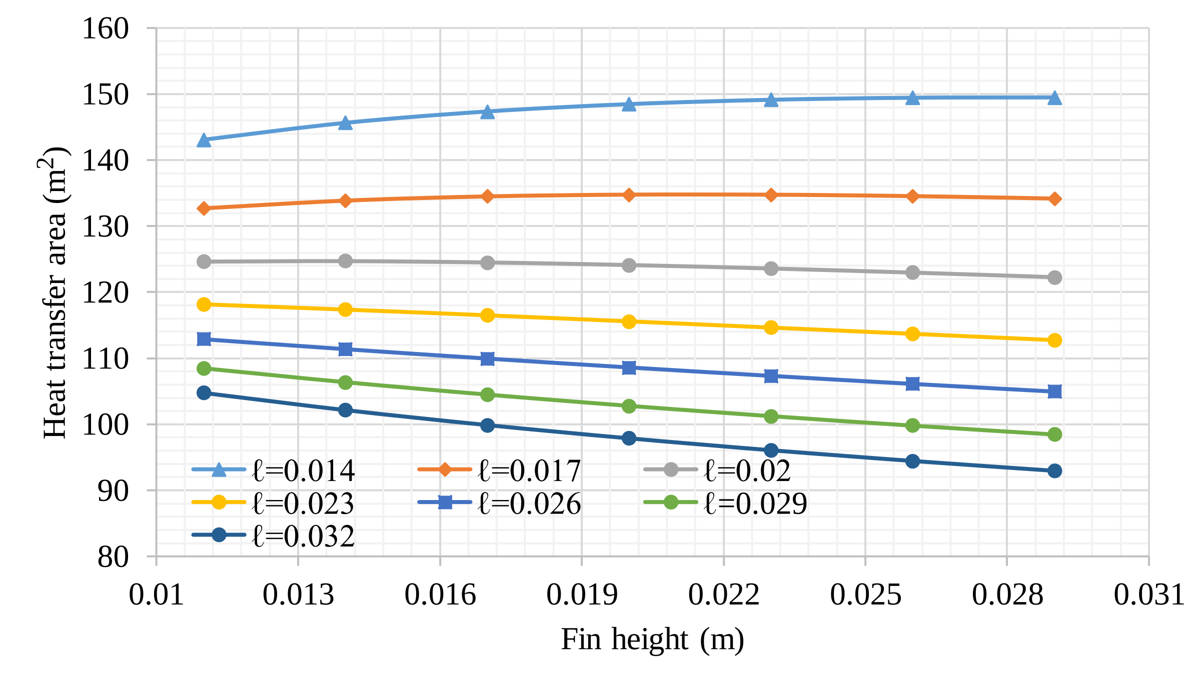

Figure 5. 1 Effects of fin height and space over heat transfer area

As Figure 5.1 shows, for smaller constant fin space when fin height increase, fin area increase and base areas decrease with equivalent range as fin area due to number of tubes in the shell decrease. But the sum of the two that is total heat transfer area increase in a small amount.

For higher constant fin space when fin height increase, fin area increase in smaller range and base area decrease with a greater range than fin area. Therefore heat transfer area decrease for higher fin space.

Table 5. 3 Effects of fin height (b) and fin space (ℓ) over overall heat transfer coefficient

ℓ (m) / b (m)	Overall heat transfer coefficient (W/ m^2.K)						
	0.014	**0.017**	**0.02**	**0.023**	**0.026**	**0.029**	**0.032**
0.011	156.024	163.6118	170.4395	176.659	182.3778	187.6754	192.6129
0.014	134.3433	141.1872	147.3873	153.069	158.3215	163.2113	167.7895
0.017	117.4813	123.6941	129.3519	134.5615	139.3991	143.9214	148.1722
0.02	103.8941	109.5587	114.7386	119.5268	123.9897	128.1768	132.1261
0.023	92.67636	97.85839	102.6128	107.022	111.1447	115.0248	118.6956
0.026	83.2522	88.00631	92.38008	96.44731	100.2607	103.8594	107.2733

0.029	75.23134	79.60439	83.63675	87.39519	90.92741	94.26871	97.44594

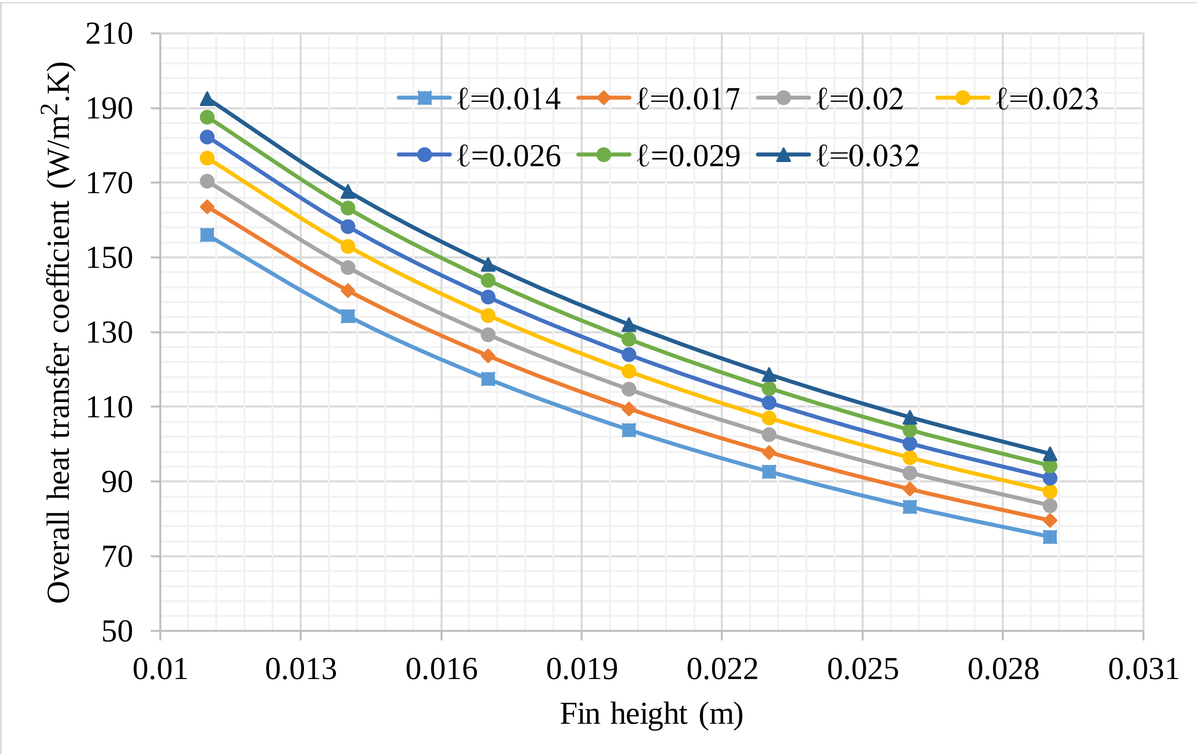

Figure 5. 2 Effects of fin height and space over heat transfer coefficient

Figure 5.2 tells that: At constant fin space, overall heat transfer coefficient decrease with increasing of fin height and at constant fin height heat transfer coefficient increase as fin space increase. But it increases with a small amount.

Table 5. 4 Effects of fin height (b) and fin space (ℓ) over fin efficiency

ℓ (m) / **b (m)**	**Overall fin efficiency (η_w)**						
	0.014	**0.017**	**0.02**	**0.023**	**0.026**	**0.029**	**0.032**
0.011	0.905199	0.907663	0.910115	0.912507	0.914818	0.917037	0.919159
0.014	0.870785	0.873391	0.87606	0.878731	0.881365	0.883941	0.886447
0.017	0.834337	0.836963	0.839727	0.842555	0.845401	0.84823	0.851023
0.02	0.796912	0.799476	0.802244	0.805139	0.808102	0.811095	0.814088
0.023	0.759381	0.761831	0.764545	0.767438	0.77045	0.773534	0.776654
0.026	0.722428	0.724739	0.72736	0.730207	0.733216	0.736335	0.739525

0.029	0.686563	0.688725	0.691234	0.694006	0.696976	0.700089	0.703303

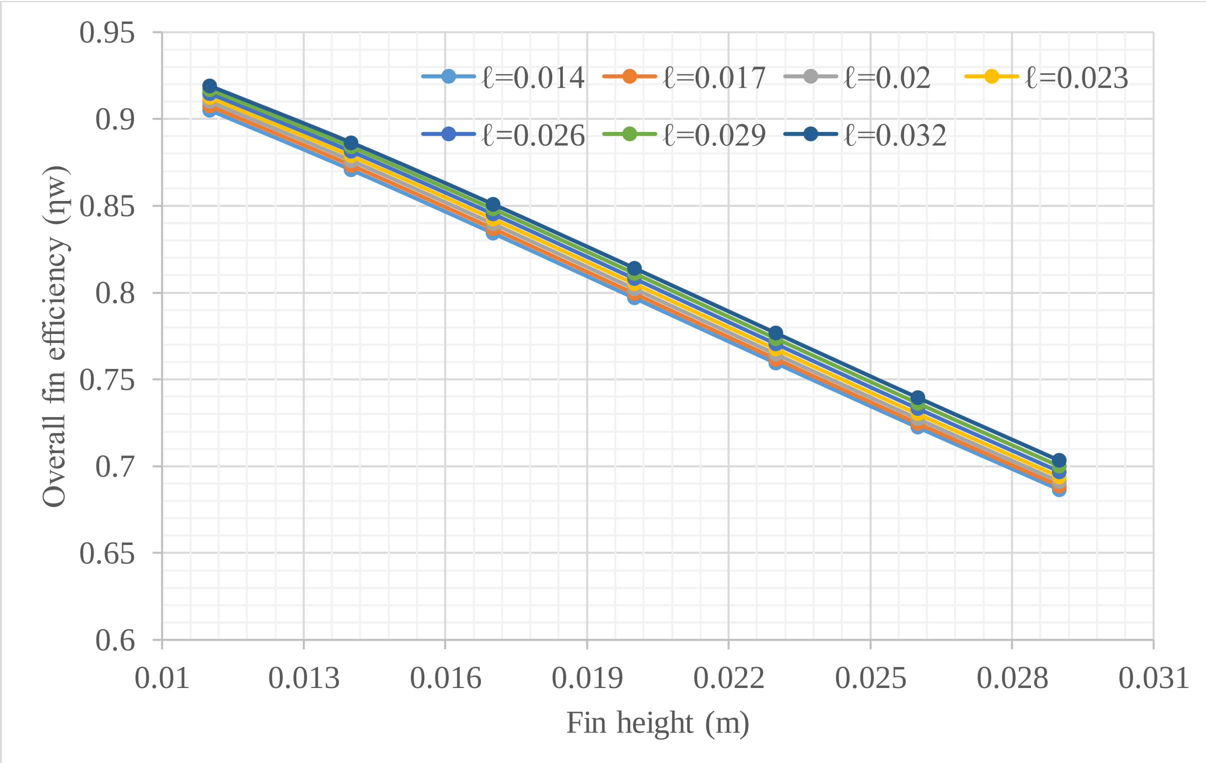

Figure 5. 3 Effects of fin height and fin space over fin efficiency

From figure 5.3: At constant fin space with increasing of fin height, fin efficiency is decreasing more rapidly.

Table 5. 5 Effects of fin height (b) and fin space (ℓ) over heat transfer rate

ℓ (m) / b (m)	Heat transfer rate (W)						
	0.014	**0.017**	**0.02**	**0.023**	**0.026**	**0.029**	**0.032**
0.011	906074.9	900850	896590.9	893115.7	890277.7	887959.7	886068.3
0.014	879461.9	871698.4	865215.6	859786.1	855224.5	851381.4	848136.5
0.017	850671.5	840509.6	831918.3	824624.7	818407.1	813086.5	808518.3
0.02	820188.6	807860	797367.9	788393.4	780679.6	774019.9	768247.5
0.023	788516.3	774300.1	762160.2	751732.7	742727.1	734911	728097.3
0.026	756147.4	740340.2	726821.5	715184.1	705105.9	696331.1	688654.6
0.029	723538	706435.1	691803.6	679195.5	668260.7	658722.5	650359.9

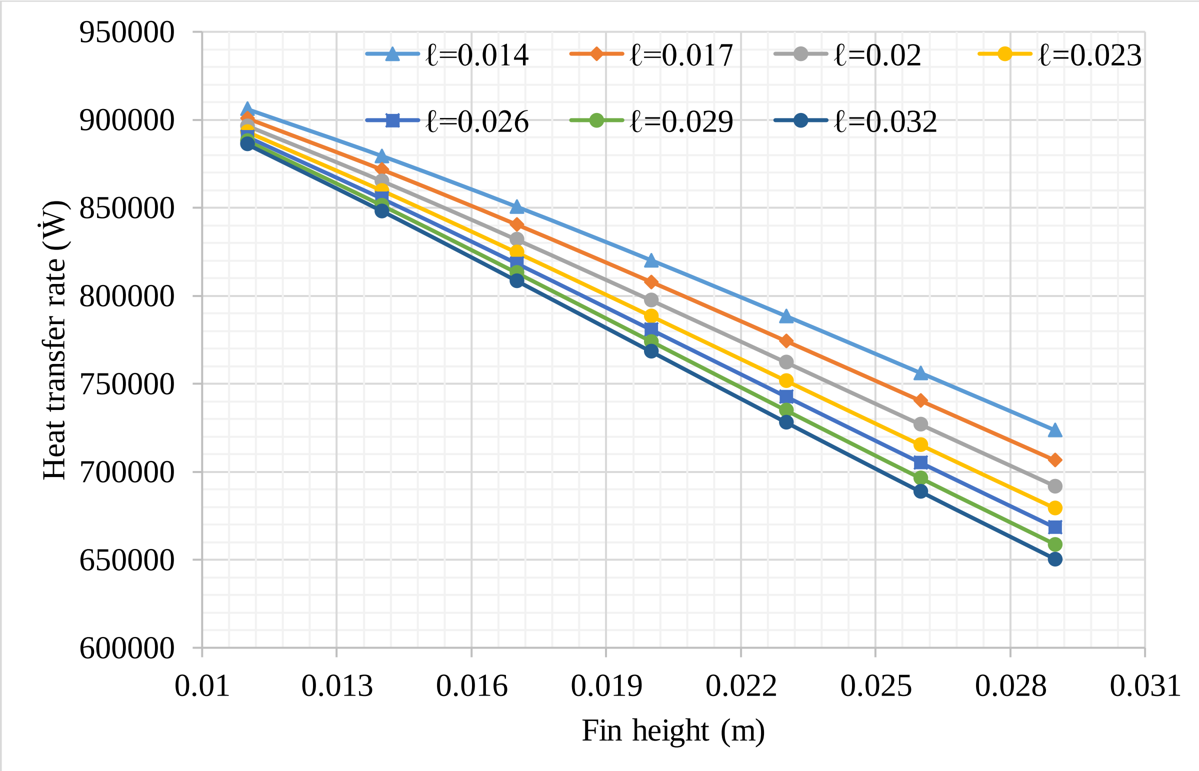

Figure 5. 4 Effects of fin height and fin space over heat transfer rate

Heat transfer rate:

At constant fin height with increasing of fin space, rate of heat transfer is decreasing in a very small amount especially for smaller fin height.

Table 5. 6 Effects of fin height (b) and space (ℓ) over pressure drop on the shell side

ℓ (m) / b (m)	Pressure drop on the shell side (Pa)						
	0.014	**0.017**	**0.02**	**0.023**	**0.026**	**0.029**	**0.032**
0.011	31596.07	28352.97	26060.29	24349.31	23020.26	21955.61	21081.71
0.014	24990.63	22260.77	20346.14	18925.84	17827.79	16951.58	16234.69
0.017	20503.29	18161.02	16527.9	15321.74	14392.45	13652.94	13049.29
0.02	17284.76	15241.76	13823.87	12780.23	11978.26	11341.41	10822.44
0.023	14878.36	13071.72	11822.57	10905.66	10202.55	9645.12	9191.471
0.026	13019.34	11403.24	10289.36	9473.61	8849.147	8354.737	7952.808
0.029	11544.81	10085.14	9081.777	8348.401	7787.816	7344.483	6984.398

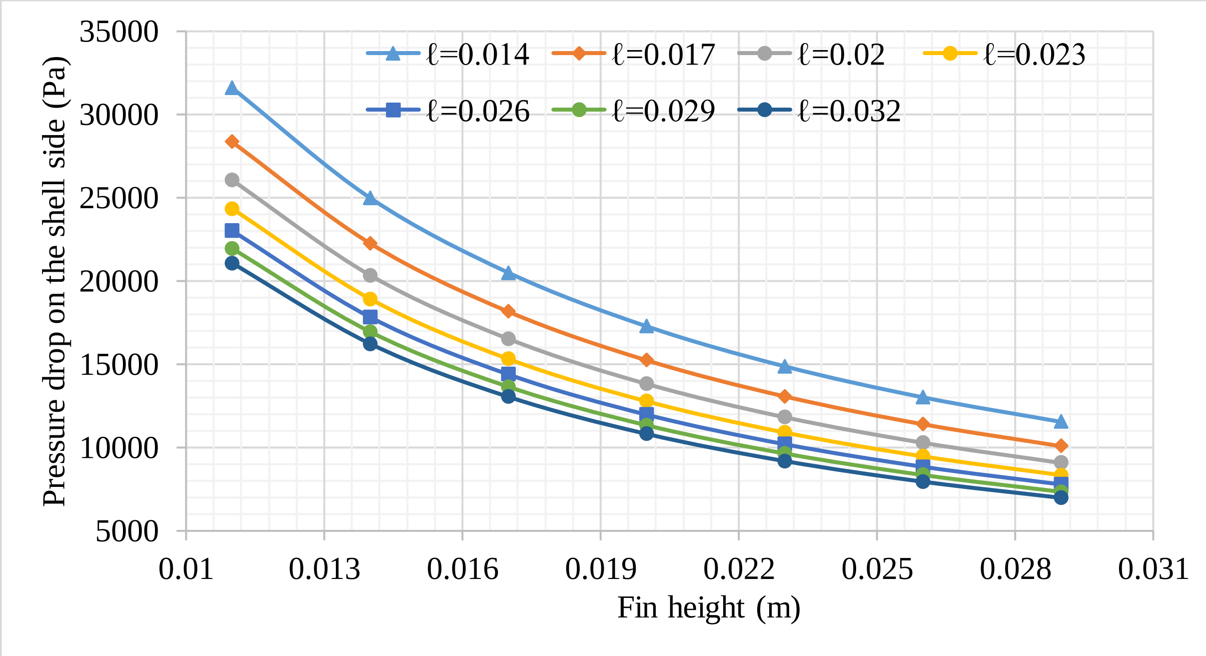

Figure 5. 5 Effects of fin height and fin space over pressure drop on the shell side

Pressure drops:

Whenever the fin space increase at constant fin height, pressure drop decrease. But the rate of decreasing of pressure drop decrease.

At constant fin space decreasing of pressure drop rates are decrease with increasing fin height.

Now conclusion can be drown that at 32 mm fin space, pressure drops and heat transfer area are decreased with a small heat transfer rate penalty. But at constant 32 mm there are 7 alternative solution as yet. Which is

Table 5. 7 Values at 32 mm fin space and variable fin heights. It is taken from appendix M.

b	**A**	$\boldsymbol{\eta_w}$	**U**	$\mathbf{\dot{Q}}$	$\boldsymbol{\Delta P_{fsT}}$	$\boldsymbol{\Delta P_{Tt}}$
0.011	104.744	0.919159	192.6129	886068.3	21081.71	367.6569
0.014	102.1451	0.886447	167.7895	848136.5	16234.69	314.5016
0.017	99.87822	0.851023	148.1722	808518.3	13049.29	271.7655
0.02	97.99125	0.814088	131.9791	768280.4	10592.62	215.4998
0.023	96.07359	0.776654	118.6956	728097.3	9191.471	208.1208
0.026	94.44417	0.739525	107.2733	688654.6	7952.808	184.0793
0.029	92.95358	0.703303	97.44594	650359.9	6984.398	163.8035

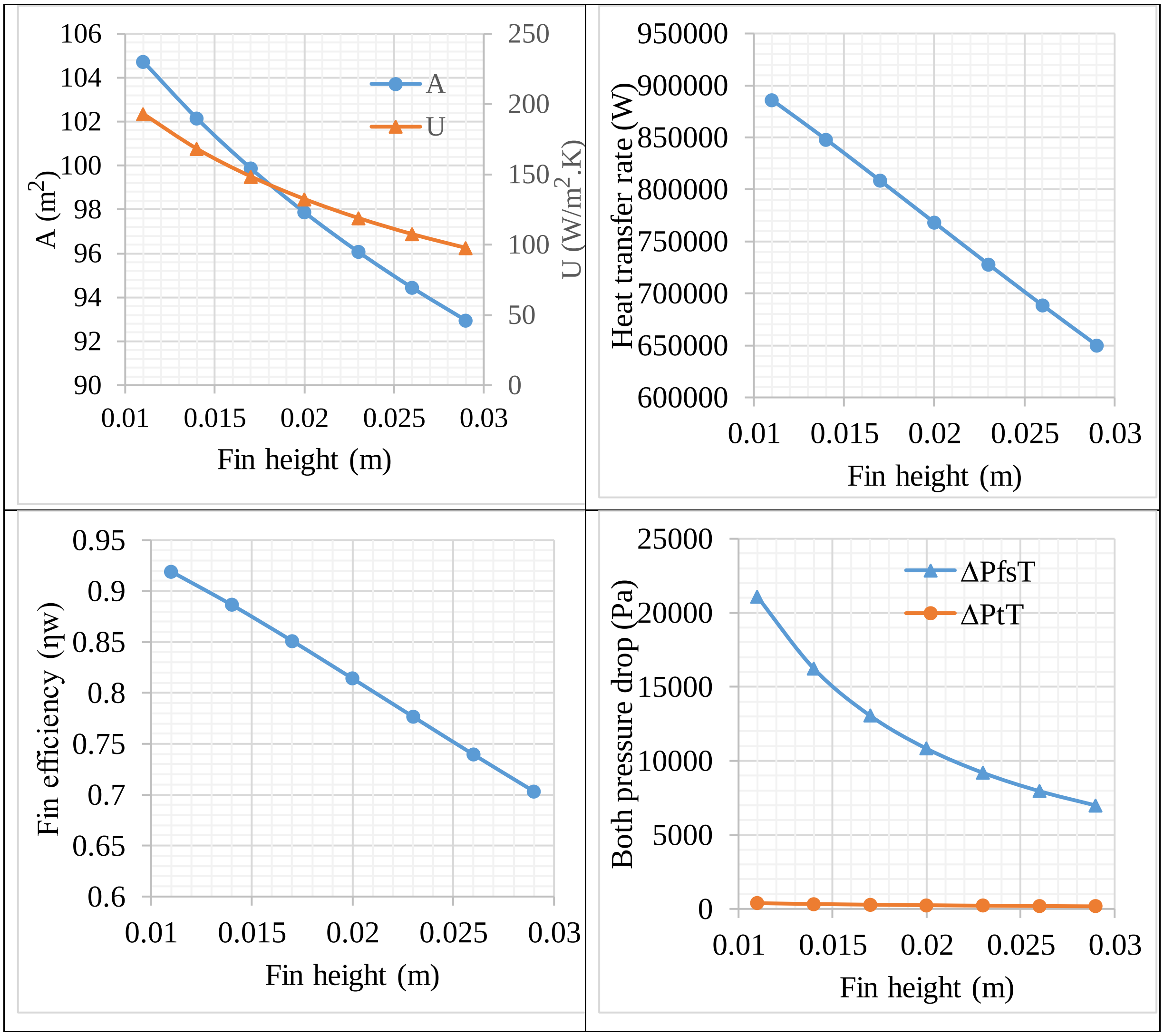

Figure 5. 6 Area, heat transfer coefficient, heat transfer rate, efficiency and pressure drops at a constant 32 mm fin space.

To select the best values to fulfill the objective functions, total cost evaluation has to be required. Functional years of original (existing) STHE $(n_y) = 20$ years, annual discount rate (i) = 10 %, unit price of electrical energy in Ethiopia $(Kel) = 0.06\,\$/kWh$ [Energy4sustainablefuture.blogspot.com], Pump efficiency $\eta = 75\ \%\ and$ the hours of operation per year$(H) = 8040$ h/year (The remaining days being nominal maintenance shutdown days).

Then by using cost estimation equations, 7 different alternative calculated values are listed in the table below.

Table 5. 8 Investment cost, operating cost and total cost

b (m)	C_{in} (\$)	C_{op} (\$)	C_T (\$)
0.011	72406.4275	3050221.19	3122627.61
0.014	71657.9338	2348930.64	2420588.58
0.017	71002.7095	1888049.46	1959052.17
0.02	61425.2315	1532500.12	1593900.35
0.023	69898.0155	1329880.1	1399778.12
0.026	69422.9297	1150663.3	1220086.23
0.029	68987.2596	1010548.22	1079535.48

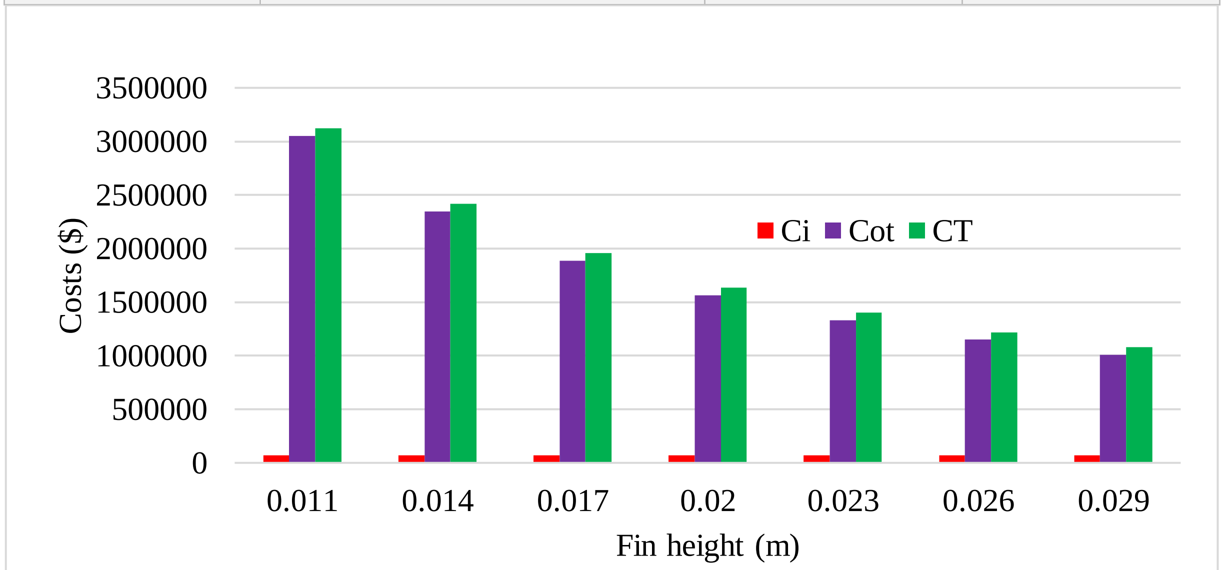

Figure 5. 7 Capital, operational and total cost of STHEX

Table 5.8 suggests that whenever fin height values varies from 11mm to 29 mm at constant 32 mm fin space there is no significant change on investment cost this means there is no significant change on heat transfer area. But not on operational cost. Figure 5.7 indicates that operating cost is the dominant cost factor in a shell and tube heat exchanger. Even if it incorporates pumping cost for hot and cold fluids, the dominant factor for this cost is pumping cost of hot fluid in the shell. As a result to minimize total cost it is better to focus on pressure drop in the shell which is responsible for operational cost.

5.2 Dual Objective Optimization Using Univariate Method

As mentioned, dual objective optimization yields Pareto solutions that constructs the Pareto curve. It can also be said that a favorable trade-off between the results of contradictive objectives is called Pareto optimum solution. Figure 5.8 and 5.9 shows the Pareto frontier constructed by the dual objective optimization of abovementioned problem objectives.

Table 5. 9 Pareto optimal solution

CT ($)	**$\dot{Q}$ (W)**
3122627.61	886068.3
2420588.58	848136.5
1959052.17	808518.3
1593900.35	768280.4
1399778.12	728097.3
1220086.23	688654.6
1079535.48	650359.9

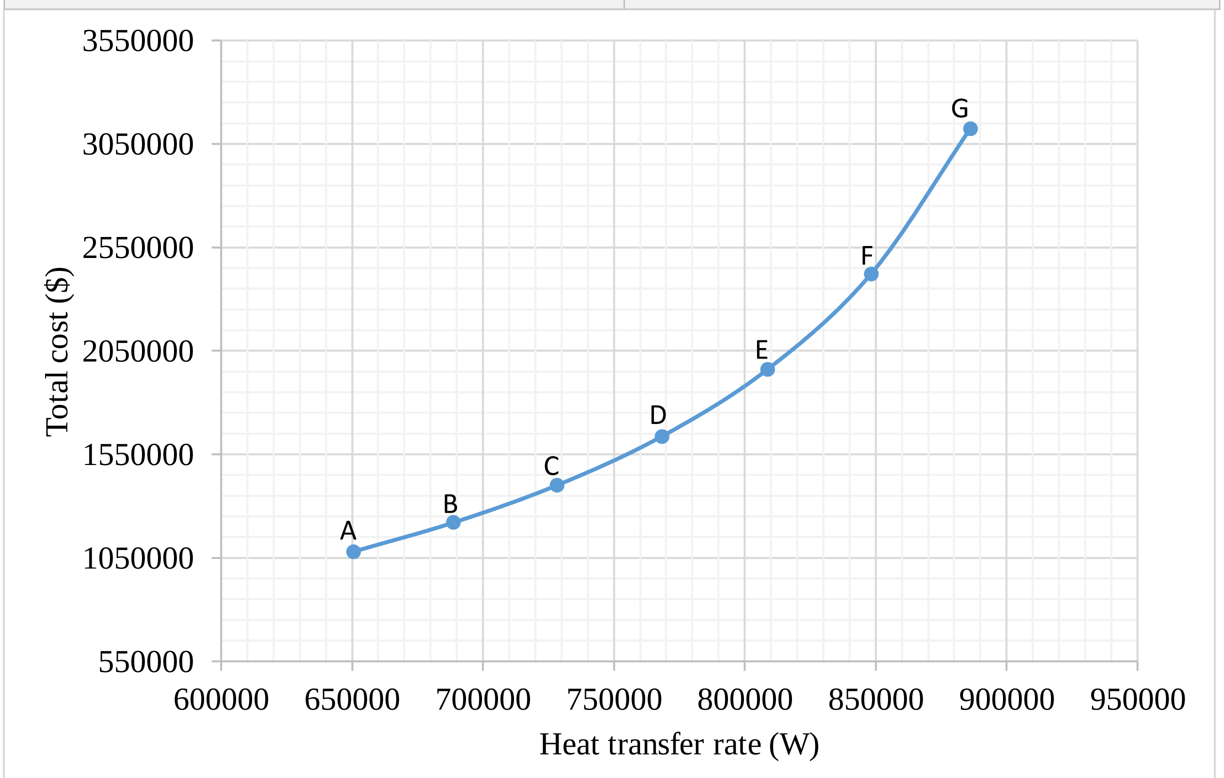

Figure 5. 8 Pareto curve of objective function

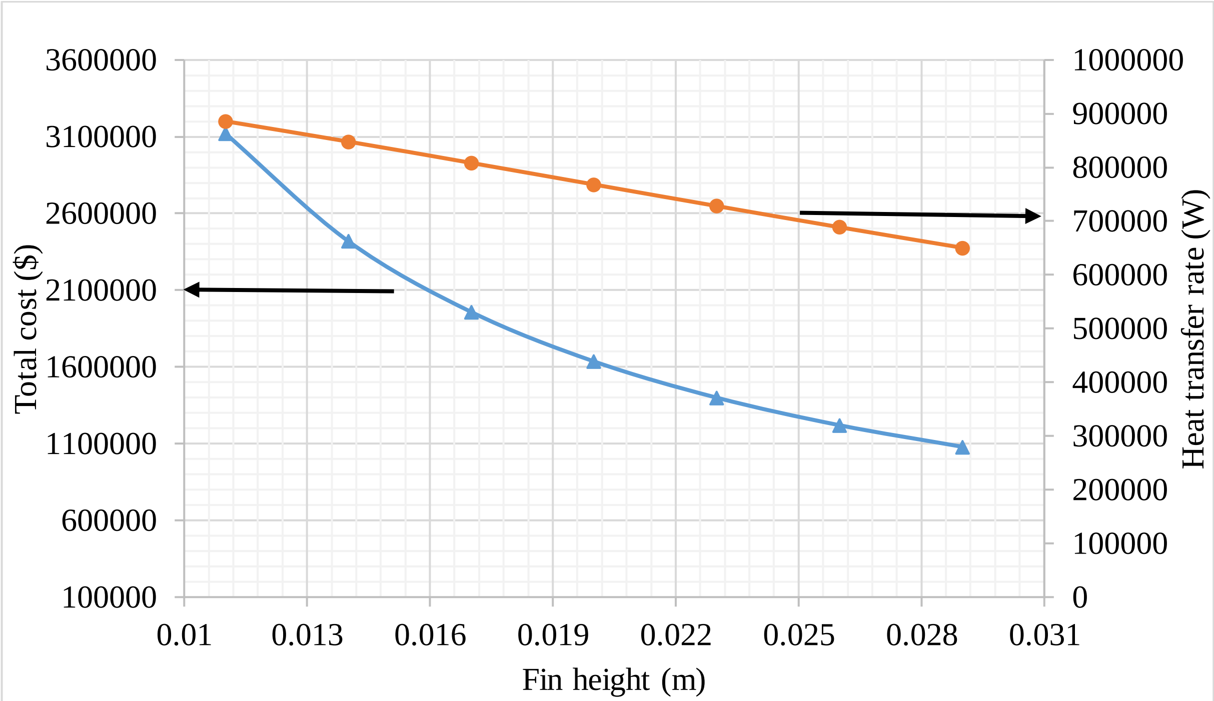

Figure 5. 9 Heat transfer rat and total cost at different fin height

Univariate optimization technique was implemented using Excel to get optimal solutions and for these optimal solutions Pareto analysis is required to decide important adjustable variables. As shown Figure 5.8 on the Pareto curve which indicates the conflict between total cost and heat transfer coefficient that is at point A both cost and heat transfer rate are minimum whereas at point G both objective functions are maximum.

Figure 5.9 indicate that whenever increasing fin height from 11 mm to 29 mm heat transfer rate decrease almost in equal ranges, while total cost drops rapidly for the first some values. But the range of decreasing values become decrease with fin height.

Finally, from Pareto optimal point solutions one point can be selected for constraint of $\dot{Q} \geq 5.133\times10^5$ W and CT $\leq 1.8294\times10^6$ \$. Due to this, it is acceptable to choose design point D at $\dot{Q} = 7.6828\times10^5$ W and CT=1.5939×10^6 \$ as modified design of shell and tube heat exchanger of for univariate optimization method.

5.3 Dual Objective Optimization Using ACO

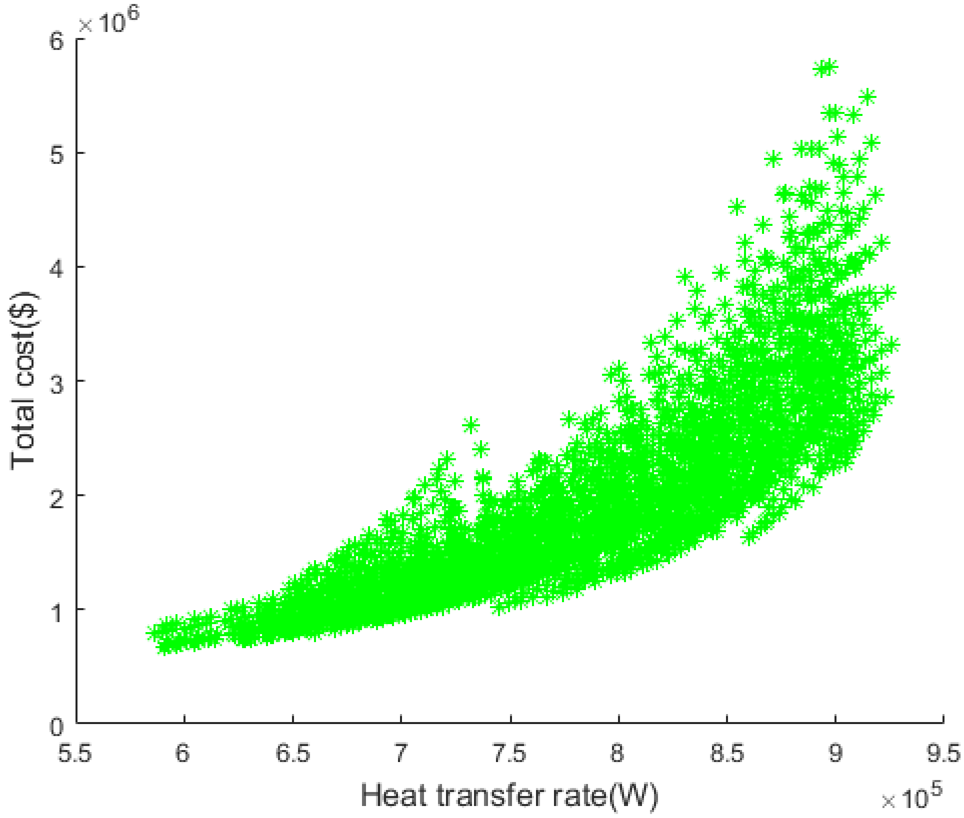

Figure 5. 10 Total cost Vs heat transfer rate Pareto fronts of STHEs without constraints.

When constraint parameters are excluded (non-constraint optimization) as shown Figure 5.10, 2,401 alternative number of STHEs which represented with its' total cost and heat transfer rate can be found by using MATLAB code.

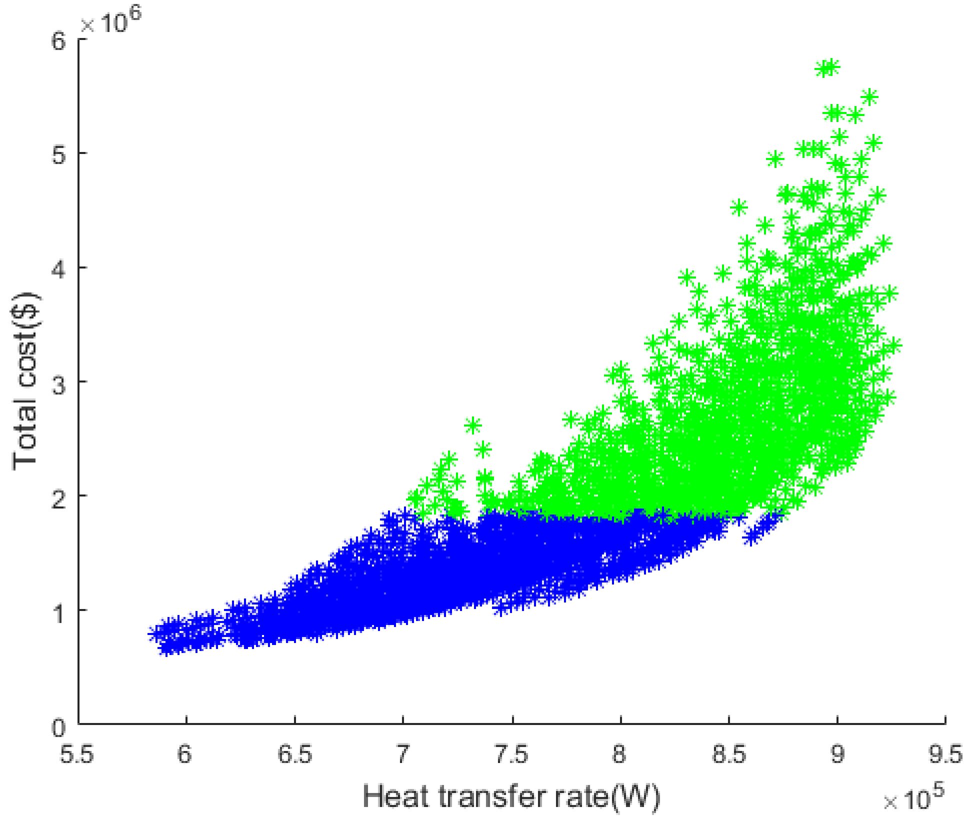

Figure 5. 11 Total cost Vs heat transfer rate Pareto fronts of STHEs for CT $\leq 1.8294\times10^6$ and CT $\geq 1.8294\times10^6$ \$ which is existing STHE cost estimation.

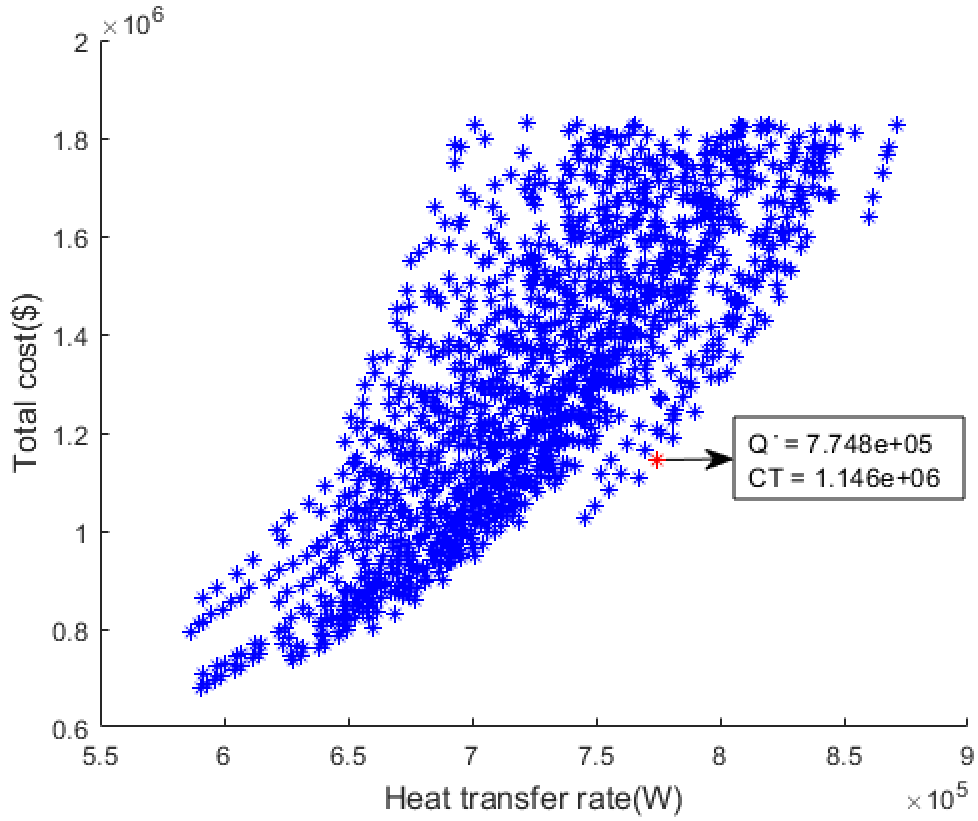

Figure 5. 12 Total cost Vs heat transfer rate Pareto front of STHEs with constraint of $\dot{Q} \geq 5.133\times10^5$ W and CT $\leq 1.8294\times10^6$ $.

As Figure 5.10, the stares in Figure 5.12 also shows different alternative STHEs. But it has constraint parameters of $\dot{Q} \geq 5.133\times10^5$ W and CT $\leq 1.8294\times10^6$ $ which is taken from existing STHE. Due to this number of alternative, STHEs are decreased from 2,401 to 1,280. Of which one optimum point with the smallest total cost to heat transfer rate ratio (CT/$\dot{Q}$ = 1.4795) is selected. At this point total cost and heat transfer rate are 1.1463× 10^6 $ and 7.74810× 10^5 W respectively.

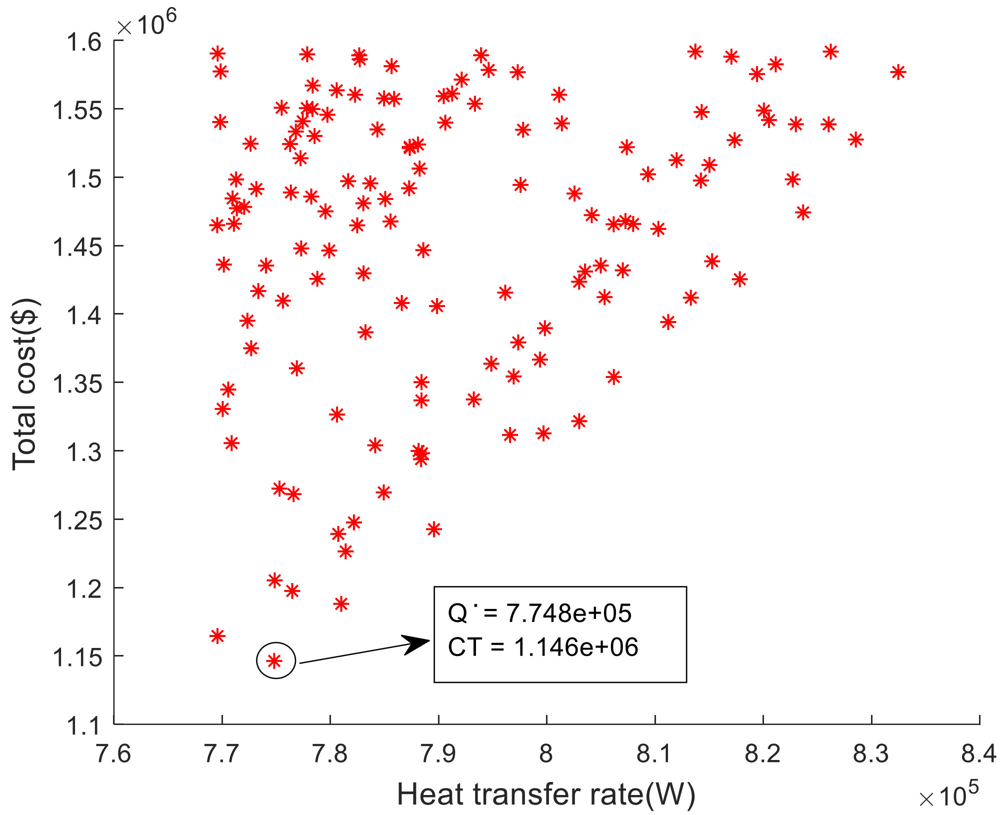

Figure 5. 13 Total cost Vs heat transfer rate Pareto front of STHEs with constraint of $\dot{Q} \geq 7.6828\times10^5$ W and CT $\leq 1.5939\times10^6$ \$.

If $\dot{Q} \geq 7.6828\times10^5$ W and CT $\leq 1.5939\times10^6$ \$ which is values of modified STHE calculated by univariate method is taken as constraints, 139 alternative heat exchangers can be found as shown in Figure 5.13.

Design optimization of heat exchanger by using Univariate and ACO have different optimal values. Existing parameter values and modified STHE optimal point values both in Univariate and ACO are listed below in Table 5.10.

Table 5. 10 Both existing and modified exchanger parameter values

Heat exchanger parameters	**Existing STHEX values**	**Modified STHE values (Univariate method)**	**Modified STHEX values (ACO method)**
Fin diameter D_f(m)	0.115	0.096	0.09
Root diameter D_r(m)	0.075	0.056	0.05
Tube diameter D_i(m)	0.04	0.04	0.034
Fin space ℓ(m)	0.023	0.032	0.029
Fin height b(m)	0.02	0.02	0.02
Fin thickness τ(m)	0.007	0.007	0.003
Number of fin per tube N_f(m)	74	55	31
Number of tube N_T(m)	64	102	114
Number of pass n_p(m)	2	3	3
Number of tube per pass	32	34	38
Number of row N_r(m)	16	23	21
Heat transfer area $A(m^2)$	94.54	97.991247	110.7173
Heat tran. coef. in tube $h_i(W/m^2.k)$	696.6	4216.76577	5168.7
Heat tran. coef. in shell $h_o(W/m^2.k)$	227	240.7993642	246.8468
Overall heat trans.coef $U(W/m^2.k)$	63.5	131.9791486	119.3063
Heat exchanger performance ε	0.3811	0.598474276	0.6036
Heat transfer rate $\dot{Q}$(W)	5.27×10^5	7.6828×10^5	7.7481×10^5
Pressure drop in shell ΔP_{fsT}(kPa)	12.209	10.5926232	7.5361
Pressure drop in tube ΔP_{tT}(Pa)	156.861	215.4997537	448.3515
Number of tubes per rows (for odd and even respectively)	4, 4	5, 4	6, 5
Investment cost C_{in}($)	6.3102×10^4	6.1425×10^4	5.6051×10^4

Operating cost C_{op} ($)	1.7663×10^{6}	1.5325×10^{6}	1.0903×10^{6}
Total cost CT($)	1.8294×10^{6}	1.5939×10^{6}	1.1463×10^{6}

The existing design and the modified STHE obtained using Univariate optimization approach and ACO method results are summarized in Table 5.10. The table demonstrates that the Univariate design approach and the ACO design approach can reduce the total cost compared to the original design approach. Quantitatively, a remarkable reduction in the total cost was achieved using the Univariate approach (by 12.87 %) and the Ant Colony Optimization approach (by 37.34 %) as compared to the original design, whereas heat transfer rate increased by 45.78 % and 47.02 % by using Univariate and ACO method respectively as compared to the original design. Therefore, design optimization of modified STHE by using ACO approach can be the best choice. The results found from univariate and ACO were selected from 49 and 2,401 alternative STHEs respectively. To get the same result in univariate technique as ACO values, Univariate technique needs 2,401 trials on Excel spreadsheet. But it is tedious and takes time and also leads to input data as well as output analysis error. That is why sensitivity analysis is used to avoid this challenge.

Result Validation

The present results in both of the optimization methods are able to provide equivalent STHE design to the related reference [40].

This related reference calculated for a fined STHE using a multi-objective optimization genetic algorism for the decision variables (tube arrangement, tube diameter, tube pitch ratio, tube length, numbers of tube, fin height, fin thickness and baffle spacing ratio) involved in optimization of the objective functions (maximum heat transfer rate and minimum total cost). In this case, the equipment life was taken $n_y = 10$ years; and the working hours H = 7500 h/year. Whereas the present work calculated for a fined STHE using a multi-objective optimization ACO and Univariate methods for the decision variables (tube arrangement, tube diameter, fin height, fin thickness and fin space) involved in optimization of the objective functions (maximum heat transfer rate and minimum total cost). The equipment life was taken $n_y = 20$ years; and the working hours H = 8040 h/year.

As shown figure 5.14, distribution of Pareto-optimal point solutions in 5.14a forms a curve line because in genetic algorisms each iteration results are updated in the next iterations.

In ACO, Pareto-optimal point solutions are randomly distributed, because of all iteration outputs are displayed. But as shown figure 5.14 all graphs have similar trend. Finally, by considering those conditions which make difference, these multi objective optimization methods for STHE design can be validated against the reference cases in the literature [40].

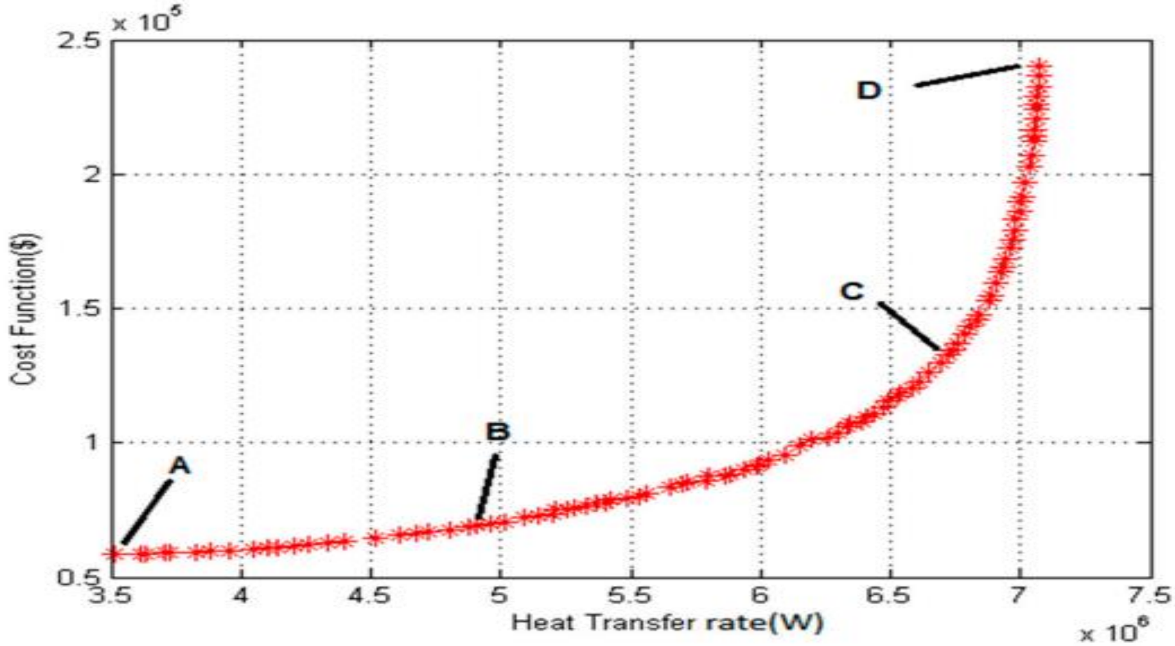

a). The distribution of Pareto-optimal point solutions using NSGA-II [40]

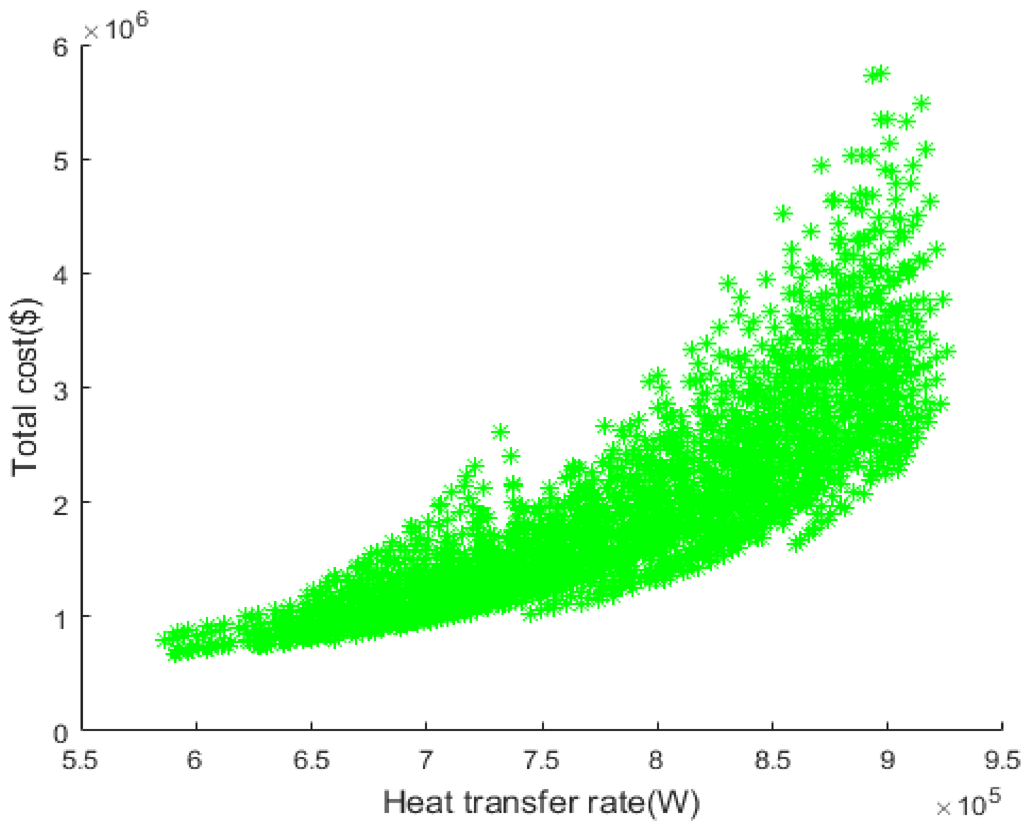

b). The distribution of Pareto-optimal point solutions using ACO

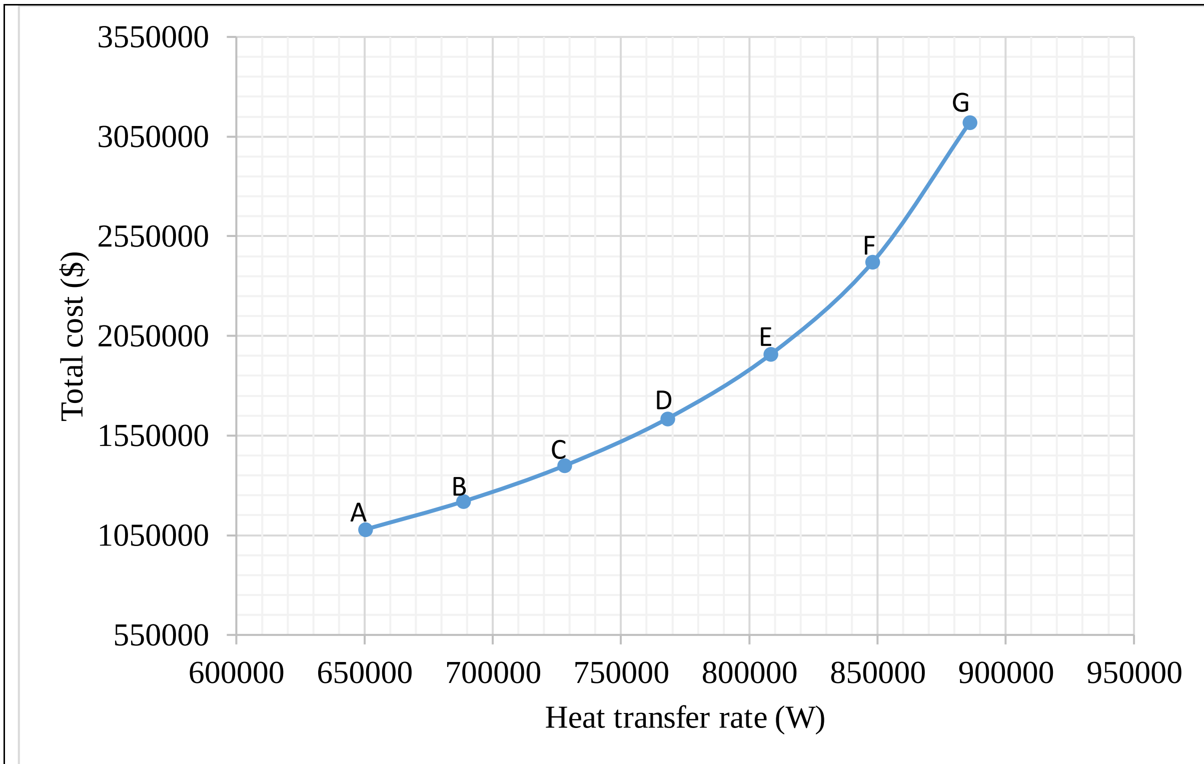

c). The distribution of Pareto-optimal point solutions using Univariate method

Figure 5. 14 Validation of present results against the reference cases in the literature

CHAPTER SIX

CONCLUSION AND RECOMMENDATION

6.1 Conclusion

In this thesis detail study of existing shell and tube heat exchanger and a modified multi-objective optimization design approach is proposed for the shell and tube heat exchanger on Microsoft Excel using univariate and ACO optimization technique with the objective functions of maximizing heat transfer rate and minimizing total cost using MATLAB. Five independent decision variables are considered, including tube arrangement, tube diameter, fin height, fin thickness and fin space. Of which, tube diameter and fin thickness have less significant change over heat transfer rate and multi objective optimization for the modification of a shell-and-tube heat exchanger allowed finding Pareto fronts with optimal decision variables both in Univariate(in Excel) and ACO(in MATLAB) techniques. From which it can be chosen one solution from all Pareto optimal solutions based on heat transfer rate as well as the cost of the design for both techniques. In Univariate and ACO methods, heat transfer rate (7.6828×10^5 W and 7.7481×10^5 W) and total cost (1.5939×10^6 \$ and 1.1463×10^6 \$) respectively have been selected.

Finally result shows that:

- The tube arrangement and fin height have more significant effects on heat transfer rate and cost of STHE.
- Operating cost is the dominant cost factor in a shell and tube heat exchanger.
- Within operating cost, pressure drop in the shell is a dominant factor.
- Heat transfer rate in both techniques have almost the same values, but it has significant difference in total cost.
- ACO approach is more cost-effective than Univariate (traditional) optimization technique.

Optimal point selected from Pareto optimal solutions of modified STHE in ACO approach was improves heat transfer rate by 47.02 % and total cost reduction by 37.34 % when compared with existing shell and tube heat exchanger.

6.2 Recommendation for Future Work

The following studies can be recommended for the future work.

- Water flow in the heat exchanger shall be analyzed as a two phase flow if two phase flow analysis measuring instruments are available.
- Experimental investigations are needed to confirm the performance of the proposed model.
- This study focuses on only economizer part. Since economizer and evaporator connected side by side, evaporator shall be suggested as an additional study along with economizer for more effective design.

REFERENCES

[1]. Shravan H. Gawande, Sunil D. Wankhede, Rahul N. Yerrawar, Vaishali J. Sonawane and Umesh B. Ubarhande, Design and Development of Shell and Tube Heat Exchanger for Beverage, Modern Mechanical Engineering, 2012, 2, 121-125.

[2]. Shah, R. K, Classification of Heat Exchangers, 1981.

[3]. Daniel Walraven, Ben Laenen and William Dhaeseleer, Optimum Configuration of Shell-and-Tube Heat Exchangers for the Use in Low-Temperature Organic Rankin Cycles, WP EN2014-13.

[4]. R. V. Patil, S. S. Bhutada, N. R. Katruwar, R. R. Rai and K. N. Dhumke, Determination of Internal Pressure in a Shell and Tube Type of Heat Exchanger by Using IBR and ASME Codes, IOSR Journal of Mechanical and Civil Engineering (IOSR-JMCE), 2014.

[5]. Abhishek Arya and Dangar Sunilbhai Dhanjibhai, Optimization of Shell and Tube Heat Exchanger, M.tech Scholar Department of Mechanical Engineering, SCE Bhopal, 2015.

[6]. Salim Fettaka, Jules Thibault and Yash Gupta, Design of Shell-and-Tube Heat Exchangers Using Multi-Objective Optimization, International Journal of Heat and Mass Transfer 343–354, 2013.

[7]. Nimish Dubey and Morrish Kumar, Design Modification in Heat Exchanger Twisted Tape for Heat Transfer Enhancement- A Review, ISSN: 2277-9655, July, 2017.

[8]. Dawit Bogale, Design and Development of Shell and Tube Heat Exchanger for Harar Brewery Company Pasteurizer Application (Mechanical and Thermal Design), American Journal of Engineering Research (AJER), 2014.

[9]. Amarjit Singh and Satbir S. Sehgal, Thermohydraulic Analysis of Shell-and-Tube Heat Exchanger with Segmental Baffles, ISRN Chemical Engineering, August 2013.

[10]. Digvendra singh and Narayan Das Pal, Designing and Performance Evaluation of a Shell and Tube Heat Exchanger Using ANSYS (Computational Fluid Dynamics), ISSN: 2395-3470, 2016.

[11]. R V Rao and V Patel, Design Optimization of Shell and Tube Heat Exchangers Using Swarm Optimization Algorithms, Department of Mechanical Engineering, S.V. National Institute of Technology, Gujarat, India, 15 February 2011.

[12]. Sandeep K. Patel and Alkesh M. Mavani, Shell and Tube Heat Exchanger Thermal

Design with Optimization of Mass Flow Rate and Baffle Spacing, International Journal of Advanced Engineering Research and Studies E-ISSN2249–8974, 2012.

[13]. Miguel Toledo-Velazquez, Pedro Quinto-Diez, Juan C. Alzelmetti-Zaragoza, Sergio R. Galvan, Juan Abugaber-Francis and Arturo Reyes-Leon, Delaware Method Improvement for the Shell and Tubes Heat Exchanger Design, Engineering, 6, 193-201, 2014.

[14]. Shridhar S. Thorat, N. K. Sane, B. S. Gawali, Vinaykumar Kabra and Ajit Gavali, Thermal Design of Shell and Tube Heat Exchanger for Concentrating Solar Power Application, International Journal of Current Engineering and Technology, E-ISSN 2277 – 4106, March 2016.

[15]. Ender Ozden and Ilker Tari, Shell Side CFD Analysis of a Small Shell-and-Tube Heat Exchanger. Middle East Technical University 2010, 06531, Ankara, Turkey.

[16]. Heidar Sadeghzadeh, Mehdi Aliehyaei and Marc A. Rosen, Optimization of a Finned Shell and Tube Heat Exchanger Using a Multi-Objective Optimization Genetic Algorithm, ISSN 2071-1050, 25 August 2015.

[17]. Fabio Toshio Kanizawa and Gherhardt Ribatski, Two-Phase Pressure Drop During Upward Cross Flow in Triangular Tube Bundle. Published by EDP Sciences, 2014.

[18]. Kevin M. Lunsford, Increasing Heat Exchanger Performance, Bryan Research and Engineering, Inc., Bryan, Texas, Hydrocarbon Engineering, March 1998.

[19]. Andressa Nakao, Andrea Valdman, Andre L. H. Costa, Miguel J. Bagajewicz and Eduardo M. Queiroz, Incorporated Fouling Modeling in to Sell-And Tube Heat Exchanger Design, Industrial & Engineering Chemistry Research, ie-2016-03564a, 14-Sep-2016.

[20]. Sandeep M and U Sathishkumar, CFD Investigation of Influence of Tube Bundle Cross-Section over Pressure Drop and Heat Transfer Rate, International Journal of Science, Engineering and Technology Research (IJSETR), Volume 4, Issue 5, May 2015.

[21]. Antonio C. Caputo, Marcello P. Pelagagge and Paolo Salini, Heat Exchanger Design Based on Economic Optimization, ENCIT 2006 -- ABCM, Curitiba, Brazil, Dec. 5-8, CIT06-0387, 2006.

[22]. Alok Shukla, Prakash Kumar and Deo. Raj Tiwari, Design Procedure of Shell and Tube Heat Exchanger, International Journal of Engineering and Technical Research (IJETR)

ISSN: 2321-0869 (O) 2454-4698 (P), Volume-3, Issue-12, December 2015.

[23]. Piyush Gupta, Avdhesh Kr. Sharma and Raj Kumar, Thermal Design of Shell and Tube Heat Exchanger Using Elliptical Tube, International Journal of Engineering and Manufacturing Science. ISSN 2249-3115 Vol. 7, 2017.

[24]. Akhilesh Mishra, A B Jayant and Ashok Kumar Gupta, Finite Element Analysis of Shell and Tube Heat Exchanger With and Without Baffles, International Journal of Engineering Science and Management(IJESM), ISSN: 2277-5528, April-June 2016.

[25]. Junichi Okamoto, Akira Usami and Hiroyuki Mimura, Sulfuric Acid Dew Resistant Steel S-TEN 1 Tube, Nippon Steel Technical Report No. 87 January 2003.

[26]. Akira Usami, Motohiro Okushima, Shunji Sakamoto, Satoshi Nishimura, Takashi Kusunoki and Kazuhiro Kojima, New S-TEN™1: An Innovative Acid-Resistant Low-Alloy Steel, Nippon Steel Technical Report No. 90 July 2004.

[27]. Ramesh K. Shah, Fundamental of Heat Exchanger Design, Rochester Institute of Technology, Rochester, New York, 2003.

[28]. Sadik Kakac and Hongtan Liu, Heat Exchangers: Selection Rating and Thermal Design, Department of Mechanical Engineering, University of Miami, Coral Gables, Florida, 2nd ed. 2002.

[29]. Usman Ur Rehman, Heat Transfer Optimization of Shell-and-Tube Heat Exchanger through CFD Studies, Chalmers University of Technology, G Oteborg, Sweden 2011.

[30]. Jussi Saari, Heat Exchanger Dimensioning, Lappeenranta University of Technology, Faculty of Technology, 2008.

[31]. Robert W. Serth, Process Heat Transfer Principles and Applications, Texas A&M University-Kingsville, Kingsville, Texas, USA, First edition 2007.

[32]. R. K. Shah, Heat Exchangers, in Encyclopedia of Energy Technology and the Environment, edited by A. Bisio and S. G. Boots, pp. 1651-1670, John Wiley & Sons, New York, 1994.

[33]. Frank P. Incropera, Theodore L. Bergman, Adrienne S. Lavine and David P. Dewitt Fundamentals of Heat and Mass Transfer, Seventh Edition, 2011.

[34]. Daniel Walraven, Optimum Configuration of Shell-and-Tube Heat Exchangers for the Use in Low-Temperature Organic Rankin Cycles, KU Leuven Energy Institute, TME Branch, July 2014.

[35]. D. Scap, M. Hoic and A. Jokic, Determination of the Pareto Frontier for Multi-Objective Optimization Problem, ISSN 1333-1124, 16 May 2013.

[36]. Indra Chandra Joseph Riadi, Cognitive Ant Colony Optimization: A New Framework in Swarm Intelligence, School of Computing, Science and Engineering College of Science and Technology University of Salford, Manchester, UK, 2014.

[37]. Hilbert, R., Janiga, G., Baron, R., and Thevenin, D., Multi-Objective Shape Optimization of a Heat Exchanger Using Parallel Genetic Algorithm, ISSN 49, 2567–2577, 2006.

[38]. R. Seidlova and J. Pozivil, Implementation of Ant Colony Algorisms in MATLAB, Institute of Chemical Technology, Department of Computing and Control Engineering Technicka , Prague , 166 28, Czech Republic, 2013.

[39]. Julien Legriel, Colas Le Guernic, Scott Cotton, and Oded Maler, Approximating the Pareto Front of Multi-Criteria Optimization Problems, CNRS- VERIMAG, 38610 Gieres, France, 2010.

[40]. Heidar Sadeghzadeh, Mehdi Aliehyaei and Marc A. Rosen, Optimization of a Finned Shell and Tube Heat Exchanger Using a Multi-Objective Optimization Genetic Algorithm, ISSN 2071-1050, 25 August 2015.

APPENDIX

Appendix A.

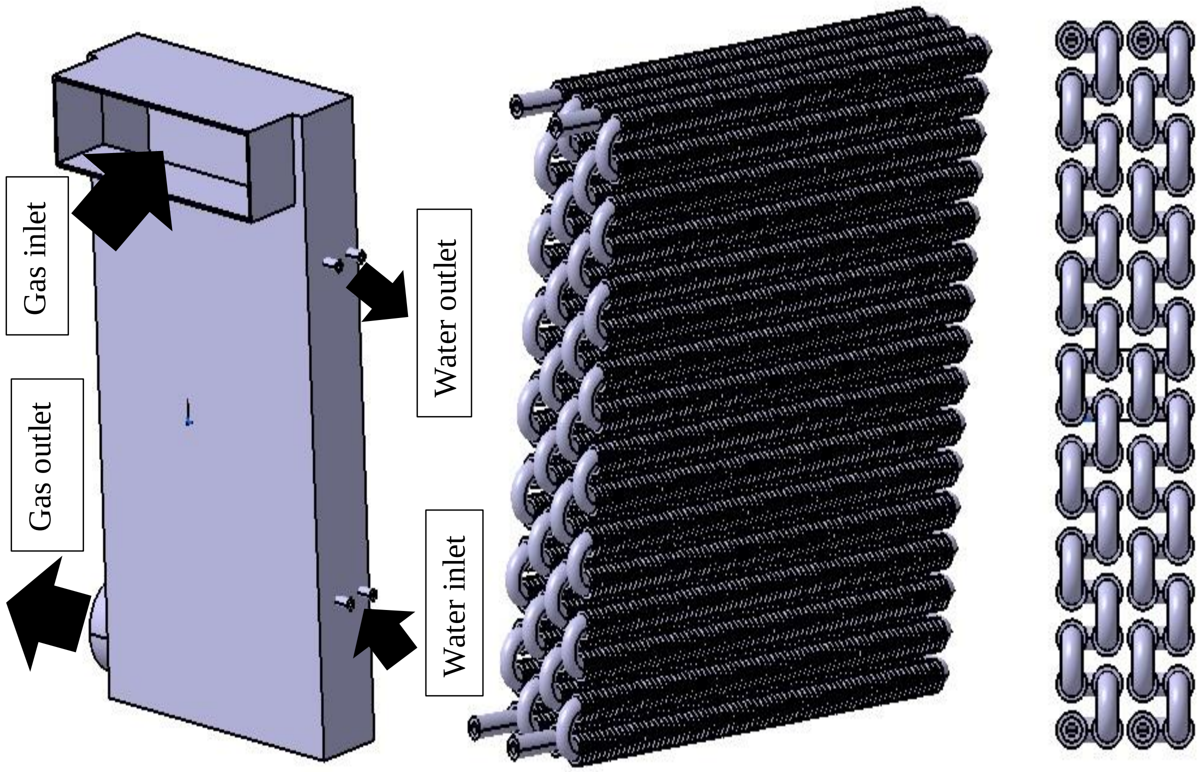

Figure A. Rough sketch of existing shell and tube heat exchanger (CATIA V5 R19)

Appendix B.

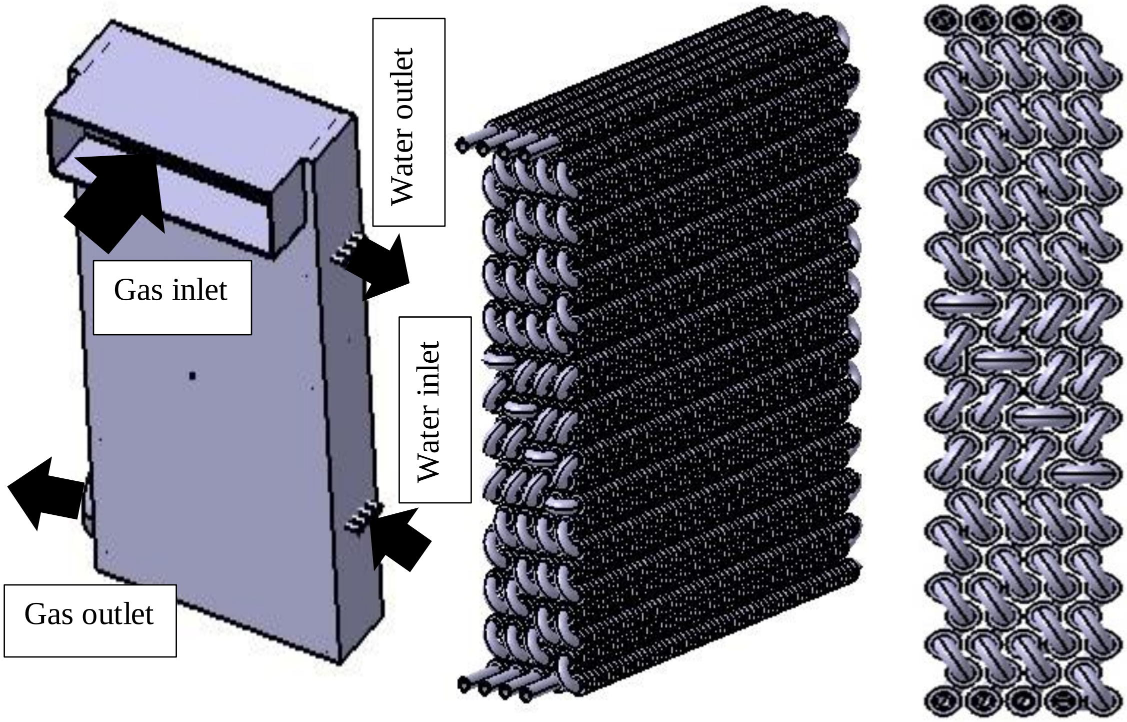

Figure B. Rough sketch modified shell and tube heat exchanger (CATIA V5 R19)

Appendix C. Effect of diameter (Di) on objective functions

Unites of parameters throughout the appendix is: D_r(m), ℓ (m), b (m), τ (m), Pt (m), X_t(m), X_L(m), D_f(m), V_{max}(m/s), h_o(W/m^2.k), D_i(m), A_b**(m^2),** A_f**(m^2),** **A**(m^2)**,** A_i**(m^2),** η_f**(%),** η_w**(%),** h_i(W/m^2.k), **(**W/m^2.k**),** $\dot{Q}$(W), A_o**(m^2),** Dh (m), $G_s(\frac{kg}{s})$**,** $G_s(\frac{kg}{s})$**,** $P_{tT}(P_a)$**,** $\Delta P_r(P_a)$, $\Delta P_{ft}(P_a)$

D_r	**ℓ**	**b**	**τ**	P_t	X_t	X_L	N_f	D_f	V_{max}	R_{es}	N_{us}	h_o	D_i	N_{T1}	N_{T2}
0.05	0.023	0.02	0.007	0.10395	0.10395	0.090023	33.33333	0.09	52.79521	77450.57	301.5313	226.1485	0.034	5.098605	4.098605
0.052	0.023	0.02	0.007	0.10626	0.10626	0.092024	33.33333	0.092	53.59605	81770.42	312.8849	225.6382	0.036	4.987766	3.987766
0.054	0.023	0.02	0.007	0.10857	0.10857	0.094024	33.33333	0.094	54.38591	86166.86	324.245	225.1702	0.038	4.881643	3.881643
0.05	0.02	0.02	0.00	0.11	0.11	0.09	33.3	0.09	55.1	9063	335.	224.	0.04	4.77	3.77

6	3		7	088	088	6025	3333	6	6502	8.33	6109	7394		9942	9942
0.058	0.023	0.02	0.007	0.11319	0.11319	0.098025	33.33333	0.098	55.93359	95183.31	346.9817	224.3416	0.042	4.682392	3.682392
0.06	0.023	0.02	0.007	0.1155	0.1155	0.100026	33.33333	0.1	56.69185	99800.33	358.3567	223.9729	0.044	4.588745	3.588745
0.062	0.023	0.02	0.007	0.11781	0.11781	0.102026	33.33333	0.102	57.43999	104487.9	369.7351	223.6301	0.046	4.498769	3.498769
N_t	n_p	A_b	A_f	**A**	A_i	**ψ**	**m**	η_f	η_w	R_{et}	N_{ut}	h_i	**U**	**NTU**	**ε**
114.9245	2.597908	30.44819	90.81504	121.2632	27.00622	0.028951	37.68401	0.730753	0.798359	82044.12	233.024	4674.187	117.8047	1.355269	0.617015
109.739	2.781118	30.23732	89.09391	119.3312	27.3046	0.028796	37.64147	0.733125	0.800748	86870.24	243.9268	4621.057	118.5436	1.342041	0.614668
104.8866	2.961695	30.01183	87.42576	117.4376	27.54709	0.02865	37.60241	0.73535	0.802983	91696.37	254.709	4571.357	119.218	1.328258	0.612185
100.3394	3.139388	29.77409	85.80857	115.5827	27.73984	0.028512	37.56643	0.737443	0.805078	96522.49	265.3783	4524.701	119.8361	1.314056	0.609585
96.07276	3.313998	29.52617	84.24034	113.7665	27.88829	0.028382	37.53317	0.739416	0.807047	101348.6	275.9414	4480.763	120.4047	1.299545	0.606885
92.06413	3.485372	29.26986	82.71916	111.989	27.99726	0.028258	37.50231	0.74128	0.8089	106174.7	286.4044	4439.268	120.9293	1.284815	0.604099
88.29334	3.653398	29.00671	81.24321	110.2499	28.07101	0.028141	37.4736	0.743043	0.810648	111000.9	296.7726	4399.976	121.4148	1.269941	0.601237
$\dot{Q}$	**a**	A_o	D_h	R_{esp}	R_{eeff}	f_s	G_s	N_r	ΔP_{fs}	ΔP_{fsT}	G_s	f_t	ΔP_{ft}	ΔP_r	ΔP_{tT}
817520.1	0.279	0.500462	0.036979	57282.37	65874.72	0.108015	39.96597	24.88244	11342.07	12476.28	62.24488	0.022203	335.0219	7.49952	342.5214
814410.5	0.274231	0.492984	0.037016	58209.78	66941.25	0.108067	40.57221	24.34151	11440.07	12584.08	62.24488	0.021877	297.7016	8.243056	305.9446
811120.7	0.269815	0.485824	0.037066	59148.39	68020.65	0.108097	41.17013	23.82361	11532.37	12685.61	62.24488	0.021573	265.8208	8.975907	274.7967

807676.3	0.265714	0.478963	0.037129	60097.64	69112.28	0.108109	41.75992	23.32728	11619.28	12781.21	62.24488	0.021289	238.3998	9.697052	248.0968
804098.9	0.261897	0.472382	0.037204	61057.03	70215.58	0.108106	42.34173	22.85122	11701.11	12871.22	62.24488	0.021022	214.6682	10.40569	225.0739
800406.5	0.258333	0.466063	0.037289	62026.12	71330.04	0.108087	42.91573	22.39419	11778.12	12955.94	62.24488	0.020771	194.0135	11.10119	205.1147
796614.5	0.255	0.459993	0.037384	63004.53	72455.21	0.108056	43.48207	21.95509	11850.57	13035.63	62.24488	0.020534	175.9438	11.7831	187.7269

Appendix D. Effect of fin space (ℓ) on objective functions

D_r	**ℓ**	**b**	**τ**	P_t	X_t	X_L	N_f	D_f	V_{max}	R_{es}	N_{us}	h_o	D_i	N_{T1}	N_{T2}
0.056	0.017	0.02	0.007	0.11088	0.11088	0.096025	41.66667	0.096	58.14369	95532.41	316.4073	211.8799	0.04	4.779942	3.779942
0.056	0.019	0.02	0.007	0.11088	0.11088	0.096025	38.46154	0.096	56.96075	93588.8	323.0769	216.3462	0.04	4.779942	3.779942
0.056	0.021	0.02	0.007	0.11088	0.11088	0.096025	35.71429	0.096	55.98446	91984.71	329.4693	220.6268	0.04	4.779942	3.779942
0.056	0.023	0.02	0.007	0.11088	0.11088	0.096025	33.33333	0.096	55.16502	90638.33	335.6109	224.7394	0.04	4.779942	3.779942
0.056	0.025	0.02	0.007	0.11088	0.11088	0.096025	31.25	0.096	54.46743	89492.17	341.5239	228.6991	0.04	4.779942	3.779942
0.056	0.027	0.02	0.007	0.11088	0.11088	0.096025	29.41176	0.096	53.86641	88504.66	347.2278	232.5186	0.04	4.779942	3.779942
0.056	0.029	0.02	0.007	0.11088	0.11088	0.096025	27.77778	0.096	53.34319	87644.99	352.7393	236.2093	0.04	4.779942	3.779942
N_t	n_p	A_b	A_f	**A**	A_i	**ψ**	**m**	η_f	η_w	R_{et}	N_{ut}	h_i	**U**	**NTU**	**ε**
100.3394	3.13942	27.50867	107.2607	134.7694	27.73984	0.028512	36.47583	0.747968	0.799412	96523.48	265.3805	4524.738	109.8592	1.404628	0.625469
100.3394	3.13942	28.37999	99.00988	127.3899	27.73984	0.028512	36.85826	0.74427	0.801242	96523.48	265.3805	4524.738	113.3629	1.370059	0.619598
100.3394	3.13942	29.12683	91.93775	121.0646	27.73984	0.028512	37.22112	0.740769	0.803137	96523.48	265.3805	4524.738	116.6809	1.340141	0.614328
100.3394	3.13942	29.77409	85.80857	115.5827	27.73984	0.028512	37.56643	0.737443	0.805078	96523.48	265.3805	4524.738	119.8362	1.314058	0.609586
100.3394	3.13942	30.34045	80.44553	110.786	27.73984	0.028512	37.89592	0.734278	0.80705	96523.48	265.3805	4524.738	122.8474	1.291172	0.605307
100.	3.13	30.8	75.7	106.	27.7	0.02	38.2	0.73	0.80	9652	265.	4524	125.	1.27	0.60

3394	942	4017	1344	5536	3984	8512	1106	1256	9039	3.48	3805	.738	7295	0981	1438
100. 3394	3.13 942	31.2 8437	71.5 0714	102. 7915	27.7 3984	0.02 8512	38.5 1313	0.72 8366	0.81 1037	9652 3.48	265. 3805	4524 .738	128. 4955	1.25 308	0.59 7933
$\dot{Q}$	**a**	A_o	D_h	R_{esp}	R_{eeff}	f_s	G_s	N_r	ΔP_{fs}	ΔP_{fsT}	G_s	f_t	ΔP_{ft}	ΔP_r	ΔP_{tT}
8287 20.8	0.26 5714	0.45 4426	0.03 0212	5154 1.71	4381 0.46	0.11 606	44.0 1477	23.3 2728	1385 7.26	1524 2.98	62.2 4552	0.02 1289	238. 404	9.69 7381	248. 1014
8209 42.1	0.26 5714	0.46 3863	0.03 2626	5452 7.45	5180 1.08	0.11 3029	43.1 1929	23.3 2728	1295 1.82	1424 7	62.2 4552	0.02 1289	238. 404	9.69 7381	248. 1014
8139 60.1	0.26 5714	0.47 1952	0.03 4929	5737 6.36	6024 5.18	0.11 0408	42.3 8024	23.3 2728	1222 1.46	1344 3.6	62.2 4552	0.02 1289	238. 404	9.69 7381	248. 1014
8076 76.6	0.26 5714	0.47 8963	0.03 7129	6009 7.64	6911 2.28	0.10 8109	41.7 5992	23.3 2728	1161 9.28	1278 1.21	62.2 4552	0.02 1289	238. 404	9.69 7381	248. 1014
8020 07.8	0.26 5714	0.48 5097	0.03 9233	6269 9.68	7837 4.59	0.10 6072	41.2 3185	23.3 2728	1111 3.78	1222 5.16	62.2 4552	0.02 1289	238. 404	9.69 7381	248. 1014
7968 81.9	0.26 5714	0.49 051	0.04 1247	6519 0.14	8800 6.69	0.10 4248	40.7 7687	23.3 2728	1068 2.99	1175 1.29	62.2 4552	0.02 1289	238. 404	9.69 7381	248. 1014
7922 37.1	0.26 5714	0.49 5321	0.04 3176	6757 6.06	9798 5.28	0.10 2603	40.3 8079	23.3 2728	1031 1.14	1134 2.25	62.2 4552	0.02 1289	238. 404	9.69 7381	248. 1014

Appendix E. Effect of Fine height (b) on objective functions

D_r	**ℓ**	**b**	**τ**	P_t	X_t	X_L	N_f	D_f	V_{max}	R_{es}	N_{us}	h_o	D_i	N_{T1}	N_{T2}
0.05 6	0.02 3	0.01 4	0.00 7	0.09 702	0.09 702	0.08 4022	33.3 3333	0.08 4	63.7 4956	1047 43.1	397. 7337	266. 3395	0.04	5.46 2791	4.46 2791
0.05 6	0.02 3	0.01 6	0.00 7	0.10 164	0.10 164	0.08 8023	33.3 3333	0.08 8	60.3 3533	9913 3.36	373. 0047	249. 78	0.04	5.21 4482	4.21 4482
0.05 6	0.02 3	0.01 8	0.00 7	0.10 626	0.10 626	0.09 2024	33.3 3333	0.09 2	57.5 225	9451 1.76	352. 6663	236. 1605	0.04	4.98 7766	3.98 7766
0.05 6	0.02 3	0.02	0.00 7	0.11 088	0.11 088	0.09 6025	33.3 3333	0.09 6	55.1 6502	9063 8.33	335. 6109	224. 7394	0.04	4.77 9942	3.77 9942
0.05 6	0.02 3	0.02 2	0.00 7	0.11 55	0.11 55	0.10 0026	33.3 3333	0.1	53.1 606	8734 4.99	321. 0785	215. 0079	0.04	4.58 8745	3.58 8745
0.05 6	0.02 3	0.02 4	0.00 7	0.12 012	0.12 012	0.10 4027	33.3 3333	0.10 4	51.4 3546	8451 0.52	308. 5294	206. 6045	0.04	4.41 2254	3.41 2254
0.05 6	0.02 3	0.02 6	0.00 7	0.12 474	0.12 474	0.10 8028	33.3 3333	0.10 8	49.9 3503	8204 5.25	297. 5695	199. 2653	0.04	4.24 8838	3.24 8838
N_t	n_p	A_b	A_f	**A**	A_i	**ψ**	**m**	η_f	η_w	R_{et}	N_{ut}	h_i	**U**	**NTU**	**ε**
132. 8068	4.15 5259	39.4 0825	77.9 5981	117. 3681	36.7 1576	0.02 0474	40.8 9574	0.81 7365	0.87 8688	9652 3.48	265. 3805	4524 .738	153. 4614	1.70 8766	0.66 8429
120. 4739	3.76 9387	35.7 4867	81.0 4512	116. 7938	33.3 0621	0.02 3107	39.6 04	0.79 0689	0.85 4756	9652 3.48	265. 3805	4524 .738	140. 6443	1.55 8388	0.64 8993
109. 739	3.43 3514	32.5 6327	83.6 3299	116. 1963	30.3 3845	0.02 5788	38.5 0915	0.76 3968	0.83 0114	9652 3.48	265. 3805	4524 .738	129. 5535	1.42 8154	0.62 9335
100.	3.13	29.7	85.8	115.	27.7	0.02	37.5	0.73	0.80	9652	265.	4524	119.	1.31	0.60

3394	942	7409	0857	5827	3984	8512	6643	7443	5078	3.48	3805	.738	8362	4058	9586
92.06413	2.880503	27.31853	87.63989	114.9584	25.45205	0.031279	36.74409	0.711319	0.779921	96523.48	265.3805	4524.738	111.2394	1.213202	0.58986
84.74209	2.651411	25.14584	89.18182	114.3277	23.4278	0.034085	36.01888	0.685759	0.754875	96523.48	265.3805	4524.738	103.575	1.123415	0.570262
78.23351	2.44777	23.21452	90.47896	113.6935	21.62844	0.03693	35.37334	0.660894	0.730134	96523.48	265.3805	4524.738	96.69948	1.043022	0.550885
$Q^{\cdot}$	**a**	A_o	D_h	R_{esp}	R_{eeff}	f_s	G_s	N_r	ΔP_{fs}	ΔP_{fsT}	G_s	f_t	ΔP_{ft}	ΔP_r	ΔP_{tT}
885641	0.2325	0.414466	0.031641	59183.44	97229.93	0.104896	48.25842	26.65975	17206.58	18927.24	62.24552	0.021289	315.5457	13.82013	329.3658
859889.3	0.243571	0.437919	0.033596	59474.44	85494.51	0.106164	45.67385	25.44795	14890.1	16379.11	62.24552	0.021289	286.243	12.25408	298.4971
833844.1	0.254643	0.459333	0.03542	59780.28	76385.92	0.107221	43.54453	24.34151	13074.59	14382.05	62.24552	0.021289	260.7372	10.89095	271.6282
807676.6	0.265714	0.478963	0.037129	60097.64	69112.28	0.108109	41.75992	23.32728	11619.28	12781.21	62.24552	0.021289	238.404	9.697381	248.1014
781540.7	0.276786	0.497022	0.038739	60423.97	63170.52	0.108859	40.24257	22.39419	10430.47	11473.52	62.24552	0.021289	218.7421	8.646573	227.3887
755574.4	0.287857	0.513692	0.040259	60757.34	58225.79	0.109493	38.93664	21.53288	9443.623	10387.99	62.24552	0.021289	201.3452	7.716811	209.062
729900.2	0.298929	0.529128	0.0417	61096.25	54046.68	0.11003	37.80082	20.73536	8613.05	9474.355	62.24552	0.021289	185.8809	6.890342	192.7713

Appendix F. Effects of fin thickness (τ) on objective functions

D_r	**ℓ**	**b**	**τ**	P_t	X_t	X_L	N_f	D_f	V_{max}	R_{es}	N_{us}	h_o	D_i	N_{T1}	N_{T2}
0.056	0.023	0.02	0.013	0.11088	0.11088	0.096025	27.77778	0.096	62.13795	102095.1	339.2751	227.1932	0.04	4.779942	3.779942
0.056	0.023	0.02	0.011	0.11088	0.11088	0.096025	29.41176	0.096	59.91066	98435.61	337.2745	225.8535	0.04	4.779942	3.779942
0.056	0.023	0.02	0.009	0.11088	0.11088	0.096025	31.25	0.096	57.58842	94620.07	335.8724	224.9145	0.04	4.779942	3.779942
0.056	0.023	0.02	0.007	0.11088	0.11088	0.096025	33.33333	0.096	55.16502	90638.33	335.6109	224.7394	0.04	4.779942	3.779942
0.056	0.023	0.02	0.005	0.11088	0.11088	0.096025	35.71429	0.096	52.6337	86479.28	337.6873	226.1299	0.04	4.779942	3.779942
0.056	0.023	0.02	0.003	0.11088	0.11088	0.096025	38.46154	0.096	49.98711	82130.81	345.4728	231.3434	0.04	4.779942	3.779942
0.056	0.023	0.02	0.001	0.11088	0.11088	0.096025	41.66667	0.096	47.21716	77579.69	376.4083	252.0591	0.04	4.779942	3.779942
N_t	n_p	A_b	A_f	**A**	A_i	**ψ**	**m**	η_f	η_w	R_{et}	N_{ut}	h_i	**U**	**NTU**	**ε**
100.3394	3.13942	24.81174	82.60307	107.4148	27.73984	0.032677	27.7163	0.793933	0.841533	96523.48	265.3805	4524.738	127.1613	1.295845	0.60619
100.3394	3.13942	26.27126	83.54587	109.8171	27.73984	0.031279	30.04183	0.782265	0.834353	96523.48	265.3805	4524.738	125.1247	1.303607	0.607646
100.3394	3.13942	27.91321	84.60651	112.5197	27.73984	0.02989	33.14338	0.764785	0.823135	96523.48	265.3805	4524.738	122.7432	1.310267	0.608885

100.3394	3.13942	29.77409	85.80857	115.5827	27.73984	0.028512	37.56643	0.737443	0.805078	96523.48	265.3805	4524.738	119.8362	1.314058	0.609586
100.3394	3.13942	31.90081	87.18235	119.0832	27.73984	0.027144	44.58649	0.691382	0.774057	96523.48	265.3805	4524.738	115.9881	1.310381	0.608906
100.3394	3.13942	34.35472	88.76748	123.1222	27.73984	0.025788	58.22067	0.603047	0.713809	96523.48	265.3805	4524.738	109.9926	1.284794	0.604095
100.3394	3.13942	37.21762	90.6168	127.8344	27.73984	0.024442	105.2593	0.384192	0.563478	96523.48	265.3805	4524.738	96.76986	1.173604	0.581468
Q˙	**a**	A_o	D_h	R_{esp}	R_{eeff}	f_s	G_s	N_r	ΔP_{fs}	ΔP_{fsT}	G_s	f_t	ΔP_{ft}	ΔP_r	ΔP_{tT}
803177.2	0.265714	0.425215	0.035469	64667.47	74367.59	0.106914	47.03843	23.32728	14579.36	16037.29	62.24552	0.021289	238.404	9.697381	248.1014
805106.2	0.265714	0.441023	0.035983	63252.84	72740.77	0.107273	45.35237	23.32728	13598.35	14958.18	62.24552	0.021289	238.404	9.697381	248.1014
806747.7	0.265714	0.458808	0.036535	61733.58	70993.62	0.107669	43.59443	23.32728	12610.99	13872.09	62.24552	0.021289	238.404	9.697381	248.1014
807676.6	0.265714	0.478963	0.037129	60097.64	69112.28	0.108109	41.75992	23.32728	11619.28	12781.21	62.24552	0.021289	238.404	9.697381	248.1014
806775.8	0.265714	0.501998	0.037771	58331.04	67080.7	0.108602	39.84371	23.32728	10625.63	11688.19	62.24552	0.021289	238.404	9.697381	248.1014
800401.2	0.265714	0.528576	0.038466	56417.48	64880.11	0.109157	37.84024	23.32728	9632.906	10596.2	62.24552	0.021289	238.404	9.697381	248.1014
770421.6	0.265714	0.559585	0.039222	54337.83	62488.5	0.109788	35.74339	23.32728	8644.567	9509.024	62.24552	0.021289	238.404	9.697381	248.1014

Appendix G. STHEs at 14mm fin space

D_r	**ℓ**	**b**	**τ**	P_t	X_t	X_L	N_f	D_f	V_{max}	R_{es}	N_{us}	h_o	D_i	N_{T1}	N_{T2}
0.056	0.014	0.011	0.007	0.09009	0.09009	0.07802	47.61905	0.078	76.29775	125424.3	403.89	270.2457	0.04	5.883006	4.883006
0.056	0.014	0.014	0.007	0.09702	0.09702	0.084022	47.61905	0.084	69.3828	114057	360.7598	241.3869	0.04	5.462791	4.462791
0.056	0.014	0.017	0.007	0.10395	0.10395	0.090023	47.61905	0.09	64.32989	105750.6	329.6025	220.5394	0.04	5.098605	4.098605
0.056	0.014	0.02	0.007	0.11088	0.11088	0.096025	47.61905	0.096	60.47615	99415.54	305.9173	204.6914	0.04	4.779942	3.779942
0.056	0.014	0.023	0.007	0.11781	0.11781	0.102026	47.61905	0.102	57.43999	94424.44	287.2305	192.188	0.04	4.498769	3.498769
0.056	0.014	0.026	0.007	0.12474	0.12474	0.108028	47.61905	0.108	54.98617	90390.66	272.0628	182.0391	0.04	4.248838	3.248838
0.056	0.014	0.029	0.007	0.13167	0.13167	0.11403	47.61905	0.114	52.96181	87062.86	259.4719	173.6145	0.04	4.025215	3.025215
N_t	n_p	A_b	A_f	**A**	A_i	**ψ**	**m**	η_f	η_w	R_{et}	N_{ut}	h_i	**U**	**NTU**	**ε**
155.0488	4.85	40.0	103.	143.	42.8	0.01	41.1	0.86	0.90	9402	259.	4430	156.	2.17	0.70

	1167	0714	0796	0868	6479	6618	9454	8405	5199	0.44	8606	.624	024	453	5813
132. 8068	4.15 5259	34.2 6805	111. 3712	145. 6392	36.7 1576	0.02 0474	38.9 3294	0.83 1027	0.87 0785	9402 0.44	259. 8606	4430 .624	134. 3433	1.90 5763	0.68 5082
114. 9245	3.59 5758	29.6 5389	117. 7078	147. 3617	31.7 7203	0.02 4442	37.2 1375	0.79 2602	0.83 4337	9402 0.44	259. 8606	4430 .624	117. 4813	1.68 6273	0.66 2655
100. 3394	3.13 942	25.8 9052	122. 5837	148. 4742	27.7 3984	0.02 8512	35.8 5173	0.75 4019	0.79 6912	9402 0.44	259. 8606	4430 .624	103. 8941	1.50 2506	0.63 891
88.2 9334	2.76 2522	22.7 8227	126. 3486	149. 1309	24.4 0958	0.03 2677	34.7 3949	0.71 5994	0.75 9381	9402 0.44	259. 8606	4430 .624	92.6 7636	1.34 6205	0.61 4238
78.2 3351	2.44 777	20.1 8654	129. 2557	149. 4422	21.6 2844	0.03 693	33.8 0981	0.67 9078	0.72 2428	9402 0.44	259. 8606	4430 .624	83.2 522	1.21 1835	0.58 9023
69.7 4941	2.18 232	17.9 9739	131. 4912	149. 4886	19.2 8292	0.04 1264	33.0 1819	0.64 3663	0.68 6563	9402 0.44	259. 8606	4430 .624	75.2 3134	1.09 5422	0.56 3621
$\dot{Q}$	**a**	A_o	D_h	R_{esp}	R_{eeff}	f_s	G_s	N_r	ΔP_{fs}	ΔP_{fsT}	G_s	f_t	ΔP_{ft}	ΔP_r	ΔP_{tT}
9060 74.9	0.21 5893	0.34 6301	0.02 1685	4857 0.17	6181 6.58	0.11 3515	57.7 5739	28.7 105	2872 3.7	3159 6.07	60.6 2715	0.02 1434	351. 8667	15.7 9019	367. 6569
8794 61.9	0.23 25	0.38 0815	0.02 3428	4771 8.94	4771 8.94	0.11 6923	52.5 2278	26.6 5975	2271 8.76	2499 0.63	60.6 2715	0.02 1434	301. 3908	13.1 1083	314. 5016
8506 71.5	0.24 9107	0.41 0727	0.02 4973	4716 1.16	3883 8.61	0.11 956	48.6 9773	24.8 8244	1863 9.35	2050 3.29	60.6 2715	0.02 1434	260. 8089	10.9 5665	271. 7655
8201 88.6	0.26 5714	0.43 6899	0.02 6366	4680 7.79	3276 5.45	0.12 165	45.7 8045	23.3 2728	1571 3.42	1728 4.76	60.6 2715	0.02 1434	227. 7096	9.19 9676	236. 9093
7885 16.3	0.28 2321	0.45 9993	0.02 7637	4660 1.67	2836 6.23	0.12 3332	43.4 8207	21.9 5509	1352 5.79	1487 8.36	60.6 2715	0.02 1434	200. 3723	7.74 8554	208. 1208
7561 47.4	0.29 8929	0.48 0521	0.02 881	4650 4.6	2504 0.94	0.12 4696	41.6 2453	20.7 3536	1183 5.76	1301 9.34	60.6 2715	0.02 1434	177. 5426	6.53 6705	184. 0793
7235 38	0.31 5536	0.49 8888	0.02 9902	4649 0.17	2244 3.53	0.12 581	40.0 9209	19.6 4403	1049 5.29	1154 4.81	60.6 2715	0.02 1434	158. 2888	5.51 4676	163. 8035

Appendix H. STHEs at 17mm fin space

D_r	**ℓ**	**b**	**τ**	P_t	X_t	X_L	N_f	D_f	V_{max}	R_{es}	N_{us}	h_o	D_i	N_{T1}	N_{T2}
0.05 6	0.01 7	0.01 1	0.00 7	0.09 009	0.09 009	0.07 802	41.6 6667	0.07 8	73.7 7042	1212 69.7	419. 4949	280. 687	0.04	5.88 3006	4.88 3006
0.05 6	0.01 7	0.01 4	0.00 7	0.09 702	0.09 702	0.08 4022	41.6 6667	0.08 4	66.9 1893	1100 06.7	374. 068	250. 2916	0.04	5.46 2791	4.46 2791
0.05 6	0.01 7	0.01 7	0.00 7	0.10 395	0.10 395	0.09 0023	41.6 6667	0.09	61.9 3373	1018 11.6	341. 3422	228. 3945	0.04	5.09 8605	4.09 8605
0.05 6	0.01	0.02	0.00	0.11	0.11	0.09	41.6	0.09	58.1	9558	316.	211.	0.04	4.77	3.77

	7		7	088	088	6025	6667	6	4369	1.25	5174	7841		9942	9942
0.056	0.017	0.023	0.007	0.11781	0.11781	0.102026	41.66667	0.102	55.16502	90684.67	296.9647	198.7012	0.04	4.498769	3.498769
0.056	0.017	0.026	0.007	0.12474	0.12474	0.108028	41.66667	0.108	52.76236	86734.99	281.1159	188.0967	0.04	4.248838	3.248838
0.056	0.017	0.029	0.007	0.13167	0.13167	0.11403	41.66667	0.114	50.78336	83481.76	267.9749	179.3039	0.04	4.025215	3.025215
N_t	n_p	A_b	A_f	**A**	A_i	**ψ**	**m**	η_f	η_w	R_{et}	N_{ut}	h_i	**U**	**NTU**	**ε**
155.0488	4.851167	42.50759	90.19467	132.7023	42.86479	0.016618	41.9828	0.864146	0.907663	94020.44	259.8606	4430.624	163.6118	2.114792	0.701743
132.8068	4.155259	36.4098	97.44976	133.8596	36.71576	0.020474	39.64454	0.826087	0.873391	94020.44	259.8606	4430.624	141.1872	1.840853	0.679035
114.9245	3.595758	31.50726	102.9943	134.5016	31.77203	0.024442	37.87068	0.787088	0.836963	94020.44	259.8606	4430.624	123.6941	1.620507	0.654739
100.3394	3.13942	27.50867	107.2607	134.7694	27.73984	0.028512	36.46758	0.748048	0.799476	94020.44	259.8606	4430.624	109.5587	1.438178	0.629306
88.29334	2.762522	24.20616	110.555	134.7612	24.40958	0.032677	35.32324	0.709684	0.761831	94020.44	259.8606	4430.624	97.85839	1.28451	0.603163
78.23351	2.44777	21.4482	113.0987	134.5469	21.62844	0.03693	34.36773	0.672538	0.724739	94020.44	259.8606	4430.624	88.00631	1.153353	0.576709
69.74941	2.18232	19.12223	115.0548	134.177	19.28292	0.041264	33.55484	0.636991	0.688725	94020.44	259.8606	4430.624	79.60439	1.040375	0.550298
$\dot{\mathbf{Q}}$	**a**	A_o	D_h	R_{esp}	R_{eeff}	f_s	G_s	N_r	ΔP_{fs}	ΔP_{fsT}	G_s	f_t	ΔP_{ft}	ΔP_r	ΔP_{tT}
900850	0.215893	0.358165	0.024183	52370.99	80936.99	0.108962	55.84421	28.7105	25775.43	28352.97	60.62715	0.021434	351.8667	15.79019	367.6569
871698.4	0.2325	0.394836	0.026429	51918.21	63043.54	0.111962	50.65763	26.65975	20237.06	22260.77	60.62715	0.021434	301.3908	13.11083	314.5016
840509.6	0.249107	0.426617	0.02842	51670.39	51670.39	0.114255	46.88383	24.88244	16510.02	18161.02	60.62715	0.021434	260.8089	10.95665	271.7655
807860	0.265714	0.454426	0.030212	51567.71	43832.56	0.116051	44.01477	23.32728	13856.14	15241.76	60.62715	0.021434	227.7096	9.199676	236.9093
774300.1	0.282321	0.478963	0.031845	51570.84	38117.58	0.117477	41.75992	21.95509	11883.38	13071.72	60.62715	0.021434	200.3723	7.748554	208.1208
740340.2	0.298929	0.500774	0.033348	51652.98	33773.11	0.118618	39.94111	20.73536	10366.58	11403.24	60.62715	0.021434	177.5426	6.536705	184.0793
706435.1	0.315536	0.520288	0.034744	51795.38	30362.81	0.119534	38.44301	19.64403	9168.306	10085.14	60.62715	0.021434	158.2888	5.514676	163.8035

Appendix I. STHEs at 20mm fin space

D_r	**ℓ**	**b**	**τ**	P_t	X_t	X_L	N_f	D_f	V_{max}	R_{es}	N_{us}	h_o	D_i	N_{T1}	N_{T2}
0.056	0.02	0.011	0.007	0.09009	0.09009	0.07802	37.03704	0.078	71.91757	118223.9	433.834	290.2814	0.04	5.883006	4.883006
0.056	0.02	0.014	0.007	0.09702	0.09702	0.084022	37.03704	0.084	65.12031	107050	386.3783	258.5285	0.04	5.462791	4.462791
0.056	0.02	0.017	0.007	0.10395	0.10395	0.090023	37.03704	0.09	60.18999	98945.11	352.2603	235.6999	0.04	5.098605	4.098605
0.056	0.02	0.02	0.007	0.11088	0.11088	0.096025	37.03704	0.096	56.45032	92797.54	326.4196	218.4097	0.04	4.779942	3.779942
0.056	0.02	0.023	0.007	0.11781	0.11781	0.102026	37.03704	0.102	53.51646	87974.64	306.0919	204.8083	0.04	4.498769	3.498769
0.056	0.02	0.026	0.007	0.12474	0.12474	0.108028	37.03704	0.108	51.1533	84089.88	289.6315	193.7945	0.04	4.248838	3.248838
0.056	0.02	0.029	0.007	0.13167	0.13167	0.11403	37.03704	0.114	49.20907	80893.81	275.9946	184.67	0.04	4.025215	3.025215
N_t	n_p	A_b	A_f	**A**	A_i	**ψ**	**m**	η_f	η_w	R_{et}	N_{ut}	h_i	**U**	**NTU**	**ε**
155.0488	4.851167	44.45238	80.17304	124.6254	42.86479	0.016618	42.6943	0.860277	0.910115	94020.44	259.8606	4430.624	170.4395	2.068957	0.698425
132.8068	4.155259	38.07561	86.62201	124.6976	36.71576	0.020474	40.2916	0.821581	0.87606	94020.44	259.8606	4430.624	147.3873	1.790164	0.673985
114.9245	3.595758	32.94877	91.55051	124.4993	31.77203	0.024442	38.47157	0.782045	0.839727	94020.44	259.8606	4430.624	129.3519	1.568608	0.648047
100.3394	3.13942	28.76724	95.34285	124.1101	27.73984	0.028512	37.03363	0.742577	0.802244	94020.44	259.8606	4430.624	114.7386	1.387047	0.621133
88.29334	2.762522	25.31364	98.27115	123.5848	24.40958	0.032677	35.86196	0.703894	0.764545	94020.44	259.8606	4430.624	102.6128	1.235211	0.593707
78.23351	2.44777	22.42949	100.5322	122.9617	21.62844	0.03693	34.88438	0.666532	0.72736	94020.44	259.8606	4430.624	92.38008	1.106427	0.566179
69.74941	2.18232	19.99711	102.2709	122.268	19.28292	0.041264	34.05324	0.630861	0.691234	94020.44	259.8606	4430.624	83.63675	0.996058	0.5389
$\dot{Q}$	**a**	A_o	D_h	R_{esp}	R_{eeff}	f_s	G_s	N_r	ΔP_{fs}	ΔP_{fsT}	G_s	f_t	ΔP_{ft}	ΔP_r	ΔP_{tT}
896590.9	0.215893	0.367393	0.026414	55765.1	101391.1	0.105378	54.4416	28.7105	23691.17	26060.29	60.62715	0.021434	351.8667	15.79019	367.6569
865215.6	0.2325	0.405741	0.029154	55732.81	79618.3	0.108063	49.29607	26.65975	18496.49	20346.14	60.62715	0.021434	301.3908	13.11083	314.5016
831918.3	0.249107	0.438977	0.031592	55821.6	65672.47	0.110093	45.56382	24.88244	15025.36	16527.9	60.62715	0.021434	260.8089	10.95665	271.7655
7973	0.26	0.46	0.03	5599	5599	0.11	42.7	23.3	1256	1382	60.6	0.02	227.	9.19	236.

67.9	5714	8058	3791	6.64	6.64	1665	3289	2728	7.15	3.87	2715	1434	7096	9676	9093
762160.2	0.282321	0.493717	0.035795	56234.66	48899.71	0.112898	40.51196	21.95509	10747.79	11822.57	60.62715	0.021434	200.3723	7.748554	208.1208
726821.5	0.298929	0.516526	0.037638	56519.64	43476.64	0.113871	38.72305	20.73536	9353.962	10289.36	60.62715	0.021434	177.5426	6.536705	184.0793
691803.6	0.315536	0.536934	0.039347	56840.28	39200.2	0.114639	37.25127	19.64403	8256.161	9081.777	60.62715	0.021434	158.2888	5.514676	163.8035

Appendix J. STHEs at 23mm fin space

D_r	ℓ	**b**	τ	P_t	X_t	X_L	N_f	D_f	V_{max}	R_{es}	N_{us}	h_o	D_i	N_{T1}	N_{T2}
0.056	0.023	0.011	0.007	0.09009	0.09009	0.07802	33.33333	0.078	70.50098	115895.2	447.1596	299.1977	0.04	5.883006	4.883006
0.056	0.023	0.014	0.007	0.09702	0.09702	0.084022	33.33333	0.084	63.74956	104796.6	397.8721	266.2191	0.04	5.462791	4.462791
0.056	0.023	0.017	0.007	0.10395	0.10395	0.090023	33.33333	0.09	58.86413	96765.56	362.4923	242.5462	0.04	5.098605	4.098605
0.056	0.023	0.02	0.007	0.11088	0.11088	0.096025	33.33333	0.096	55.16502	90684.67	335.7277	224.6378	0.04	4.779942	3.779942
0.056	0.023	0.023	0.007	0.11781	0.11781	0.102026	33.33333	0.102	52.2669	85920.51	314.693	210.5633	0.04	4.498769	3.498769
0.056	0.023	0.026	0.007	0.12474	0.12474	0.108028	33.33333	0.108	49.93503	82087.19	297.673	199.1752	0.04	4.248838	3.248838
0.056	0.023	0.029	0.007	0.13167	0.13167	0.11403	33.33333	0.114	48.01822	78936.19	283.5816	189.7465	0.04	4.025215	3.025215
N_t	n_p	A_b	A_f	**A**	A_i	ψ	**m**	η_f	η_w	R_{et}	N_{ut}	h_i	**U**	**NTU**	ε
155.0488	4.851167	46.00821	72.15573	118.1639	42.86479	0.016618	43.34504	0.85672	0.912507	94020.44	259.8606	4430.624	176.659	2.033272	0.695718
132.8068	4.155259	39.40825	77.95981	117.3681	36.71576	0.020474	40.88649	0.817429	0.878731	94020.44	259.8606	4430.624	153.069	1.749894	0.669755
114.9245	3.595758	34.10197	82.39545	116.4974	31.77203	0.024442	39.02631	0.777392	0.842555	94020.44	259.8606	4430.624	134.5615	1.526904	0.642365
100.3394	3.13942	29.77409	85.80857	115.5827	27.73984	0.028512	37.55794	0.737525	0.805139	94020.44	259.8606	4430.624	119.5268	1.345651	0.614142
88.29334	2.762522	26.19961	88.44403	114.6436	24.40958	0.032677	36.36232	0.698547	0.767438	94020.44	259.8606	4430.624	107.022	1.195082	0.585584
78.23351	2.44777	23.21452	90.47896	113.6935	21.62844	0.03693	35.36534	0.660986	0.730207	94020.44	259.8606	4430.624	96.44731	1.068071	0.557113
69.74941	2.18232	20.697	92.04382	112.7408	19.28292	0.041264	34.51812	0.6252	0.694006	94020.44	259.8606	4430.624	87.39519	0.959717	0.529079

$\dot{Q}$	**a**	A_o	D_h	R_{esp}	R_{eeff}	f_s	G_s	N_r	ΔP_{fs}	ΔP_{fsT}	G_s	f_t	ΔP_{ft}	ΔP_r	ΔP_{tT}
893115.7	0.215893	0.374775	0.028418	58814.46	122975.7	0.102456	53.36924	28.7105	22135.74	24349.31	60.62715	0.021434	351.8667	15.79019	367.6569
859786.1	0.2325	0.414466	0.031641	59213.29	97278.97	0.104888	48.25842	26.65975	17205.31	18925.84	60.62715	0.021434	301.3908	13.11083	314.5016
824624.7	0.249107	0.448864	0.034523	59655.81	80710.8	0.106708	44.56015	24.88244	13928.85	15321.74	60.62715	0.021434	260.8089	10.95665	271.7655
788393.4	0.265714	0.478963	0.037129	60127.95	69147.15	0.108101	41.75992	23.32728	11618.39	12780.23	60.62715	0.021434	227.7096	9.199676	236.9093
751732.7	0.282321	0.505521	0.039509	60620.44	60620.44	0.109181	39.56604	21.95509	9914.238	10905.66	60.62715	0.021434	200.3723	7.748554	208.1208
715184.1	0.298929	0.529128	0.0417	61127.07	54073.94	0.110021	37.80082	20.73536	8612.372	9473.61	60.62715	0.021434	177.5426	6.536705	184.0793
679195.5	0.315536	0.55025	0.043731	61643.59	48889.74	0.110673	36.34979	19.64403	7589.455	8348.401	60.62715	0.021434	158.2888	5.514676	163.8035

Appendix K. STHEs at 26mm fin space

D_r	**ℓ**	**b**	**τ**	P_t	X_t	X_L	N_f	D_f	V_{max}	R_{es}	N_{us}	h_o	D_i	N_{T1}	N_{T2}
0.056	0.026	0.011	0.007	0.09009	0.09009	0.07802	30.30303	0.078	69.3828	114057	459.6437	307.5509	0.04	5.883006	4.883006
0.056	0.026	0.014	0.007	0.09702	0.09702	0.084022	30.30303	0.084	62.67023	103022.3	408.6773	273.4489	0.04	5.462791	4.462791
0.056	0.026	0.017	0.007	0.10395	0.10395	0.090023	30.30303	0.09	57.82201	95052.45	372.1371	248.9996	0.04	5.098605	4.098605
0.056	0.026	0.02	0.007	0.11088	0.11088	0.096025	30.30303	0.096	54.15615	89026.21	344.5208	230.5213	0.04	4.779942	3.779942
0.056	0.026	0.023	0.007	0.11781	0.11781	0.102026	30.30303	0.102	51.28712	84309.87	322.8326	216.0096	0.04	4.498769	3.498769
0.056	0.026	0.026	0.007	0.12474	0.12474	0.108028	30.30303	0.108	48.9806	80518.23	305.2946	204.2748	0.04	4.248838	3.248838
0.056	0.026	0.029	0.007	0.13167	0.13167	0.11403	30.30303	0.114	47.08592	77403.6	290.7813	194.5639	0.04	4.025215	3.025215
N_t	n_p	A_b	A_f	**A**	A_i	**ψ**	**m**	η_f	η_w	R_{et}	N_{ut}	h_i	**U**	**NTU**	**ε**
155.0488	4.851167	47.28117	65.59612	112.8773	42.86479	0.016618	43.94594	0.85342	0.914818	94020.44	259.8606	4430.624	182.3778	2.005179	0.693508
132.8068	4.155259	40.4986	70.87255	111.3712	36.71576	0.020474	41.43796	0.813573	0.881365	94020.44	259.8606	4430.624	158.3215	1.717463	0.666202

114.9245	3.595758	35.04551	74.90496	109.9505	31.77203	0.024442	39.54209	0.773069	0.845401	94020.44	259.8606	4430.624	139.3991	1.492903	0.637522
100.3394	3.13942	30.59788	78.00779	108.6057	27.73984	0.028512	38.0466	0.732832	0.808102	94020.44	259.8606	4430.624	123.9897	1.311634	0.608133
88.29334	2.762522	26.9245	80.40367	107.3282	24.40958	0.032677	36.82959	0.693581	0.77045	94020.44	259.8606	4430.624	111.1447	1.161923	0.578569
78.23351	2.44777	23.85682	82.2536	106.1104	21.62844	0.03693	35.81522	0.655838	0.733216	94020.44	259.8606	4430.624	100.2607	1.036248	0.549263
69.74941	2.18232	21.26965	83.6762	104.9458	19.28292	0.041264	34.95356	0.61995	0.696976	94020.44	259.8606	4430.624	90.92741	0.929469	0.520561
$\dot{Q}$	**a**	A_o	D_h	R_{esp}	R_{eeff}	f_s	G_s	N_r	ΔP_{fs}	ΔP_{fsT}	G_s	f_t	ΔP_{ft}	ΔP_r	ΔP_{tT}
890277.7	0.215893	0.380815	0.030228	61569.06	145526.9	0.100011	52.52278	28.7105	20927.51	23020.26	60.62715	0.021434	351.8667	15.79019	367.6569
855224.5	0.2325	0.421604	0.033919	62401.7	115888.9	0.102235	47.44137	26.65975	16207.08	17827.79	60.62715	0.021434	301.3908	13.11083	314.5016
818407.1	0.249107	0.456954	0.037238	63208	96671.05	0.103881	43.77127	24.88244	13084.04	14392.45	60.62715	0.021434	260.8089	10.95665	271.7655
780679.6	0.265714	0.487886	0.040251	63990.66	83187.86	0.105128	40.9962	23.32728	10889.33	11978.26	60.62715	0.021434	227.7096	9.199676	236.9093
742727.1	0.282321	0.515178	0.043008	64752.33	73198.28	0.106081	38.82435	21.95509	9275.045	10202.55	60.62715	0.021434	200.3723	7.748554	208.1208
705105.9	0.298929	0.539438	0.04555	65495.44	65495.44	0.106813	37.07831	20.73536	8044.679	8849.147	60.62715	0.021434	177.5426	6.536705	184.0793
668260.7	0.315536	0.561144	0.047909	66222.24	59371.66	0.107371	35.64404	19.64403	7079.833	7787.816	60.62715	0.021434	158.2888	5.514676	163.8035

Appendix L. STHEs at 29mm fin space

D_r	**ℓ**	**b**	**τ**	**P_t**	**X_t**	**X_L**	**N_f**	**D_f**	**V_{max}**	**R_{es}**	**N_{us}**	**h_o**	**D_i**	**N_{T1}**	**N_{T2}**
0.056	0.029	0.011	0.007	0.09009	0.09009	0.07802	27.77778	0.078	68.47773	112569.2	471.4122	315.4253	0.04	5.883006	4.883006
0.056	0.029	0.014	0.007	0.09702	0.09702	0.084022	27.77778	0.084	61.79833	101589	418.8898	280.2821	0.04	5.462791	4.462791
0.056	0.029	0.017	0.007	0.10395	0.10395	0.090023	27.77778	0.09	56.98136	93670.52	381.2716	255.1116	0.04	5.098605	4.098605
0.056	0.029	0.02	0.007	0.11088	0.11088	0.096025	27.77778	0.096	53.34319	87689.8	352.8621	236.1025	0.04	4.779942	3.779942
0.056	0.029	0.023	0.007	0.11781	0.11781	0.102026	27.77778	0.102	50.49827	83013.09	330.5643	221.1829	0.04	4.498769	3.498769

0.056	0.029	0.026	0.007	0.12474	0.12474	0.108028	27.77778	0.108	48.21267	79255.85	312.542	209.1241	0.04	4.248838	3.248838
0.056	0.029	0.029	0.007	0.13167	0.13167	0.11403	27.77778	0.114	46.33622	76171.18	297.634	199.149	0.04	4.025215	3.025215
N_t	n_p	A_b	A_f	A	A_i	ψ	m	η_f	η_w	R_{et}	N_{ut}	h_i	U	NTU	ε
155.0488	4.851167	48.34196	60.12978	108.4717	42.86479	0.016618	44.50497	0.850338	0.917037	94020.44	259.8606	4430.624	187.6754	1.98289	0.691702
132.8068	4.155259	41.40722	64.9665	106.3737	36.71576	0.020474	41.95251	0.80997	0.883941	94020.44	259.8606	4430.624	163.2113	1.691061	0.663208
114.9245	3.595758	35.83179	68.66288	104.4947	31.77203	0.024442	40.02445	0.769029	0.84823	94020.44	259.8606	4430.624	143.9214	1.464854	0.633377
100.3394	3.13942	31.28437	71.50714	102.7915	27.73984	0.028512	38.50442	0.728449	0.811095	94020.44	259.8606	4430.624	128.1768	1.283339	0.602945
88.29334	2.762522	27.52858	73.70336	101.2319	24.40958	0.032677	37.268	0.688947	0.773534	94020.44	259.8606	4430.624	115.0248	1.134184	0.57248
78.23351	2.44777	24.39207	75.39913	99.7912	21.62844	0.03693	36.23784	0.651037	0.736335	94020.44	259.8606	4430.624	103.8594	1.009515	0.542427
69.74941	2.18232	21.74685	76.70318	98.45004	19.28292	0.041264	35.36302	0.615058	0.700089	94020.44	259.8606	4430.624	94.26871	0.903978	0.513131
$\dot{Q}$	a	A_o	D_h	R_{esp}	R_{eeff}	f_s	G_s	N_r	ΔP_{fs}	ΔP_{fsT}	G_s	f_t	ΔP_{ft}	ΔP_r	ΔP_{tT}
887959.7	0.215893	0.385848	0.031872	64069.67	168910.9	0.097924	51.83764	28.7105	19959.64	21955.61	60.62715	0.021434	351.8667	15.79019	367.6569
851381.4	0.2325	0.427552	0.036013	65333.32	135333.3	0.099973	46.78133	26.65975	15410.53	16951.58	60.62715	0.021434	301.3908	13.11083	314.5016
813086.5	0.249107	0.463695	0.03976	66508.17	113455.1	0.101473	43.13489	24.88244	12411.77	13652.94	60.62715	0.021434	260.8089	10.95665	271.7655
774019.9	0.265714	0.495321	0.043176	67610.14	98034.71	0.102595	40.38079	23.32728	10310.37	11341.41	60.62715	0.021434	227.7096	9.199676	236.9093
734911	0.282321	0.523226	0.046311	68651.74	86560.89	0.103443	38.22719	21.95509	8768.291	9645.12	60.62715	0.021434	200.3723	7.748554	208.1208
696331.1	0.298929	0.54803	0.049206	69642.9	77678.62	0.104083	36.49699	20.73536	7595.216	8354.737	60.62715	0.021434	177.5426	6.536705	184.0793
658722.5	0.315536	0.570224	0.051896	70591.63	70591.63	0.104562	35.07652	19.64403	6676.803	7344.483	60.62715	0.021434	158.2888	5.514676	163.8035

Appendix M. STHEs at 32mm fin space

D_r	ℓ	b	τ	P_t	X_t	X_L	N_f	D_f	V_{max}	R_{es}	N_{us}	h_o	D_i	N_{T1}	N_{T2}
0.056	0.032	0.01	0.00	0.09	0.09	0.07	25.6	0.07	67.73	11134	482.5	322.8	0.04	5.88	4.88

		1	7	009	009	802	4103	8	014	0.2	615	854		3006	3006
0.056	0.032	0.014	0.007	0.09702	0.09702	0.084022	25.64103	0.084	61.07929	100407	428.5849	286.7692	0.04	5.462791	4.462791
0.056	0.032	0.017	0.007	0.10395	0.10395	0.090023	25.64103	0.09	56.2889	92532.2	389.9571	260.9231	0.04	5.098605	4.098605
0.056	0.032	0.02	0.007	0.11088	0.11088	0.096025	25	0.096	52.47666336	86265.33736	359.881622	240.7993642	0.04	5	4
0.056	0.032	0.023	0.007	0.11781	0.11781	0.102026	25.64103	0.102	49.84949	81946.58	337.9326	226.1131	0.04	4.498769	3.498769
0.056	0.032	0.026	0.007	0.12474	0.12474	0.108028	25.64103	0.108	47.58145	78218.2	319.4545	213.7493	0.04	4.248838	3.248838
0.056	0.032	0.029	0.007	0.13167	0.13167	0.11403	25.64103	0.114	45.72025	75158.61	304.1747	203.5254	0.04	4.025215	3.025215
N_t	n_p	A_b	A_f	A	A_i	ψ	m	η_f	η_w	R_{et}	N_{ut}	h_i	U	NTU	ε
155.0488	4.851167	49.23956	55.50441	104.744	42.86479	0.016618	45.02819	0.847443	0.919159	94020.44	259.8606	4430.624	192.6129	1.96512	0.690229
132.8068	4.155259	42.17606	59.96908	102.1451	36.71576	0.020474	42.43523	0.806586	0.886447	94020.44	259.8606	4430.624	167.7895	1.669387	0.660681
114.9245	3.595758	36.4971	63.38112	99.87822	31.77203	0.024442	40.47776	0.765237	0.851023	94020.44	259.8606	4430.624	148.1722	1.441492	0.629819
102	3	32.5697	65.4214	97.99124	28.19892	0.0285121	38.88552	0.72481	0.81627734	88382.3529	247.317640	4216.76577	131.979148	1.259700	0.598474
88.29334	2.762522	28.03972	68.03387	96.07359	24.40958	0.032677	37.68106	0.684604	0.776654	94020.44	259.8606	4430.624	118.6956	1.110743	0.567172
78.23351	2.44777	24.84497	69.5992	94.44417	21.62844	0.03693	36.63639	0.646543	0.739525	94020.44	259.8606	4430.624	107.2733	0.986828	0.536447
69.74941	2.18232	22.15064	70.80294	92.95358	19.28292	0.041264	35.74947	0.610482	0.703303	94020.44	259.8606	4430.624	97.44594	0.882276	0.506617
$\dot{Q}$	a	A_o	D_h	R_{esp}	R_{eeff}	f_s	G_s	N_r	ΔP_{fs}	ΔP_{fsT}	G_s	f_t	ΔP_{ft}	ΔP_r	ΔP_{tT}
886068.3	0.215893	0.390107	0.03337	66349.87	193017.8	0.096113	51.27172	28.7105	19165.19	21081.71	60.62715	0.021434	351.8667	15.79019	367.6569
848136.	0.2325	0.43258	0.03794	68037.9	155515.4	0.098013	46.23702	26.6597	14758.81	16234.69	60.62715	0.021434	301.3908	13.11083	314.5016

5		5	6	8				5								
808518.3	0.249107	0.4694	0.04211	69582.23	130978.3	0.099387	42.6107	24.88244	11862.99	13049.29	60.62715	0.021434	260.8089	10.95665	271.7655	
768280.4	0.265714	0.5035	0.046038	70922.13	113475.42	0.10042	39.724834	23	9629.6574	10592.623	56.991544	0.0217796	207.84468	7.6550689	215.49975	
728097.3	0.282321	0.530036	0.049432	72337.76	100643.8	0.101161	37.73606	21.95509	8355.883	9191.471	60.62715	0.021434	200.3723	7.748554	208.1208	
688654.6	0.298929	0.5553	0.052682	73585.79	90567.12	0.101722	36.01916	20.73536	7229.825	7952.808	60.62715	0.021434	177.5426	6.536705	184.0793	
650359.9	0.315536	0.577906	0.055706	74765.8	82500.19	0.102132	34.61023	19.64403	6349.453	6984.398	60.62715	0.021434	158.2888	5.514676	163.8035	

Appendix N.

Existing Shell and Tube Heat Exchanger Cost Estimation MATLAB Code

```
%A=Heat transfer area
%PtT=Pressure drop in the tube
%PfsT=Pressure drop in the shell
%CopT=Oprating cost
%Cin=Investment cost
%CT=Total cost
clc
clear
A=94.54;
PtT=149.74;
PfsT=12209;
P=1/0.75*(20*PfsT/0.757+2.5*PtT/954.675);
Co=P*8040*0.06/1000;
```

```
sum=0;
for i=1:1:20
   Cop=Co/(1.1^i);
   sum=sum+Cop;
end
CopT=sum;
CB=exp(11.667-0.809*log(A*0.09290304)+0.009005*(log(A*0.09290304))^2);
Fm=1.55+(A*0.09290304/100)^0.05;
Cin=CB*Fm*1.25*0.9876;
CT=Cin+CopT;
```

Appendix O

Modified Shell and Tube Heat Exchanger MATLAB Code

```
clc
clear
for Di=0.031:0.003:0.049            %Di tube diameter
   for b=0.011:0.003:0.029          %Fin height
      for l=0.014:0.003:0.032       %Fin space
         for t=0.001:0.002:0.013    %Fin thickness
Dr=Di+0.016;                        %Root diameter
Pt=1.155*(Dr+2*b);                  %Tube pitch
XT=Pt;                              %Transvers pitch
XL=3^0.5/2*Pt;                      %Longitudnal pitch
Nr1=(0.53/XT);                      %Number of tubes in the 1st, 3rd, 5th...nth rows
Nr2=Nr1-1;                          %Number of tubes in the 2nd, 4th, 6th...rows
Nf=1/(l+t);                         %Number of fin in a meter length
Nf=floor(Nf);
Df=Dr+2*b;                          %Fin diameter
```

```
% Heat transfer coefficients both in shell and tube sides
NT=1/(2*XT*XL)*(1.1872+0.53*XL+(0.53-XT)*(2.24-XL));        %Total number of tubes
NT=ceil(NT);                                   %Gets rid of decimal part and add 1 to the integer part
np=19.5548*NT*Di^2;                            %Total number of pass
np=ceil(np);                                   %Gets rid of decimal part and add 1 to the integer part
NTp=floor(NT/np);
NT=NTp*np;
for Nr=ceil(2.24/XL)                                  %Number of tube rows)
Nr1=ceil(0.53/XT);
Nr2=Nr1-1;
if mod(Nr,2)==0
   Nr=ceil(2*NT/(Nr1+Nr2));
   NT=NTp*np;
else
   Nr=ceil(2*(NT-Nr1)/(Nr1+Nr2));
   NT=NTp*np;
end
end
Vmax=12.01/(((0.53/XT)-1)*((XT-Dr)-(Df-Dr)*t*Nf)+(XT-Dr)-(Df-Dr)*t*Nf); %Maximum
gas velocity in ashell
Res=2.9355*10^4*Dr*Vmax;                              %Renolds number of gas in the shell
Nus=0.12*Res^0.681*(l/b)^0.2*(l/t)^0.1134;        %Nusselt number in the shell
ho=0.03747*Nus/Dr;                                    %Heat transfer coefficient of gas in the shell
Ab=6.9115*Dr*NT*(1-Nf*t);                             %Base heat transfer area
Af=6.9115*((Df^2-Dr^2)/2+Df*t)*Nf*NT;           %Fin heat transfer area
A=Ab+Af;                                              %Total heat transfer area
Ai=6.9115*NT*Di;                                      %Area in the pipe
w=0.5*(Df+t-Dr)*(1+0.35*log((Df+t)/Dr));
m=(2*ho/45.5/t)^0.5;
eff=tanh(m*w)/(m*w);                                       %Efficiency of single fin
efw=(Ab+eff*Af)/A;                                         %Overall fin efficiency
```

```
Ret=120200*np/(NT*Di);                                   %Renolds number of water in the tube
if Ret>=10^4
Nut=0.0273*Ret^0.8;                                      %Nusselt number in the tube
elseif 2100<Ret<10^4
    Nut=0.137625*(Ret^(2/3)-125)*(1+(Di/2.2)^(2/3));
else
  Nut=1.86*(0.7591*Ret*Di)^(1/3);
end
hi=0.682*Nut/Di;                                         %Heat transfer coefficient in the tube
U=(A/(Ai*hi)+0.00017611*A/Ai+0.00044030/efw+1/(efw*ho)+A*0.001589959*log(Dr/Di)/
NT)^(-1); %Overall heat transfer coefficient
NTU=A*U/10266.57;                                        %Number of transfer units
C=0.5;                                                   %Heat capacity rate ratio
e=2*(1+C+(1+C^2)^0.5*(1+exp(-(NTU)*(1+C^2)^0.5))/(1-exp(-(NTU)*(1+C^2)^0.5)))^(-1);
%Heat exchanger effectivness
Q=1283731.757*e;                                         %Heat transfer rate
% presure drops both in the shell and tube side
a=(Pt-Df)/Dr;
Ao=2.2*((0.53/XT-1)*(XT-Dr-(Df-Dr)*t*Nf)+XT-Dr-(Df-Dr)*t*Nf);         %Minimum
free-flow area in the shell
Dh=8.96*Ao/A;                                            %Haydrolic diameter
Resp=29355.9*Dh*Vmax;                                    %Renolds number in haydrolic diameter
Reeff=Resp*(l/b);
fs=(1+2*exp(-a/4)/(1+a))*(0.012+27.2/Reeff+0.29/Reeff^0.2);           %Pressure drop
factore in the shell
Gs=0.757*Vmax;                                           %Gas mass flux
%gets rid of decimal part and add 1 to the integer part
chPfs=2.642*fs*Nr*Gs^2;                                  %Pressure drop in the shell
chPfsT=0.1*chPfs+chPfs;                                  %Pressure drop including additional factors
Gt=3.1831*np/(NT*Di^2);                                  %Mss flux in the tube
if Ret>=3000
```

```
ft=0.4137*Ret^(-0.2585);
else
ft=64/Ret;
end
chPft=0.0011522*ft*NT*Gt^2/Di;
chPr=0.00052374*(2*np-1.5)*Gt^2;                    %Pressure drop on bending of tubes
chPtT=chPr+chPft;
% Total cost estimation of shell and tube heat exchanger
P=1/0.75*(20*chPfsT/0.757+2.5*chPtT/954.675);    %Pumping power for both gas and water
Co=P*8040*0.06/1000;                                  %The annual current cost
sum=0;
for i=1:1:20                                          %Oprating years
    Cop=Co/1.1^i;
    sum=sum+Cop;
end
CopT=sum;
CB=exp(11.667-0.809*log(A*0.09290304)+0.009005*(log(A*0.09290304))^2);      %Capital
cost factor for STHEx types
Fm=1.55+(A*0.09290304/100)^0.05;         %Capital cost factor of material
Cin=CB*Fm*1.25*0.9876;
CT=Cin+CopT;
scatter(Q,CT,'g*');                          %Heat transfer rate and total cost of heat
exchanger with out constraints
hold on;
xlabel('Heat transfer rate(W)','fontsize',12)
ylabel('Total cost($)','fontsize',12)
if ((Q>=768280.4) && (CT<=1.5939*10^6))                 %Heat transfer rate and total cost
of heat exchanger when heat transfer rate greater than values gotten from Excel value
scatter(Q,CT,'k*');
hold on ;
xlabel('Heat transfer rate(W)','fontsize',12)
```

```
ylabel('Total cost($)','fontsize',12)
end
% Problem constraints
if ((Q>=5.133*10^5) && (CT<=1829400))                    %Heat transfer rate and total cost of
heat exchanger
disp(Q);
disp(CT);
disp(chPfsT);
disp(chPtT);
disp(e);
disp(CT/Q);
disp(U);
disp(np);
disp(e);
disp(A);
disp(Dr);
disp(Di);
disp(b);
disp(l);
disp(t);
disp(Nf);
disp(NT);
disp(NTp);
disp(Nr);
disp(Nr1);
disp(Nr2);
scatter(Q,CT,'b*');
hold on ;
xlabel('Heat transfer rate(W)','fontsize',12)
ylabel('Total cost($)','fontsize',12)
 end
```

```
            end
         end
      end
   end
```